QUANTIFYING THE EFFECTS OF EPIPHYTIC ALGAE ON THE GROWTH OF A SUBMERSED MACROPHYTE

By

JING GUAN

A DISSERTATION PRESENTED TO THE GRADUATE SCHOOL
OF THE UNIVERSITY OF FLORIDA IN PARTIAL FULFILLMENT
OF THE REQUIREMENTS FOR THE DEGREE OF
DOCTOR OF PHILOSOPHY

UNIVERSITY OF FLORIDA

2017

To my parents and husband

ACKNOWLEDGMENTS

Certain things cannot be completed alone, and completion of this dissertation definitely should be ranked as one of them. Without inspiration and guidance from my committee, this work would not have been done. My committee chair, Dr. Thomas Frazer, was always there with an open ear and sage advice on managing my progress and staying on track. He made me feel more confident and convinced me that what I am doing is worthwhile. I cannot thank him enough for his support. My co-chair Dr. Charles Jacoby provided encouragement and guidance when things didn't work out and drove me to follow-up when things did work. He was amazingly motivated, dedicated, and selfless with his time and energy. Dr. Frazer always challenged me to step back to take a look at the big picture of my research system, and Dr. Jacoby helped me home-in on specific questions. I very much appreciate their consistent and combined efforts to provide me with a doctoral research experience that had freedom and direction. Dr. Greg Kiker was selfless with his time and energy, and I thank him for his encouragement and willingness to share his experience of the modeling world. Dr. Mark Brenner was always a welcoming presence and positive influence that encouraged me to keep going. His frank and insightful questions provoked thought and discussion that immensely improved this product.

I also would like to thank my lab mates: Jessica Frost, Joelle Laing, and Morgan Farrell. Thanks for their selfless and amazing dedication in the field. Field days with them were some of the most enjoyable and memorable highlights of my doctoral study. I could not have asked for a better group.

Most importantly, none of this could have happened without the loving support of my parents and husband. Their constant love, understanding, and encouragement gave me huge motivation.

Finally, I thank all who have added spice to my life during these four years of study. Their encouragement and support made completing this research as enjoyable as possible.

TABLE OF CONTENTS

page

LIST OF TABLES

LIST OF FIGURES

Abstract of Dissertation Presented to the Graduate School
of the University of Florida in Partial Fulfillment of the
Requirements for the Degree of Doctor of Philosophy

QUANTIFYING THE EFFECTS OF EPIPHYTIC ALGAE ON THE GROWTH OF A SUBMERSED MACROPHYTE

By

Jing Guan

December 2017

Chair: Thomas K. Frazer
Co-chair: Charles A. Jacoby
Major: Interdisciplinary Ecology

Declines in the abundance of submersed macrophytes in Florida's spring systems are attributed, in large part, to the proliferation of nuisance algae. Macroalgal mats and increased epiphytic burdens on the leaves of native macrophytes are particularly problematic as these algae intercept incident light necessary for photosynthesis. Prolonged shading leads to loss of macrophytes and the refuge, foraging habitat and other important ecosystem services they provide. In the Chassahowitzka River, a spring-fed system along the west coast of peninsular Florida, documented increases in epiphytes on macrophytes were temporally concordant with losses of important macrophytes, such as *Vallisneria americana*, and I explored the causal link between these events by studying the impacts of epiphytic loads on light attenuation and growth of *V. americana*. My results suggest that even low loads of epiphytes result in a marked reduction of the light available for growth. Therefore, to provide water resource managers with an objective tool to support decisions and improve water management activities, a simulation model of the growth of *Vallisneria*

americana was developed. The model, based on observations in the laboratory and the field, predicts the growth of *V*. *americana* under different loads of epiphytes.

CHAPTER 1
INTRODUCTION

Status of Florida's Spring Systems

The landscape of peninsular Florida between latitudes 27º and 31º is punctuated by a large number and diversity of springs, due, in large part, to a highly permeable karst geology, abundant rainfall and a vast aquifer (Wetland Solutions Inc. 2010). These springs continuously discharge freshwater that supplies the downstream lakes, streams, rivers and estuaries that form Florida's spring systems. These springs are characterized by clear water that is rich in dissolved nutrients and gases and constant in temperature and chemical content (Knight and Notestein 2008). These characteristics create favorable habitats for myriad aquatic flora and fauna in Florida's springs and their downstream receiving waters. Besides these ecological values, clear water and associated plants and animals have been important economic resources that support various recreational activities, attract a large number of visitors and generate millions of dollars of annual revenue for local economies (Bonn 2004, Scott et al. 2002).

Unfortunately, many springs in Florida show signs of substantial degradation, including a proliferation of nuisance algae, declines in native macrophytes, altered food webs, and deteriorating aesthetics (Wetland Solutions Inc. 2010). In the famous Silver Springs, for example, fish populations have experienced significant declines (Munch et al. 2006). Human activities, such as pumping groundwater and more intensive use of the land in watersheds of springs likely underlie many of the observed problems (Cohen et al. 2007). Groundwater depletion and nutrient pollution are of particular concern because they can reduce flows and lead to eutrophication (Knight and Notestein 2008). This predicament creates significant negative feedbacks on ecological health, public

health, and local economies; therefore, a greater emphasis on ecological research and monitoring in Florida's spring systems has become a focus.

One focus for recent studies has been submersed macrophytes, which always have been recognized as a crucial part of Florida's spring systems (Choice et al. 2014, Canfield and Hoyer 1988, Mattson et al. 1995). Submersed macrophytes are vascular aquatic plants that have internal transport structures and true roots, and they are principally angiosperms that can flower and produce enclosed seeds on a seasonal basis (Sculthorpe 1985). Common native macrophytes in Florida's springs include sagittaria (*Sagittaria kurziana*), wild celery/eel grass (*Vallisneria americana*), southern naiad (*Najas guadalupensis*), coontail (*Ceratophyllum demersum*), and fanwort (*Cabomba caroliniana*), with Eurasian milfoil (*Myriophyllum spicatum*) and hydrilla (*Hydrilla verticillata*) being common invasive species. The favorable substrate, flow and light environment in Florida's springs facilitate the productivity of submersed macrophytes. For example, the total annual production of leaves for *V. americana* can reach 2704 g m^{-2} in Kings Bay, which belongs to the Crystal River/Kings Bay spring complex (Hauxwell et al. 2007). As some of the most important primary producers in Florida's springs, submersed macrophytes play important ecological roles. They provide food for a number of grazers, enrich the water with oxygen that sustains high abundances of aquatic animals, provide a refuge from predators, reduce turbidity by stabilizing the river bed, and improve water quality by taking up nutrients (Smart et al. 1994, Rogers et al. 1995, Wigand et al. 2000).

Given the important ecological roles they play, submersed macrophytes represent a useful indicator for evaluating the ecological health of Florida's springs. In

recent decades, declines in the abundance of submersed macrophytes have been observed in several springs, lakes, estuaries, and rivers in Florida (Hauxwell et al. 2004, Knight and Notestein 2008). Declines of native submersed macrophytes in Florida's springs have been attributed to climate change, degradation of water quality (e.g., excessive loads of nutrients, herbicides and other chemical pollutants), increased disturbance (e.g., trampling and propeller scars), competition from exotic species (e.g., hydrilla), and light limitation (Canfield and Hoyer 1988).

Among those factors contributing to declines of native submersed macrophytes in Florida's springs, light limitation caused by algal proliferation has been widely recognized as a main causal factor. In recent decades, massive macroalgal mats and heavy loads of epiphytic algae have become increasingly common in Florida's spring ecosystems. For example, a survey of 29 Florida springs found that almost all of them harbored macroalgae, and approximately 50% of the benthic substrate was covered by algal mats with an average thickness of 0.5 m and a maximum thickness in some springs of 2 m (Stevenson et al. 2007). These algal communities consist of myriad microalgae, diatoms, cyanobacteria, microbes, and macroalgae (Notestein 2001). Macroalgae that grow in Florida's spring systems include the genera *Chara* and *Nitella* that resemble vascular plants, and filamentous genera, principally green algae and cyanobacteria, such as *Cladophora*, *Enteromorpha*, *Lyngbya*, and *Vaucheria* (Knight and Notestein 2008). These epiphytic algae appeared to have proliferated rapidly, possibly stimulated by reductions in flow and nutrient enrichment in springs (Hauxwell et al. 2004, Hoyer et al. 2004, Heffernan et al. 2010). Once established, these algae have been shown to intercept a large proportion of incident light necessary for photosynthesis

and growth of submersed macrophytes (Phillips et al. 1978). Evidence suggests the occurrence of a fundamental shift in dominance from submersed macrophytes to nuisance algae, with this event being a major concern for a broad group of environmental scientists and managers of natural resources (Springs Management Plan 2016).

The Chassahowitzka River

One place where increased epiphytic loads on macrophytes have been documented is the Chassahowitzka River (Latitude 28°42'54", Longitude 82°34'35"), a spring-fed system on Florida's west coast (Figure 1-1). These increases were temporally concordant with losses of important macrophyte species, such as *Vallisneria americana* (Notestein 2001). Such an observation suggests a cause and effect relationship, so the system may be particularly suitable for a study of the impacts of epiphytes on macrophytes.

The Chassahowitzka River is located in southwest Citrus County, FL. The climate in this area is subtropical, with mean annual precipitation ranging from 132 cm to 142 cm (United States Fish and Wildlife Service 1988). This spring-fed, coastal river originates at the Chassahowitzka Spring, which is a first magnitude spring (Yobbi and Knockenmus 1989), and it also is fed by several smaller spring vents located in its tributaries (Crab, Baird, and Potter Creeks, Notestein 2001). The discharge from the main spring complex ranges from 2 to 8 $m^3 s^{-1}$, and the mean discharge between 1930 and 1972 was 3.92 $m^3 s^{-1}$ (Rosenaur et al. 1977). The river flows west approximately 4 km from the main spring boil to a coastal marsh complex and then another 4 km to the Gulf of Mexico (Notestein 2001). Given a gradient in elevation of 3 m or less, mean flow rates are generally less than 0.20 m s^{-1} (Frazer et al. 2006).

Such low flow rates mean that tidal cycles influence both spring discharge and flow within the river (Yobbi 1992), with tidal mixing creating brackish creeks and bays in the lower river. Above the marsh complex, the depth of the midstream channel ranges from 0.5 m to 2.6 m, with a mean depth of 1.2 m (Notestein 2001). The upper portion of the river is narrow, with a minimum width of 44 m and a maximum width of 175 m midway downstream, and in total, the wetted surface area of the river (above the marsh complex) is approximately 360,000 m^2 (Notestein 2001). Approximately 3% the wetted area is covered by a canopy of riparian vegetation (Notestein 2001). Water clarity in the river is good and light attenuation coefficients (K_d) are generally less than 1.5 (Frazer et al. 2006). The primary substrate along the river bottom is sand (~ 54%), with varying mixtures of mud and rock (Frazer et al. 2006). Mud is more prevalent near the shoreline, and small patches of exposed limestone appear throughout the river (~ 1% of the total bottom area), which is indicative of the dominance of limestone in the underlying geology (Brooks 1981). The influence of groundwater keeps water temperature along the length of the river fairly uniform, ranging from 20.7°C to 26.4°C, but temporal variations caused by seasonal changes in air temperatures did occur during my sampling.

In combination, the light environment and substrate in the Chassahowitzka River appear favorable for the growth of primary producers, with macrophytes, macroalgae, and periphyton observed throughout most of the river (Notestein 2001). The density of submersed aquatic vegetation declines gradually with distance downstream because of higher salinities (Yobbi and Knochenmus 1989). Common macrophytes include *Vallisneria americana*, *Potamogeton pectinatus*, *Najas guadalupensis*, *Myriophyllum*

spicatum, and *Hydrilla verticilla*. Some *Sagittaria kurziana*, *Ruppia maritima*, *Potamogeton illinoensis*, and *Ceratophyllum demersum* also have been observed in this river (Frazer et al. 2006). Based on visual estimates, *V. americana* is the dominant macrophyte in the river (Notestein 2001). In addition, benthic algae represent approximately 43% of the total SAV biomass, composed primarily of *Lyngbya* sp. and *Chaetomorpha* sp., with *Gracilaria* sp. and *Enteromorpha* sp. also abundant (Notestein 2001).

Although a large portion of the river and estuary are protected in the Chassahowitzka National Wildlife Refuge, the system has exhibited increasing anthropogenic impacts, including nitrate concentrations at the headspring that have increased from 0.01 mg L^{-1} to over 0.5 mg L^{-1}, or more than 50-fold since the 1960s (Jones et al. 1997, Frazer 2000, Scott et al. 2004). These increased nutrient concentrations may have stimulated macroalgal blooms, which can impact the survival of macrophytes and ultimately the ecological, economic and social value of the resource (Pinckney et al. 2001). Therefore, important questions regarding spring macrophytes and epiphytic algae are: “How much light is intercepted by epiphytic algae on macrophytes?”; “How much epiphytic biomass causes damage or dysfunction for macrophytes?”; and “Can we effectively model the performance of macrophytes subject to different loads of epiphytes?”

Objectives

Toward this end, laboratory and field measurements, and a model were used to answer these questions and achieve three main objectives: 1) empirically model the relationship between epiphytic biomass on *V. americana* leaves and light transmission (Chapter 2); 2) document the impacts of epiphytes on the growth of *V. americana* in the

field (Chapter 3); and 3) employ these data to develop and calibrate a model that predicts the performance of *V. americana* under different loads of epiphytes (Chapter 4). The overarching objectives of this research were to develop a more comprehensive understanding of the impacts of epiphytes on macrophytes and to provide water resource managers with objective tools to assess the vulnerability of macrophytes to the negative impacts of increased loads of epiphytes.

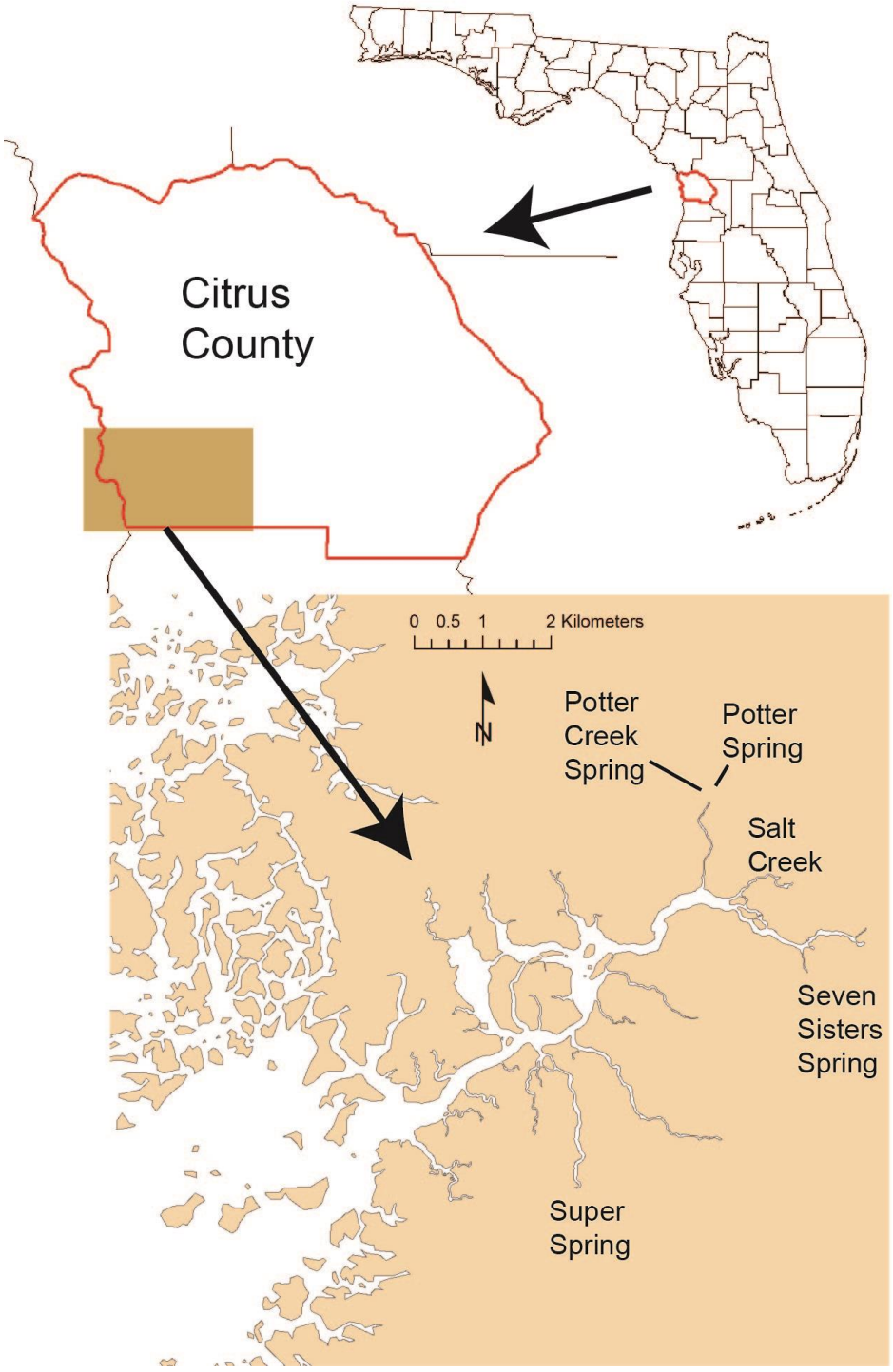

Figure 1-1. Location of the Chassahowitzka River and its estuary. Labels indicate spring vents and tributaries. Reprinted with permission from Chassahowitzka.net, http://www.chassahowitzka.net/rmap.htm (November 18, 2017).

CHAPTER 2
LIGHT ATTENUATION BY EPIPHYTES ON *VALLISNERIA AMERICANA*

Background

Florida has abundant spring resources, which have important economic and ecological value (Scott et al. 2002, Bonn 2004). In these valuable spring systems, submersed freshwater macrophytes historically dominated primary production because of the shallow water and suitable sediments. As some of the most important primary producers, submersed macrophytes play important roles in regulating the aquatic environment by providing food, enriching the water with oxygen, stabilizing the sediment, cycling nutrients, and acting as food and a refuge that sustains high abundances of animals (Smart et al.1994, Rogers et al. 1995, Wigand et al. 2000).

Because macrophytes fill such an important ecological niche in Florida's spring systems, they represent a useful indicator of environmental health. In recent decades, environmental reports have documented declines in the abundance of macrophytes in several lakes, estuaries and rivers in Florida (Hauxwell et al. 2004). The decline of macrophytes in Florida's springs may be attributed to many factors: climatic change, water quality degradation (e.g., excessive nutrients and agricultural herbicides), increased human activities (e.g., trampling and scarring from anchors or propellers), competition from exotic species (e.g., *Hydrilla verticillata*), and reduced availability of light.

Among those factors responsible for declines in macrophytes, a frequently cited influence is low light availability, which decreases net photosynthesis (Kimber et al. 1995, Hauxwell et al. 2007). The minimum light requirement for survival of freshwater macrophytes is approximately 13% of light reaching the water's surface

(Carter et al. 2000, Kemp et al. 2004). The amount of light available to submersed aquatic macrophytes can be affected by many environmental factors, such as riparian canopies, phytoplankton and turbidity that reduce water clarity, and algae that grow on the leaves of macrophytes (Carter et al. 2000). Algae can intercept a large proportion of incident light that macrophytes need to support their metabolism and growth, and available light has always been considered an important cause of loss of macrophytes (Sand-Jensen 1977, Phillips et al. 1978, Orth and Moore 1983, Twilley et al. 1985, Cambridge et al. 1986, Silberstein et al. 1986, Canfield and Hoyer 1988). The influence of algae has become especially evident in recent decades, with massive macroalgal mats and large quantities of epiphytic algae becoming increasingly common in Florida's spring systems (Knight and Notestein 2008). In some springs, there may have been a fundamental ecological shift in the aquatic primary producer communities from native macrophytes to nuisance algae (Springs Management Plan 2016). Such ecological shifts can be attributed to chemical, physical, and biological changes in the aquatic systems, including excessive anthropogenic loads of nutrients, reduced water velocities, and declines in abundance of grazers (Hauxwell et al. 2004, Hoyer et al. 2004, Heffernan et al. 2010).

Excessive proliferation of macroalgal mats and epiphytes on leaves of macrophytes are particularly problematic as these algae can intercept the incident light that macrophytes require for photosynthesis. Thus, it is necessary to quantify the relationship between epiphytic loads on macrophytes and light attenuation and to formulate a numerical model incorporating the effect of epiphytes on the growth of macrophytes.

The relationship between epiphytic loads and light attenuation has been quantified using different methods to measure light transmission through epiphytes (Table 2-5). Most studies used an indirect method to measure transmission of light that involved removing epiphytes from leaves and measuring light transmission through a resuspended slurry (Sand-Jensen and Borum 1984, Neckles et al. 1993, Dixon 2000). This method is easy to apply, but it destroys the three-dimensional (3D) structure of the submersed epiphytic communities. This 3D-structure recently was demonstrated to be a very important influence on light attenuation, especially by filamentous epiphytes (Vermaat and Hootsmans 1994, Brush and Nixon 2002, Drake et al. 2003, Stankelis et al. 2003). Filamentous epiphytes that are underwater extend away from the leaves of macrophytes (Brush and Nixon 2002), whereas coralline algae and diatoms form flat sheets that may be more suitable for evaluation by the indirect method (Vermaat and Hootsmans 1994, Drake et al. 2003). Some other studies used artificial leaves, such as Mylar™ strips, as an alternative to natural leaves (Phillips et al. 1978, Van-Dijk 1993, Glazer 1999, Stankelis et al. 2003, Notestein 2001). Although this method can document the age of epiphytes on artificial leaves, the significant differences between artificial leaves and natural leaves may lead to important differences in the epiphytes that, in turn, may affect estimates of light transmission (Bulthuis and Woelkerling 1983, Brush and Nixon 2002). In addition, artificial light sources also were used widely in previous studies (Sand-Jensen and Borum 1984, Sand-Jensen 1990, Van-Dijk 1993), but Drake et al. (2003) found that artificial light sources do not mimic the quality of natural light accurately, which may be a very important influence on photosynthesis by aquatic plants.

After light attenuation was measured for different epiphytic loads, three equations were used to describe light attenuation as a function of the loads. The least used approach was the linear equation of Glazer (1999) that described light transmission through epiphytic bryozoans; however, the linear model fit well only at very low densities of epiphytes (0 to 5 mg DW cm^{-2}). In aquatic science, the most widely used equation to model epiphyte light attenuation is an exponential decay function ($I_e = I_0 \mathrm{e}^{-K_e B_e}$) derived from the Beer-Lambert Law (Kirk 1994, Burt et al. 1995, Stankelis et al. 2003), where I_0 is incident light, K_e is the coefficient of epiphytic light attenuation, and I_e is attenuated light that decreases exponentially with B_e or loads of epiphytes. Some studies, however, found that a hyperbolic decay equation was applicable and superior in explaining variation in light attenuation with differences in loads caused by epiphytic communities with various morphologies (e.g., microalgal films, coralline algal crusts, and filamentous macroalgae, Van-Dijk 1993, Vermaat and Hootsmans 1994, Brush and Nixon 2002).

In my study area, the spring-fed Chassahowitzka River on the west coast of peninsular Florida, increases in epiphytes on macrophytes were temporally concordant with losses of important species, such as *Vallisneria americana* (Notestein 2001). This observation suggests a cause-and-effect relationship, although the direct effects of epiphytes on light attenuation and the performance of macrophytes in the system have not been investigated. The objectives of this chapter were to measure and model light transmission through different loads of epiphytes found on *V. americana* leaves. The method used by Brush and Nixon (2002) to directly measure light attenuation was employed in this study. Thus, all measurements of light attenuation were obtained using leaves of *V. americana* that were collected in the field and held underwater so the 3D

structure of epiphytic communities were maintained as they were exposed to natural light. The resulting measurements became the basis for fitting exponential and hyperbolic decay models to describe the relationship between the density of epiphytes and light attenuation. These two mathematical models were evaluated to identify the best fit to the results and the most useful numerical model for predicting growth of macrophytes under differing loads of epiphytes.

Materials and Methods

Study Site and Environmental Data

Sampling was conducted in a large, continuous *V. americana* meadow in the Chassahowitzka River. The meadow covered ~ 2700 m^2 of the underlying sand/mud substrate. The study area is in the mid-upper reaches of the river (Latitude 28°43'8", Longitude 82°35'32"), about 1.8 km west of the head springs and 2.2 km upstream of the coastal marsh complex (Figure 2-1). River flows are primarily from spring discharge so water temperatures remain about 25.8ºC. Although freshwater contributes 99% of the flow, the study area is a tidally influenced freshwater-oligohaline system, with a mean salinity of 2.96‰ and 1-m tidal range. Through my sampling period (August 2015-October 2015), light attenuation coefficients (K_d) in the water and average concentrations of total nitrogen (TN), total phosphorus (TP), and chlorophyll-a (Chl-a) ranged from 1.5 to 3.2, 640 to 950 µg TNL^{-1}, 20 to 55 µg TPL^{-1}, and 2.79 to 16.09 µg Chl-a L^{-1}, respectively. The riparian canopy does not shade much of the water at my site, and mean *in-situ* surface irradiance ranged from 1606 to 1914 µE m^{-2} s^{-1}.

Sampling

Between August and October 2015, samples of leaves were collected from the Chassahowitzka River. A snorkeler haphazardly tossed five quadrats (0.25 m

by 0.25 m) within the meadow, and within the quadrats, leaves of *V. americana* with varying amounts of epiphytes were clipped carefully at their bases and placed in 1-L Nalgene® jars filled with ambient water. Jars containing 4-6 leaves were stored on ice in a cooler prior to processing (within 24 hr of collection).

Determination of Light Transmission Through Varying Epiphytic Loads

Attenuation of natural photosynthetically active radiation (PAR) by epiphytes was measured. Measurements were taken with a LI-1400 datalogger (Figure 2-2A) and two, 2-π underwater quantum sensors (LI-COR UWQ5754 and LI-COR UWQ 5692, Figure 2-2B). One sensor measured light through a leaf of *V*. *americana* and the other simultaneously measured natural, incident irradiance at the same depth. The sensors were submersed in an outdoor tank filled with water (108 cm long $\times$ 62 cm wide $\times$ 48 cm high) at the University of Florida (Figure 2-2C). In order to minimize errors caused by dramatic changes in incident light (e.g., edge effects introduced by passing clouds), all measurements were made under direct light on clear days when incident light was greater than 1300 µE m^{-2} s^{-1}.

In addition to limiting variation in the quantity and quality of light, efforts were made to limit variation arising from the heterogeneous distribution of epiphytes on *V*. *americana* leaves. Therefore, leaves were separated into a series of sections approximately 6 cm long that had relatively homogeneous distributions of epiphytes.

The effect of epiphytes on light penetration was measured via a two-step process (Figure 2-3). Before measuring the penetration of PAR, one side of each section was scraped with a scalpel to remove epiphytes that were saved for taxonomic identification. Each processed section was placed on one of the submerged sensors, which ensured

the epiphytes extended into the water column. When the uncovered sensor indicated that incident irradiance was stable, the quantity of light hitting that sensor and the quantity of light passing through the section of leaf and its attached epiphytes were recorded. Recordings were made at 1-s intervals for 30 s at three points along each section. Next, the epiphytes on the other side of each section were removed and saved for determination of epiphytic biomass per unit area (mg dry weight cm^{-2} of leaf, mg ash-free dry weight cm^{-2} of leaf, mg ash dry weight cm^{-2} of leaf, and µg chlorophyll-a cm^{-2} of leaf). The resulting clean sections of leaves were placed over the appropriate submerged sensor, and incident light and light passing through the section were measured. Sections were saved, and their lengths and widths were measured to determine their surface areas (cm^2). For each section, light attenuation by epiphytes (percent reduction in transmission of PAR) was calculated from the amount of incident light passing through both the epiphytes and the leaf (I) relative to the amount of light passing through the leaf only (I_0): $\text{PAR Transmission Percentage} = I/I_0 * 100\%$. The effects of scraping were determined by comparing transmission of incident light before and after scraping sections of five leaves that had no visible epiphytes.

The epiphytes initially removed from leaves were processed to determine the species composition of assemblages. Prior to examination under an anatomical lens, the samples were distributed as a single layer in a wet petri dish. Representative types of algae were chosen according to their morphology (e.g., filaments, mats, tufts, or slurry) and color (e.g., green, blue-green, or red). Next, a small sample of each of the chosen algae was transferred with tweezers or an eyedropper to a separate wet glass

slide for microscopic analysis. Thereafter, algae were examined at 100X and 400X and identified using standard keys.

The epiphytes scraped from the other side of each section were used to determine biomass per unit area, as chlorophyll-a content, and various measures of mass. To measure the mass of epiphytes, half of each sample was placed in a pre-weighed, 20-ml aluminum tray. Samples in aluminum trays were processed to yield dry weight (DW), ash weight (AW), and ash-free dry weight (AFDW). Dry weights were measured after the pre-weighed wet samples were held in a forced-air drying oven maintained at approximately 65ºC for 36 to 48 hr. Ash weights were measured after dried samples had been heated to 450ºC in a muffle furnace for 4 hr. Dry weight and ash weight for each sample were measured to the nearest 0.001 g on a Mettler P 163 balance. Ash-free dry weight is the difference between dry weight and ash weight. The other half of each sample was wrapped in 47-mm-diameter Whatman GF/F glass microfiber filters that were stored in a freezer at -20ºC for no more than 2 days. Chlorophyll pigments were extracted from the epiphytes with 90% ethanol in a 79ºC water bath, and chlorophyll-a concentrations were determined spectrophotometrically (Montana Department of Environmental Quality 2011). Using these data, various measures of epiphytic density were determined by dividing the DW, AFDW, AW and chlorophyll-a concentrations by the relevant areas for sections of leaves (one side of each section only).

Modeling Light Transmission Through Epiphytes

Mean values of three replicate measures of percent light transmission for individual sections were used in subsequent analyses. Empirical relationships between

light transmission through epiphytes and epiphytic biomass were investigated with regression based on a standard least squares approach.

Exponential and hyperbolic decay models were fit to the mean values, and the results were compared to determine the relative suitability of these different regression models. Exponential decay functions and negative hyperbolic functions were fit in both two-parameter and three-parameter forms: i.e., $y = ae^{(-\frac{x}{b})}$, $y = c + ae^{(-\frac{x}{b})}$, and $y = \frac{a}{1+x/b}$, and $y = a(1 + \frac{cx}{b})^{(-\frac{1}{c})}$. In the relevant equations, y is the transmittance of PAR through epiphytes (I/I_0 %) expressed as percent of incident light passing through both epiphytes and leaves relative to the amount of light passing through the leaves only; x is the epiphytic density expressed as mg DW cm^{-2}, mg AFDW cm^{-2}, mg AW cm^{-2}, and µg chlorophyll-a cm^{-2}; and a, b and c are constants. All models were evaluated in both constrained (100% light transmission at a load of zero) and unconstrained forms. Parameter estimates together with coefficients of determination (R^2) were calculated with CurveExpert statistical software and Python matplotlib.

All models were evaluated with the Akaike Information Criterion (AIC, Akaike 1973, Burnham and Anderson 2001). This criterion assesses goodness of fit with a likelihood function, and it includes a penalty related to overfitting that is calculated on the basis of the number of model parameters. Thus, AIC is used to determine if increased complexity significantly increases the amount of variation explained by a model.

The preferred model is the one with the minimum AIC value. The general form for calculating AIC is: $AIC = 2K - 2\ln(L)$; where K is the number of parameters included in

the model, $\ln(L)$ is the natural logarithm of likelihood of the model, and the likelihood (L) reflects the overall fit of the model (larger values indicate better fit). AIC also could be calculated in a more conventional formula: $AIC = 2K + n * \ln(RSS/n)$, where K is the number of parameters included in the model, n is the sample size, and RSS is the residual sum of squares. For small sample sizes (n/K< 40), AIC requires a bias-adjustment, which yields a second-order Akaike Information Criterion (AICc) or $AICc = AIC + \frac{2K(K+1)}{n-K-1}$, where variables are as defined above. As sample sizes (n) increase, the last term of the AICc approaches zero, and AICc approximately equals AIC (Burnham and Anderson 2002).

The AICc value itself has no meaning; AICc values become meaningful when they are compared among a series of candidate models. The model with the lowest AICc is the best model. To compare models, $\Delta AICc$ and Akaike weight (w_i) are used. The difference between the model with the lowest AICc (the best fitting model) and the others is expressed as: $\Delta_i = AICc_i - \min AICc$, where $AICc_i$ is the AICc value of model i, and $\min AICc$ is minimum AIC value for all models. Akaike weights (w_i) is an another method of measuring the suitability of each model, which is represented as the normalized relative likelihood value of the model: $w_i = \frac{\exp(-0.5*\Delta_i)}{\sum_{r=1}^{R}\exp(-0.5*\Delta_r)}$, where w_i is the Akaike weight for model i, the numerator is the relative likelihood for model i, and the denominator is the sum of the relative likelihoods for the whole set of R candidate models.

Results

Composition of Epiphytic Communities

The epiphytes on *V. americana* leaves collected in the Chassahowitzka River were dominated by a green filamentous macroalgae, *Enteromorpha* sp. (Figure 2-4) that was mixed with a small amount of *Cladophora* sp. (Figure 2-5A) and diatoms (Figure 2-5B). Epiphytes mostly adhered directly to the surfaces of leaves.

Determination of Light Transmission Through Different Epiphytic Loads

Direct measurements of the light attenuation by epiphytic loads were obtained from a total of 120 samples. Blades without epiphytes attenuated 93.52 $\pm$ 2.6% of incident light (mean $\pm$ SD, n = 60). A comparison of light passing through sections of leaves without epiphytes before and after they were scraped indicated that scraping did not alter light attenuation substantially, with scraped blades transmitting approximately 0.48% less incident light. The epiphytic loads ranged from 0.21 to 16.66 mg DW cm^{-2} of leaf (Figure 2-6A), 0.11 to 8.14 mg AFDW cm^{-2} of leaf (Figure 2-6B), 0.05 to 8.52 mg Ash DW cm^{-2} of leaf (Figure 2-6C), and 1.05 to 47.35 µg chlorophyll-a cm^{-2} of leaf (Figure 2-6D). Biotic (AFDW) and abiotic (ash DW) components showed that abiotic materials the epiphytic communities comprised 21.90% to 77.10% of the epiphytic communities. Epiphytic communities on macrophytes were not homogeneously distributed, with greater accumulation on the older portions of leaves near their tips and less or no epiphytes on the new or basal portions of leaves. Light transmission expressed as percentage of the incident irradiance (I_0) that penetrated to the leaves (I) ranged from 4.48 to 87.15%. Four scatter plots of light transmission versus different measures of epiphytic loads display similar trends (Figure 2-6): transmission of light decayed rapidly at low epiphytic loads and then

gradually leveled off as epiphytic loads increased. Incident light could be attenuated by 80% at ~ 6.29 mg DW cm^{-2} of leaf (or 3.43 mg AFDW cm^{-2} of leaf, 2.88 mg Ash DW cm^{-2} of leaf or 17.08 µg chlorophyll-a cm^{-2} of leaf), and transmission could be attenuated by 90% at ~ 17.73 mg DW cm^{-2} of leaf (or 4.53 mg AFDW cm^{-2} of leaf, 3.23 mg Ash DW cm^{-2} of leaf or 22.49 µg chlorophyll-a cm^{-2} of leaf).

Modeling Light Transmission Through Epiphytes

The 32 regression models captured 30.69 - 83.22% of the variation in observations of light transmission through different epiphytic loads (R^2 values in Table 2-1 and Table 2-2). The correlation coefficients (|r|) of all regressions were greater than 0.55, ranging from +0.61 to +0.91. The |r| of regressions that expressed epiphytic loads as mg DW cm^{-2} of leaf were as high as 0.9. Models based on dry weight (mg DW cm^{-2} of leaf) had the best performance with R^2 as high as 0.83. Models based on loads expressed as chlorophyll-a (µg chlorophyll-a cm^{-2} of leaf) had inferior fits relative to other models. Comparisons of determination coefficients (R^2) of all candidate models revealed that the unconstrained models captured more of the variation than constrained models.

Candidate models were ranked according to their suitability (Table 2-3) as determined by AICc values, differences (Δ_i) between each model's AICc and the lowest AICc, and Akaike weights (w_i). A value of $\Delta_i < 2$ suggested substantial evidence for the suitability of the model, values of $3 < \Delta_i < 7$ indicated that the model had considerably less support, whereas a $\Delta i > 10$ indicated that the model did not explain a substantial portion of the variation in the data (Burnham and Anderson 2002). AICc values ranged from 268.68 to 351.88. The values of Δ_i for the first five models

(Unconstrained_DW_Three-parameter exponential decay, Unconstrained_DW_Two-parameter exponential decay, Unconstrained_DW_Three-parameter hyperbolic decay, Unconstrained_DW_Two-parameter hyperbolic decay, and Unconstrained_AFDW_Two-parameter hyperbolic decay) were < 2, suggesting these models explained a substantial amount of variation in the data. The values of Δ_i for models 6 to 10 (Unconstrained_AFDW_Two-parameter exponential decay, Unconstrained_AFDW_Three-parameter hyperbolic decay, Constrained_DW_Two-parameter hyperbolic decay, Unconstrained_AFDW_Three-parameter exponential decay, and Constrained_DW_Three-parameter hyperbolic decay) were between 3 and 7, so they explained considerably less of the variation in the data. Models with Δ_i values ≥12 explained very little of the variation in the data. These results indicated that model 1 (Unconstrained_DW_Three-parameter exponential decay) was the best of the 32 candidate models, with the minimum Δ_i and an Akaike weight (w_i) of 0.23 (Table 2-3).

Discussion

Most of the epiphytic loads were < 10 mg DW cm^{-2} of leaf, with only a few samples reaching 16.66 mg DW cm^{-2} of leaf. Epiphytic loads up to 100 mg DW cm^{-2} of leaf were noted by Brush and Nixon (2002), and the lower epiphytic loads in my study may be a consequence of the relatively low phosphorus concentrations in the Chassahowitzka River. In addition, epiphytes may be more abundant on macrophytes with complex morphologies or rough leaf surfaces (Notestein 2001); therefore, lower epiphytic loads may reflect the simple structure of the leaves of *V. americana*.

The four scatter plots relating light transmission and epiphytic loads show similar trends: transmission decayed rapidly at low epiphytic loads and then reductions in transmission approached zero as epiphytic loads increased (Figure 2-6). These trends illustrated the dramatic capacity of epiphytes to produce shade, even at low loads (thin layers). Beyond a certain point, increasing epiphytic loads did not attenuate much more light than thinner layers.

The regressions in Figures 2-8 to 2-15 are consistent with those of most previous studies (Figure 2-7, Brush & Nixon 2002). Linear regressions were used in a few studies (Glazer 1999, Bulthuis and Woelkerling 1983, Agustí et al.1994), but they failed to describe light transmission through a wide range of epiphytic densities (Brush and Nixon 2002), so a linear model may be suitable only for epiphytic communities composed of bryozoans or microalgae, rather than macroalgae. Theoretically, light transmission should be 100% when the epiphytic load is zero, but all models to pass through that point yielded lower R^2 values (Table 2-1 and Table 2-2). The unconstrained three-parameter exponential decay model based on dry weight of epiphytes (model 1 in Table 2-3) captured most of the variation in the data, with the highest AICc value 268.68 and minimum Δ_i and Akaike weight (w_i). The reliability of three-parameter, exponential decay models was noted in previous studies (Silberstein et al. 1986, Stankelis et al. 2003, Frankovich and Zieman 2005). However, model 2 also could be considered appropriate because model 1 is only 1.46 times as likely to be the best (evidence ratio = 0.23/0.16, Table 2-3). This model describes light transmission through epiphytes as $y = ae^{-x/b}$, which generates an epiphytic light attenuation coefficient (K_e) that parallels the water column attenuation coefficient (K_d). Thus, transmission of light

through both the water column and a load of epiphytes can be communicated simply by modifying the standard Beer-Lambert model (Frankovich and Zieman 1994, Kemp et al. 2000): $\text{Availiable Light} = I_0 * (e^{-K_d * Z})(e^{-K_e * B})$. Although the regressions were similar between this study and previous investigations, there were still differences in slopes and asymptotes (Table 2-4). For a given epiphytic load, light transmission through epiphytes varied from previous studies, with the epiphytic loads that reduce light transmission by 50% ranging from 1.06 to 22.12 mg DW cm^{-2} of leaf (Table 2-4). These differences may be caused by the composition and morphologies of the epiphytic communities. In my study area, the green filamentous macroalga *Enteromorpha* sp. was the dominant species on leaves of *V. americana*, which agreed with observations reported in Notestein's (2001) study of the Chassahowitzka River. In my study, about 1.69 mg DW cm^{-2} of *Enteromorpha* sp. could attenuate 50% of incident light, whereas in Florida Bay and the Florida Keys, coralline algae and associated carbonate sediment comprised most of the epiphytic load, and it took ~ 4.36 mg DW cm^{-2} to reduce transmission of light by 50% (Frankovich and Zieman 2005). Furthermore, ~ 22.12 mg DW cm^{-2} of *Cladophora* sp. attenuated transmission of light by 50% in Brush and Nixon's (2002) study of *Zostera marina*. *Enteromorpha* sp. may have attenuated light more strongly because it is darker in color and forms long, dense patches on leaves of macrophytes. In addition, coralline algae may absorb less light because pigment contents of symbiotic algae in corals are lower than in other algal species (Vásquez-Elizondo and Enríquez 2017, Losee and Wetzel 1983).

Light transmission decreases to an asymptote as epiphytic loads increase because the filamentous algae extend away from the surfaces of leaves, so lengthening

filaments increase the epiphytic load more than they affect the areal coverage on leaves or the amount of light attenuation. Filamentous *Enteromorpha* sp. in this study reduced light transmission to approximately 10% of incident light, and three other filamentous algae, *Ulothrix* sp., *Cladophora* sp., and *Polysiphonia* sp. reduced light transmission to 15%, 30%, and 18% of incident light, respectively (Brush and Nixon 2002). The asymptotic value may be determined by the detailed architecture of the epiphytic load, which is a topic for further study.

Besides differences related to the composition and morphology of epiphytic communities, the method used to measure transmission of light could lead to differences among the results of investigations (Table 2-4). The method used to measure transmission of light in this study kept the epiphytes in their natural orientations because they were submersed (Borum and Wium-Anderson 1980, Sand-Jensen and Borum 1984, Twilley et al. 1985, Neckles et al. 1993). This method is suitable for many algal morphologies, including film-like, crustose and filamentous algae (Van-Dijk 1993, Vermaat and Hootsmans 1994, Burt et al. 1995, Brush and Nixon 2002, Stankelis et al. 2003). Submergence is particularly important for algae that elongate from a relatively small base because the collapse of the three-dimensional structure to a two-dimensional structure can lead to overestimation of light attenuation (Brush and Nixon 2002). In fact, Cebrián et al. (1999) found that a given biomass of encrusting red algae attenuated more light than a similar load of erect, brown algae because the brown algal blades floated and let more light pass. Therefore, the geometric structure of an epiphytic community is an essential factor when considering light attenuation.

Another consideration is how samples are processed prior to measurement of light attenuation. A key element in processing is whether light attenuation is measured through the epiphytic load on one or both sides of a leaf. Based on field observations in my study area, I chose to measure light attenuation by epiphytes on one side of *V. americana* leaves because epiphytic loads on the two sides of leaves were substantially different (Figure 2-16). Thus, my processing involved removing epiphytes from one side of each leaf before measuring light passing through the remaining layer of epiphytes and the leaf. This approach eliminates the assumption that both sides of each leaf have the same composition and amount of epiphytes. In addition, two-layer method relies on a different equation: $\text{Light transmission } (\%) = 100\% * \sqrt{\frac{I_y}{I_0}}$, where I_y is the amount of light passing through the leaf and two layers of epiphytes and I_0 is amount of incident light. This difference arises because two layers of epiphytes generate a multiplicative effect on light attenuation rather than an additive one (Vermaat and Hootsmans 1994). The two-layer method may be most suitable for large accumulations of crustose coralline algae and delicate film-like algae. These firmly attached epiphytes generally are removed with acid after transmission of light has been measured.

Another methodological consideration is the choice of the metric for characterizing epiphytic loads. Because photosynthetic pigments in epiphytes (e.g., chlorophyll-a, chlorophyll-b, chlorophyll-c, fucoxanthin, and phycocyanins) are considered to be the dominant factors that influence light attenuation (Losee and Wetzel 1983, Agustí et al. 1994), many studies used total chlorophyll-a mass per unit area to describe epiphytic loads (Stankelis et al. 1999). In my study, results expressing epiphytic loads as µg chlorophyll-a cm^{-2} of leaf yielded the poorest predictions of light

transmission as shown by lower R^2 values (Table 2-1 and 2-2). Epiphytic loads described as total dry weight (mg DW cm^{-2} of leaf) yielded the best predictions, with R^2 values up to 0.83. Even other measures of epiphytic loads (mg AFDW cm^{-2} and mg Ash DW cm^{-2}) yielded better results than those of chlorophyll-a. This discrepancy may be a consequence of unpigmented mucous, frustules, calcium carbonate, and trapped detritus that all attenuate light without contributing chlorophyll-a (Lin 1995). In my samples, inorganic matter (ash dry weight) represented up to 77.10% of epiphytic loads. Such large amounts of abiotic matter may become trapped in the epiphytic matrix when sediments are resuspended by diurnal tidal currents. Thus, useful estimates of epiphytic loads come from dry weights, without the need to extract chlorophyll-a or use a muffle furnace.

My results indicated that 90% of incident light is attenuated at ~ 7.73 mg DW cm^{-2}. Thus, it is not necessary for epiphytic loads to be conspicuous before they have the potential to affect the growth of macrophytes. Previous studies reported that 13% of incident light at the water's surface was the average minimal light requirement for survival of freshwater angiosperms (Chamber and Kalff 1985) and marine macrophytes needed about 11% of incident light at the water's surface (Duarte 1991). Based on these minimum light requirements and my results, I hypothesized that the critical epiphytic load for *V*. *americana* is approximately 6 mg DW cm^{-2}, i.e., the level at which transmission of PAR reaches 15% of incident light at a given depth. This hypothesis was tested by measuring growth and epiphytic loads for *V*. *americana* in the Chassahowitzka River.

Table 2-1. Parameter estimates and coefficients of determination (R^2) for unconstrained models of light transmission through epiphytes.

		Two-parameter exponential decay	Three-parameter exponential decay	Two-parameter hyperbolic decay	Three-parameter hyperbolic decay
Epiphytic loads	Equation	$y = ae^{-x/b}$	$y = c + ae^{-x/b}$	$y = \frac{a}{1 + x/b}$	$y = a * (1 + c * x/b)^{-1/c}$
mg DW cm^{-2}		a=79.61	a=74.22	a=93.31	a=84.93
		b=3.63	b=2.78	b=1.63	b=2.61
			c=8.36		c=0.44
	R^2	0.82	0.83	0.82	0.83
	AICc	269.44	268.68	270.12	269.78
mg AFDW cm^{-2}		a=73.31	a=67.53	a=83.37	a=78.41
		b=2.36	b=1.79	b=1.09	b=1.57
			c=8.01		c=0.56
	R^2	0.82	0.82	0.82	0.82
	AICc	271.21	271.6	270.22	271.27
mg Ash DW cm^{-2}		a=87.71	a=81.14	a=101.05	a=95.63
		b=1.25	b=0.84	b=0.6	b=0.82
			c=13.05		c=0.6
	R^2	0.72	0.33	0.73	0.73
	AICc	298.06	351.88	295.84	296.56
µg Chl-a cm^{-2}		a=53.76	a=63.41	a=74.09	a=835.19
		b=29.88	b=4.49	b=9.14	b=0.005
			c=25.77		c=2.7
	R^2	0.31	0.54	0.42	0.51
	AICc	311.1	288.95	300	292.31

Table 2-2. Parameter estimates and coefficients of determination (R^2) for constrained models of light transmission through epiphytes.

		Two-parameter exponential decay	Three-parameter exponential decay	Two-parameter hyperbolic decay	Three-parameter hyperbolic decay
Epiphyte loads	Equation	$y = ae^{-x/b}$	$y = c + ae^{-x/b}$	$y = \frac{a}{1 + x/b}$	$y = a * (1 + c * x/b)^{-1/c}$
mg DW cm^{-2}		a=100	a=84.258	a=100	a=100
		b=2.63	b=1.695	b=1.41	b=1.409
			c=15.746		c=1.007
	R^2	0.73	0.79	0.82	0.82
	AICc	295.58	281.91	271.3	273.45
mg AFDW cm^{-2}		a=100	a=79.73	a=100	a=100
		b=1.45	b=0.693	b=0.725	b=0.52
			c=20.254		c=1.53
	R^2	0.60	0.74	0.79	0.81
	AICc	319.28	295.64	280.81	277.55
mg Ash DW cm^{-2}		a=100	a=85.97	a=100	a=100
		b=1.05	b=0.76	b=0.613	b=0.725
			c=14.08		c=0.69
	R^2	0.69	0.75	0.73	0.73
	AICc	302.49	291.97	295.86	296.83
µg Chl-a cm^{-2}		a=100	a=73.277	a=100	a=100
		b=8.403	b=3.778	b=4.926	b=2.217
			c=26.72		c=2.342
	R^2	0.31	0.53	0.38	0.50
	AICc	337.51	289.887	304.632	293.63

Table 2-3. Candidate models ranked from best to worse based on AICc value, difference values (Δ_i), and Akaike weights (w_i).

Rank	Model	AICc	Δ_i	w_i
1	Uncon_DW_Three-parameter exponential decay	268.68	0.00	2.28E-01
2	Uncon_DW_Two-parameter exponential decay	269.44	0.76	1.56E-01
3	Uncon_DW_Three-parameter hyperbolic decay	269.78	1.10	1.32E-01
4	Uncon_DW_Two-parameter hyperbolic decay	270.12	1.44	1.11E-01
5	Uncon_AFDW_Two-parameter hyperbolic decay	270.22	1.54	1.06E-01
6	Uncon_AFDW_Two-parameter exponential decay	271.21	2.53	6.45E-02
7	Uncon_AFDW_Three-parameter hyperbolic decay	271.27	2.59	6.26E-02
8	Con_DW_Two-parameter hyperbolic decay	271.30	2.62	6.17E-02
9	Uncon_AFDW_Three-parameter exponential decay	271.60	2.92	5.31E-02
10	Con_DW_Three-parameter hyperbolic decay	273.45	4.77	2.10E-02
11	Con_AFDW_Three-parameter hyperbolic decay	277.55	8.87	2.71E-03
12	Con_AFDW_Two-parameter hyperbolic decay	280.81	12.13	5.31E-04
13	Con_DW_Three-parameter exponential decay	281.91	13.23	3.06E-04
14	Uncon_Chl-a_Three-parameter exponential decay	288.95	20.27	9.06E-06
15	Con_Chl-a_Three-parameter exponential decay	289.89	21.21	5.67E-06
16	Con_Ash DW_Three-parameter exponential decay	291.97	23.29	2.00E-06
17	Uncon_Chl-a_Three-parameter hyperbolic decay	292.31	23.63	1.69E-06
18	Con_Chl-a_Three-parameter hyperbolic decay	293.63	24.95	8.73E-07
19	Con_DW_Two-parameter exponential decay	295.58	26.90	3.29E-07
20	Con_AFDW_Three-parameter exponential decay	295.64	26.96	3.20E-07
21	Uncon_Ash DW_Two-parameter hyperbolic decay	295.84	27.16	2.89E-07
22	Con_Ash DW_Two-parameter hyperbolic decay	295.86	27.18	2.86E-07
23	Uncon_Ash DW_Three-parameter hyperbolic decay	296.56	27.88	2.02E-07
24	Con_Ash DW_Three-parameter hyperbolic decay	296.83	28.15	1.76E-07
25	Uncon_Ash DW_Two-parameter exponential decay	298.06	29.38	9.53E-08
26	Uncon_Chl-a_Two-parameter hyperbolic decay	300.00	31.32	3.61E-08
27	Con_Ash DW_Two-parameter exponential decay	302.49	33.81	1.04E-08
28	Con_Chl-a_Two-parameter hyperbolic decay	304.63	35.95	3.56E-09
29	Uncon_Chl-a_Two-parameter exponential decay	311.10	42.42	1.40E-10
30	Con_AFDW_Two-parameter exponential decay	319.28	50.60	2.35E-12
31	Con_Chl-a_Two-parameter exponential decay	337.51	68.83	2.59E-16
32	Uncon_Ash DW_Three-parameter exponential decay	351.88	83.20	1.96E-19

Table 2-4. Comparison of models and key parameters relating light transmission to loads of epiphytes in this and previous studies.

Author (Year)	Equation	Epiphytic loads (mg DW cm^{-2} of leaf) at 50% light transmission	Asymptote % of incident light
Present study	Two-parameter exponential	1.69	10%
Brush and Nixon (2002)	Three-parameter hyperbolic	3.61	15%
	Three-parameter hyperbolic	22.12	30%
Frankovich and Zieman(2005)	Three-parameter hyperbolic	2.59	18%
	Two-parameter exponential	4.36	10%
	Two-parameter hyperbolic	4.27	15%
Silberstein et al. (1986)	Three-parameter exponential	3.47	10%
Burt et al. (1995)	Two-parameter exponential	1.80	20%
Stankelis et al. (2003)	Three-parameter exponential	1.50	0%
Van-Dijk(1993)	Two-parameter hyperbolic	1.06	0%

Table 2-5. Comparison of methods in this and previous studies.

		Sample processing		Method of measurement			
Author (year)	Study area	One/Two layers	Suspend/not	Light	Leaf	Method	Epiphytes
Present study	Florida Chassahowitzka Spring Freshwater	one	underwater	natural	natural	directly	*Chaetomorpha sp.*
Brush and Nixon (2002)	Rhode Island Mesocosms Marine	one	underwater	natural	natural	directly	*Ulothrix sp., Cladophora sp., Polysiphonia sp.*
Frankovich and Zieman (2005)	Florida Bay and Florida Key Marine	one & two	underwater	artificial	artificial	directly	calcium carbonate sediment & corallines, *Polysiphonia sp.*
Burt et al. (1995)	Australia Success Bank Marine	two	underwater	artificial	artificial	directly	Rhodophyta, Phaeophyta, Cyanophyta and some coralline algae
Silberstein et al. (1986)	Australia Cockurn Sound Marine	two	underwater	artificial	artificial	directly	combination of filamentous algae and coralline communities
Stankelis et al. (2003)	Maryland Patuxent estuary Mesohaline	two	underwater	artificial	artificial	directly	diatoms
Van-Dijk (1993)	Lake Veluwe Freshwater	one	underwater	artificial	artificial	directly	diatoms and green algae
Cebrian et al. (1999)	Spanish Cala Jonquet Marine	one	dry	artificial	artificial	indirectly	red encrusting algae, brown erect algae, bryozoa and hydrozoa

Figure 2-1. Location of the sampling area (Latitude 28°43’8”, Longitude 82°35’32”) and head springs in the Chassahowitzka River, Citrus County, Florida. The sampling area is a large continuous *Vallisneria americana* meadow (bright green area) that covers approximately 2700 m^2 and is located about 1.8 km west of the head springs. Reprinted with permission from Google Earth, https://www.google.com/earth/ (November 18, 2017).

A B C

Figure 2-2. Apparatus used to measure attenuation of natural photosynthetically active radiation (PAR) by epiphytes. A) A LI-1400 datalogger. B) Two, 2-π underwater quantum sensors (LI-COR UWQ5754 and LI-COR UWQ 5692). C) The apparatus was submerged in an outdoor tank filled with freshwater. Photos courtesy of author.

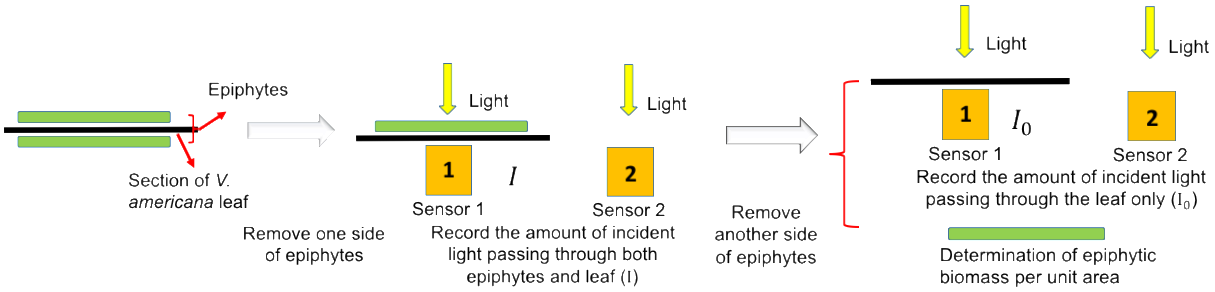

Figure 2-3. Schematic representation of measuring the effect of epiphytes on light penetration. Before measuring, one side of each leaf section was scraped to remove epiphytes. Each scraped section was placed on an underwater sensor (No. 1). When the uncovered sensor (No. 2) indicated that incident irradiance was stable, irradiation passing through both the blade section and attached epiphytes was recorded. Next, the epiphytes on the other side of each section were removed and saved for determination of epiphytic load per unit area. The resulting clean sections were placed over the appropriate underwater sensor, and light passing through the blade was measured.

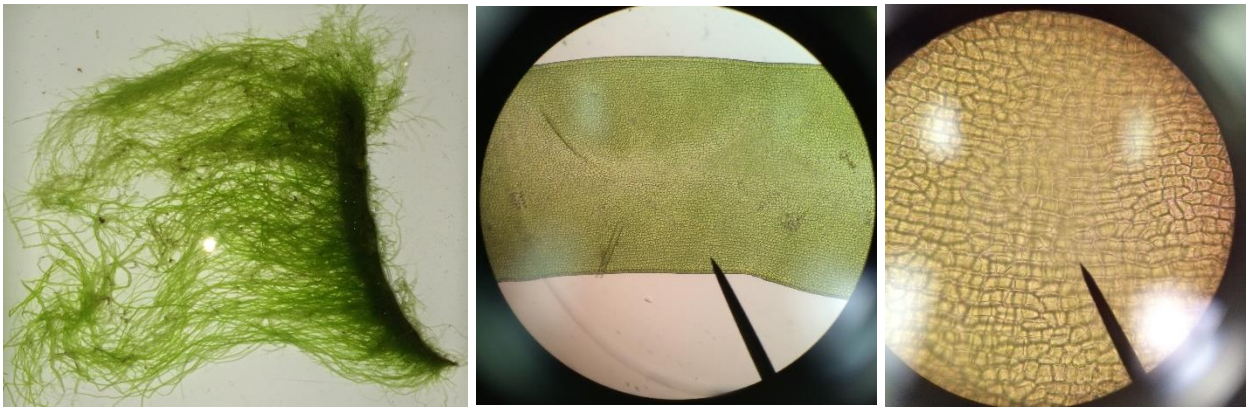

A B C

Figure 2-4. The dominant green filamentous macroalgae *Enteromorpha* sp. in my study site. A) Characteristic distribution of *Enteromorpha* sp. B) *Enteromorpha* sp. branching filament at 100x magnification. C) *Enteromorpha* sp. branching filament at 400x magnification. Photos courtesy of author.

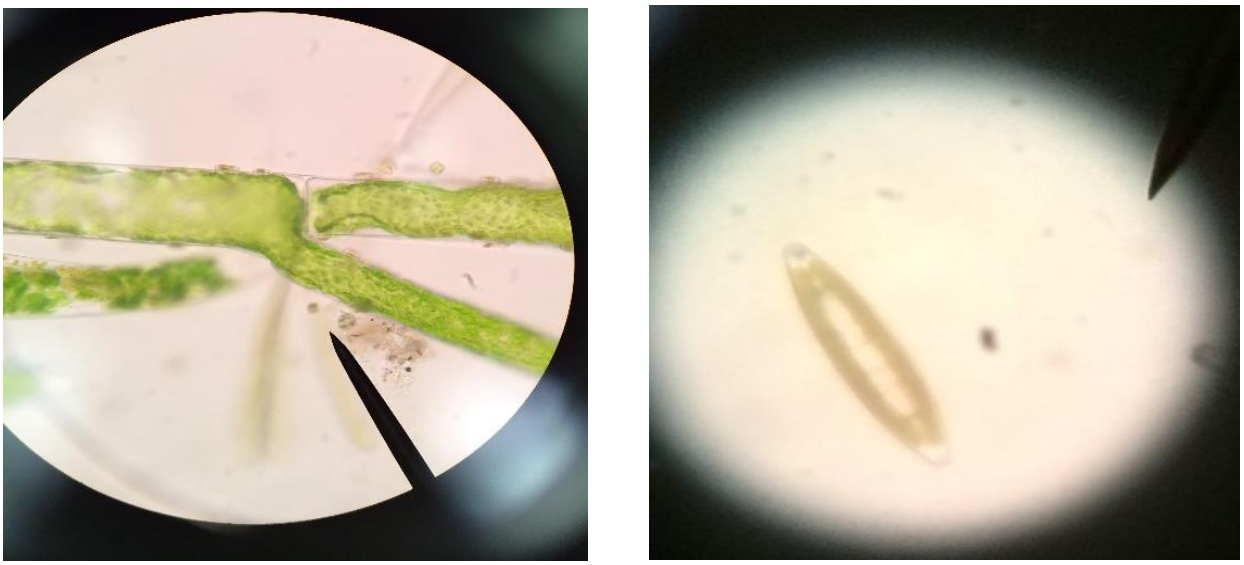

A B

Figure 2-5. Other epiphytes in my study site. A) *Cladophora* sp. branching filament at 400x magnification. B) Ubiquitous diatoms at 400x magnification. Photos courtesy of author.

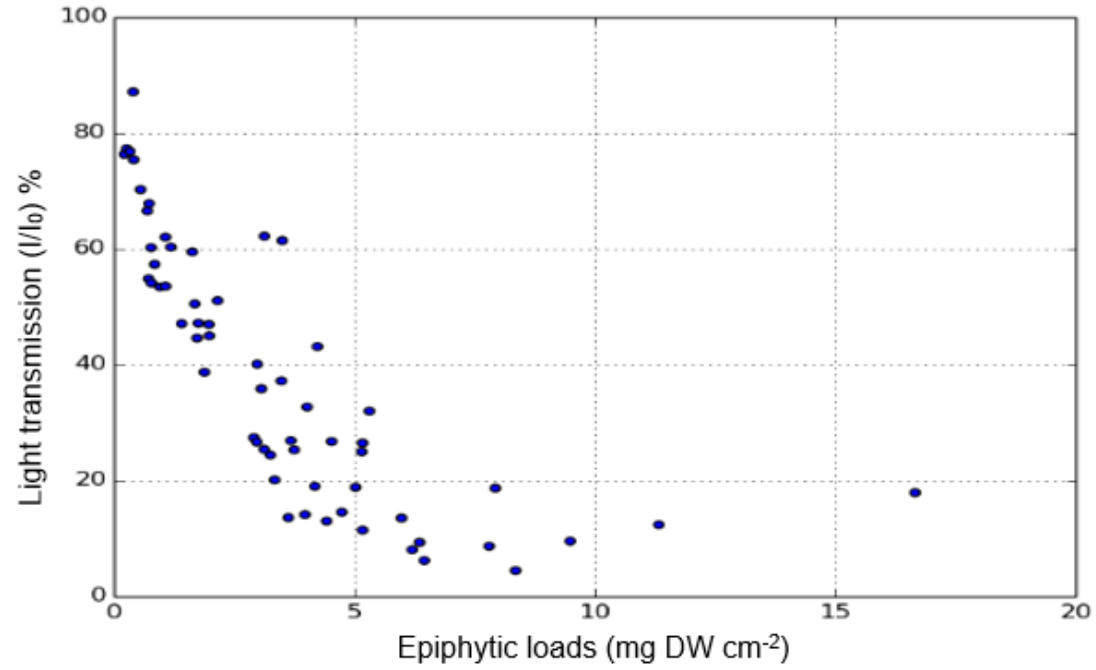

A

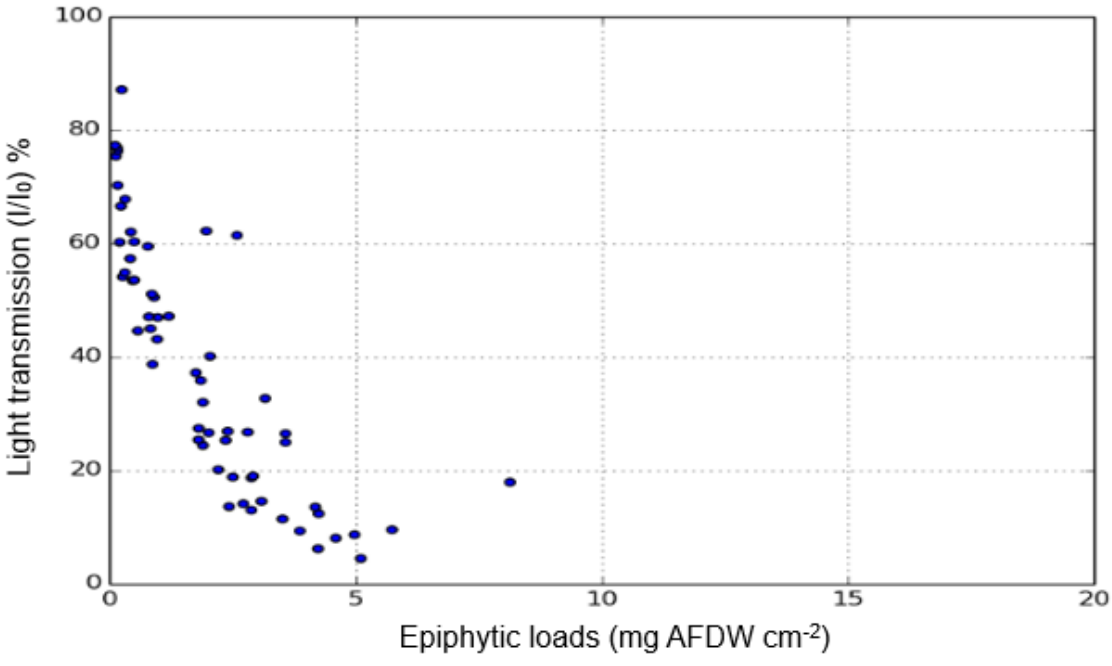

B

Figure 2-6. Scatter plots showing the relationships between epiphytic loads and light transmission. Light transmission (I) expressed as percentage of incident irradiance (I_0). A) Epiphytic loads expressed as mg dry weight cm^{-2} of leaf (mg DW cm^{-2}). B) Epiphytic loads expressed as mg ash free dry weight cm^{-2} of leaf (mg AFDW cm^{-2}). C) Epiphytic loads expressed as mg ash dry weight cm^{-2} of leaf (mg ash DW cm^{-2}). D) Epiphytic loads expressed as µg Chlorophyll-a cm^{-2} of leaf.

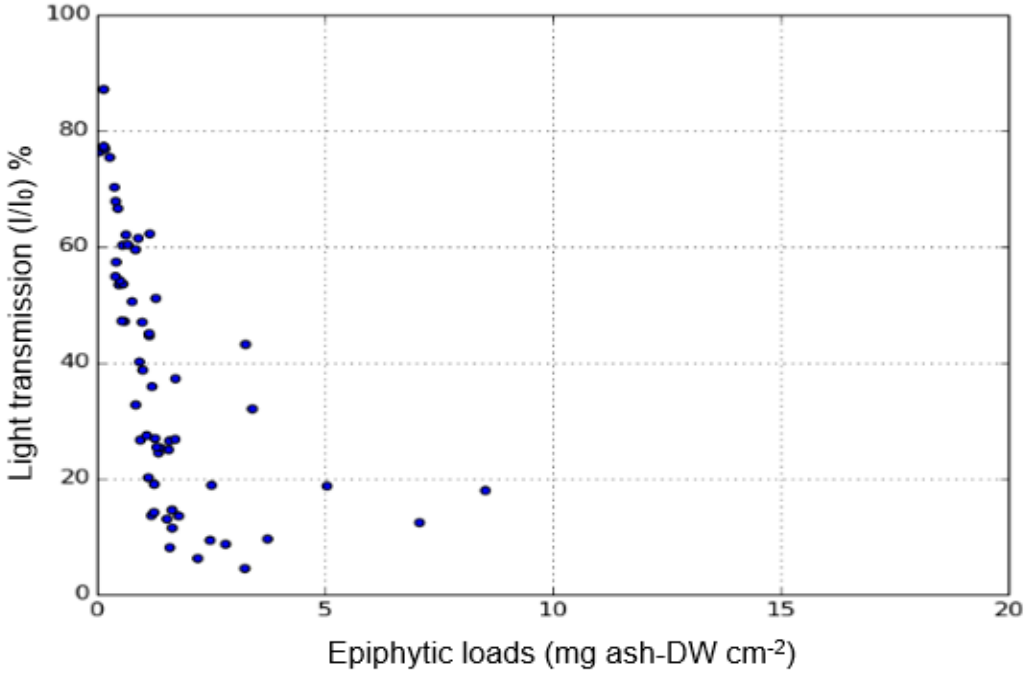

C

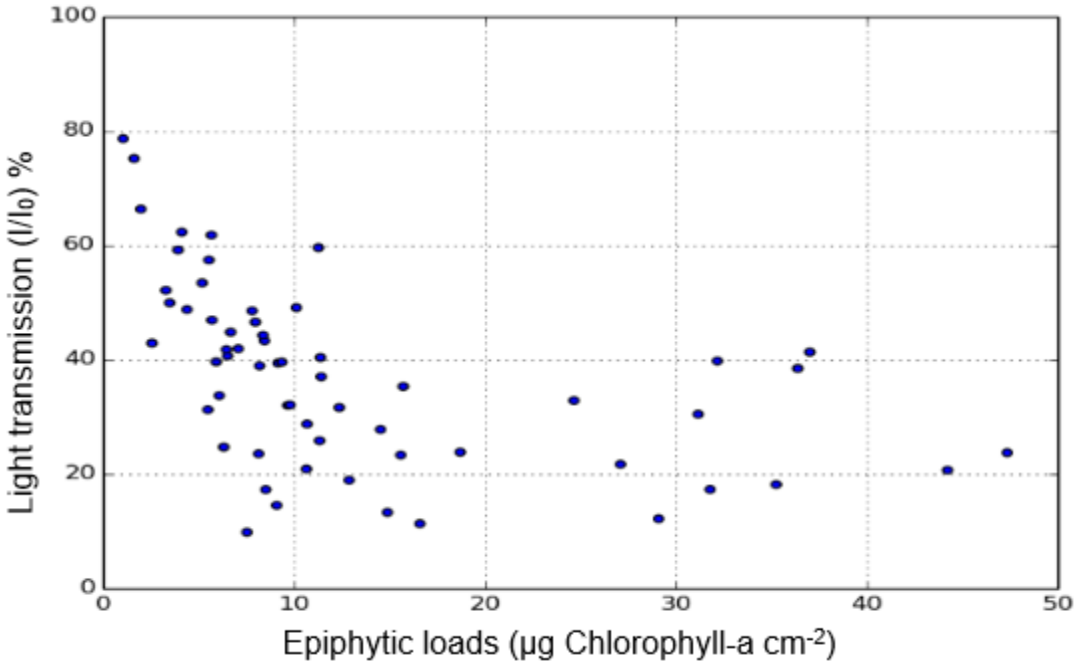

D

Figure 2-6. Continued.

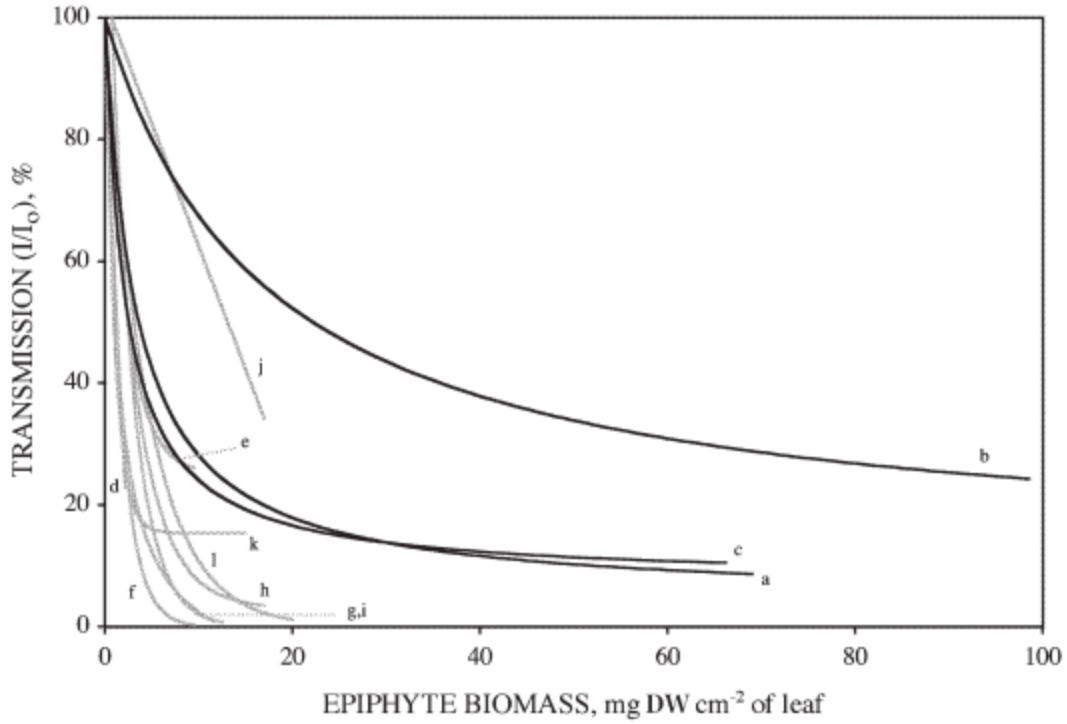

Figure 2-7. Comparison of relationships between epiphytic loads, as mg dry weight cm^{-2} of leaf, and light transmission, in previous studies. Reproduced with permission from Brush and Nixon (2002).

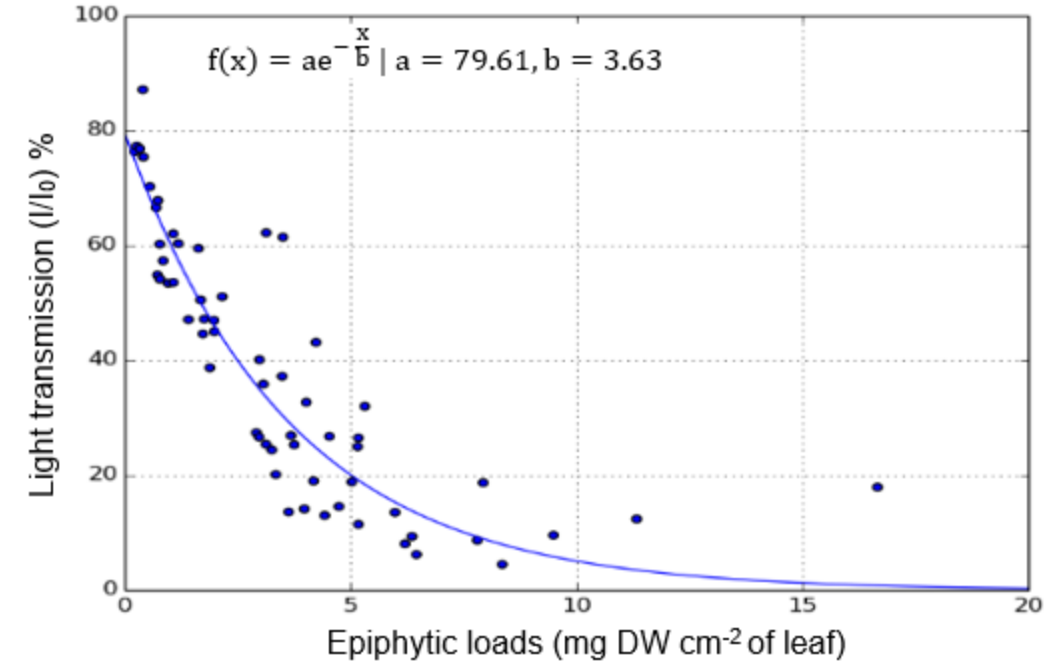

A

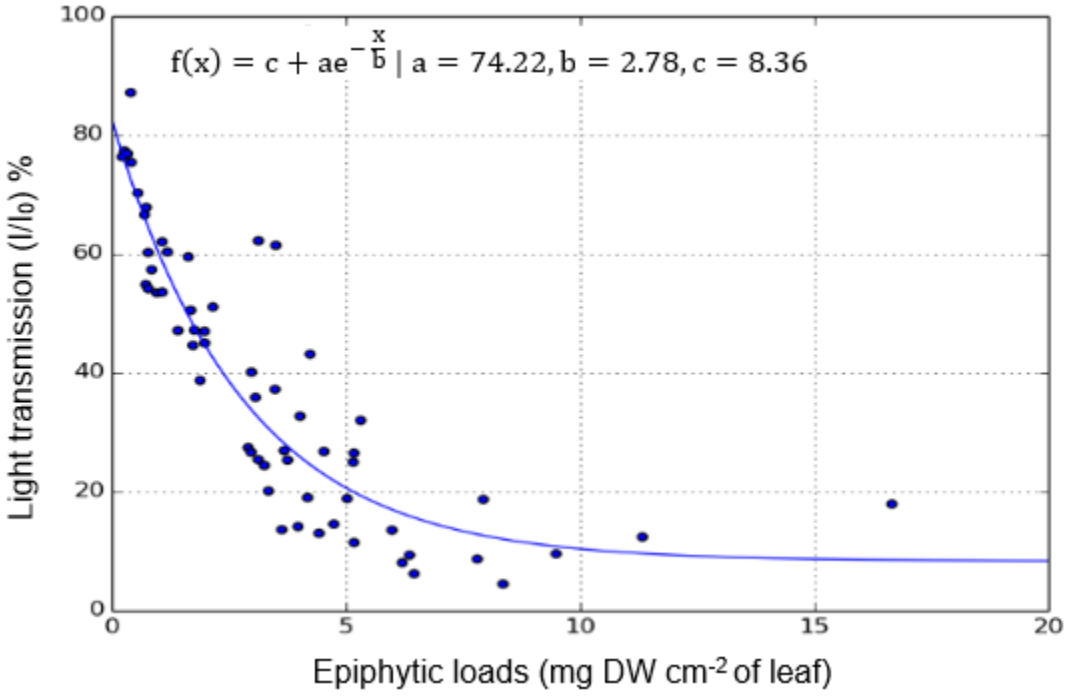

B

Figure 2-8. Decay equations fit to the relationships between total epiphytic loads (mg dry weight cm^{-2} of leaf) and light transmission. A) Two-parameter exponential equation. B) Three-parameter exponential equation. C) Two-parameter hyperbolic equation. D) Three-parameter hyperbolic equation. Parameter estimates for regression equations are listed.

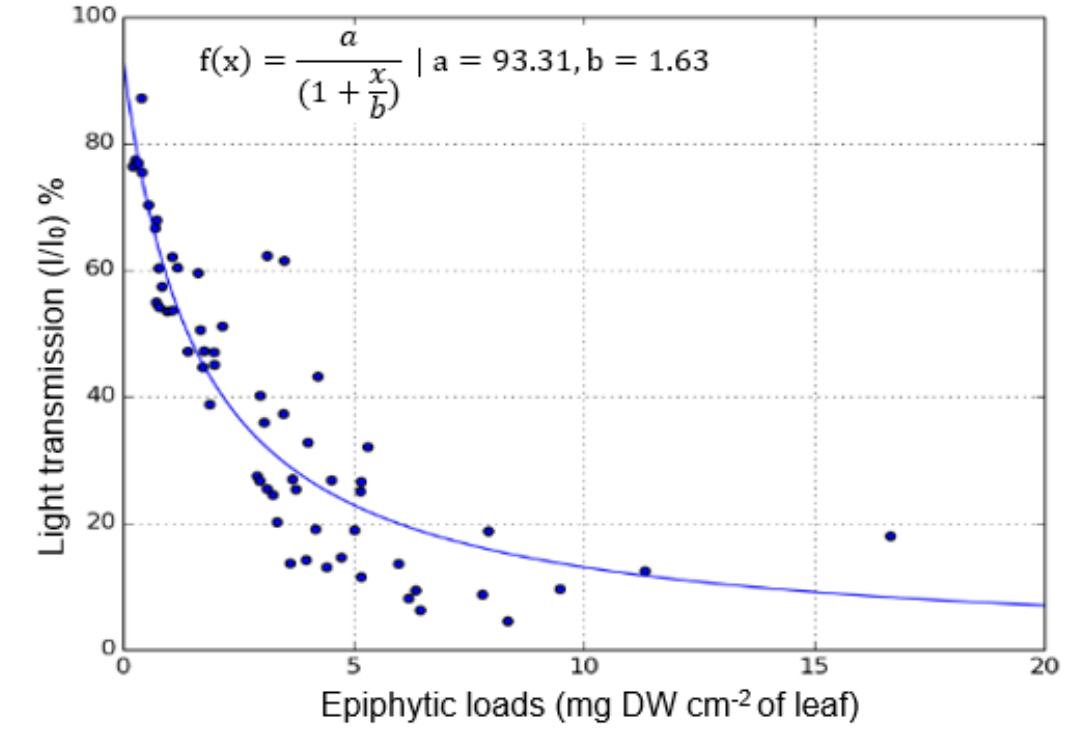

C

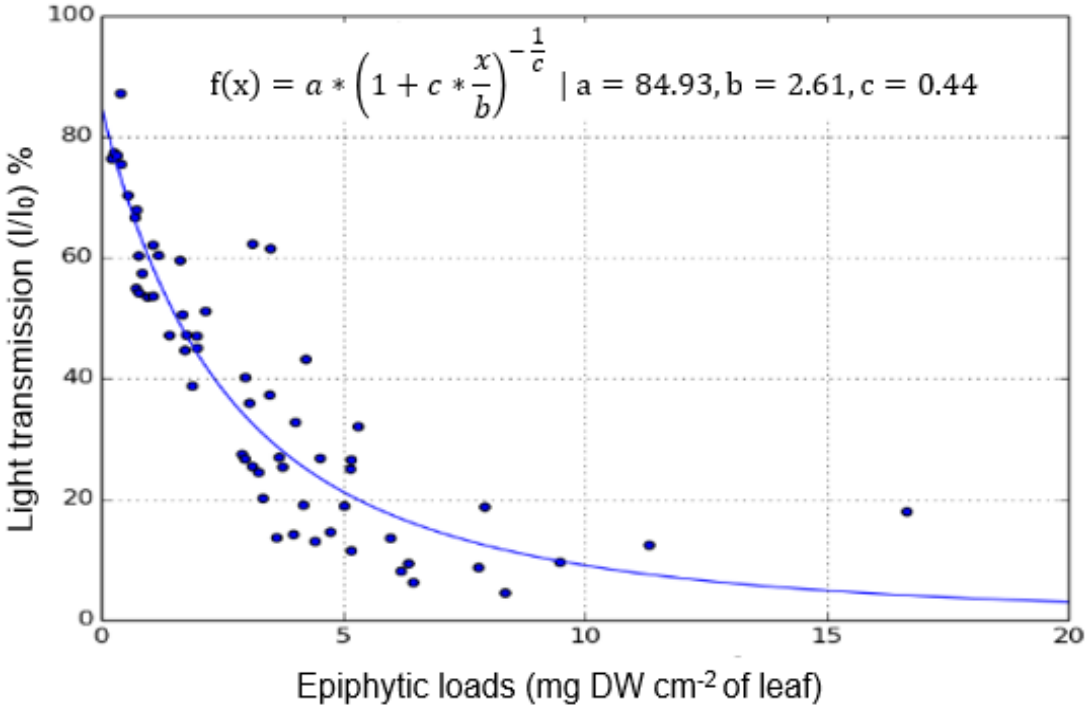

D

Figure 2-8. Continued.

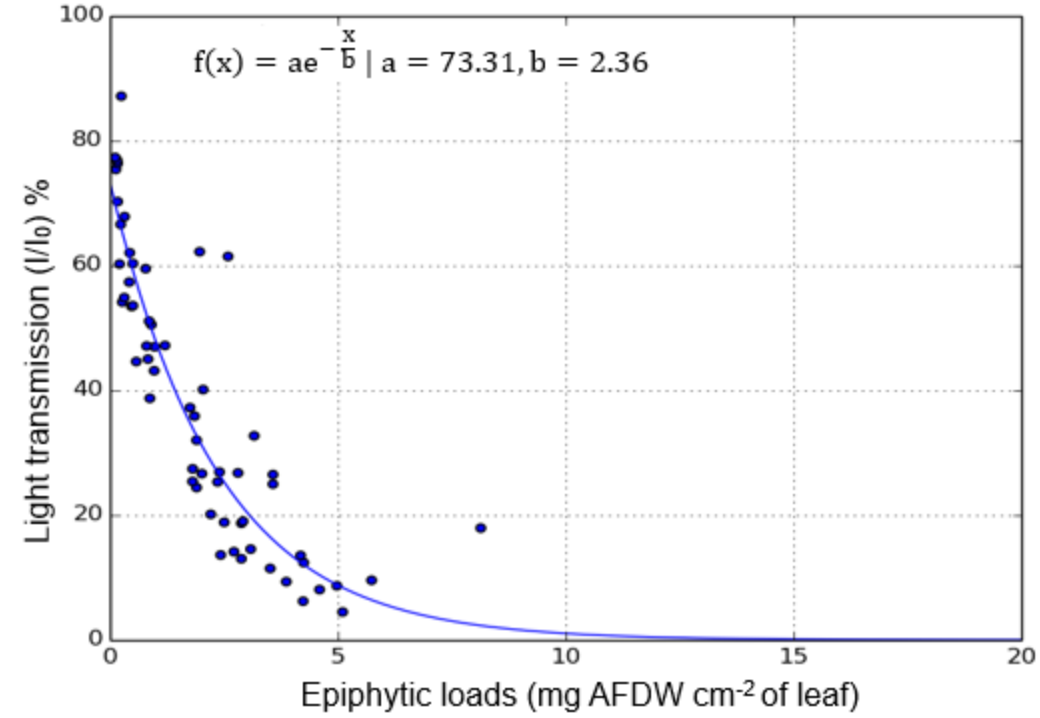

A

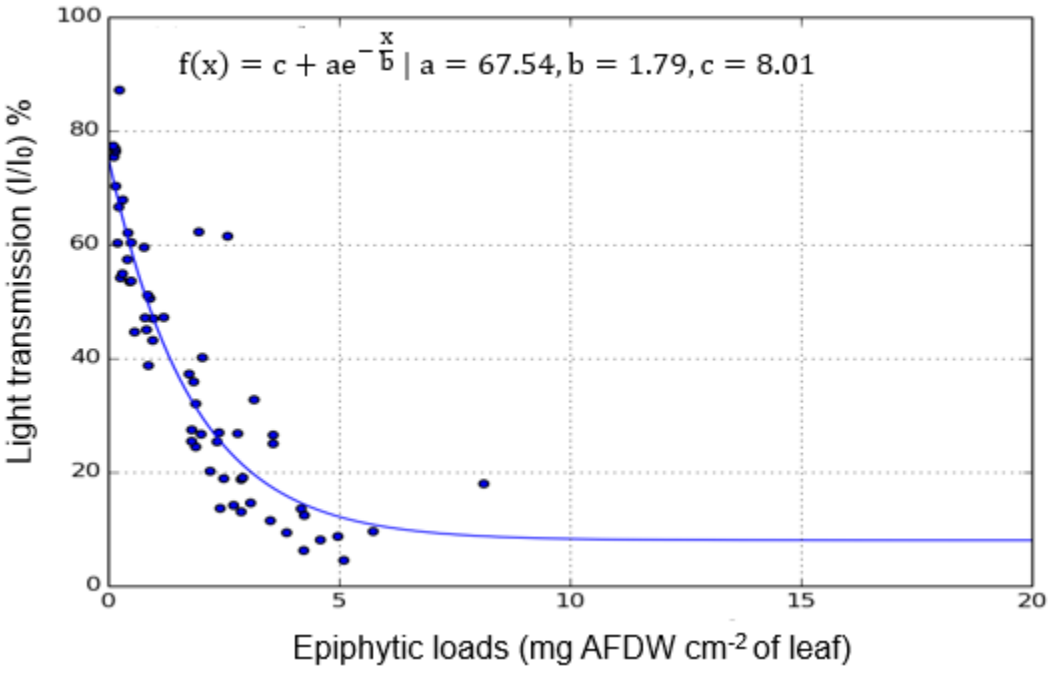

B

Figure 2-9. Decay equations fit to the relationships between total epiphytic loads (mg ash-free dry weight cm^{-2} of leaf) and light transmission. A) Two-parameter exponential equation. B) Three-parameter exponential equation. C) Two-parameter hyperbolic equation. D) Three-parameter hyperbolic equation. Parameter estimates for regression equations are listed.

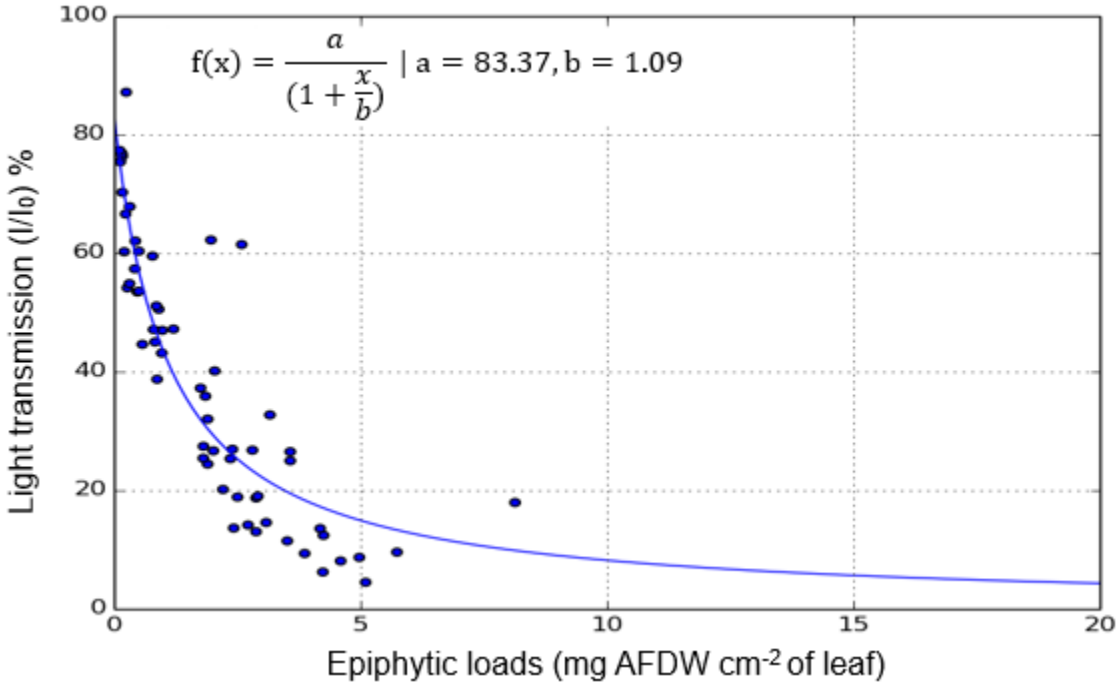

C

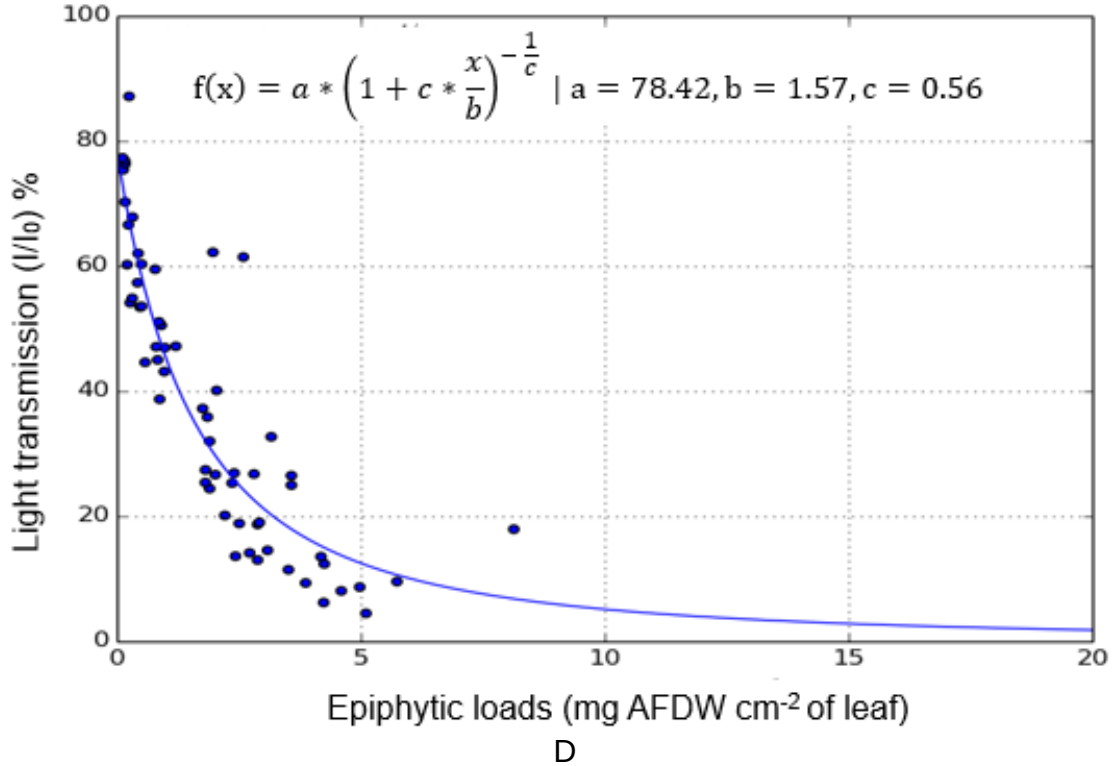

D

Figure 2-9. Continued.

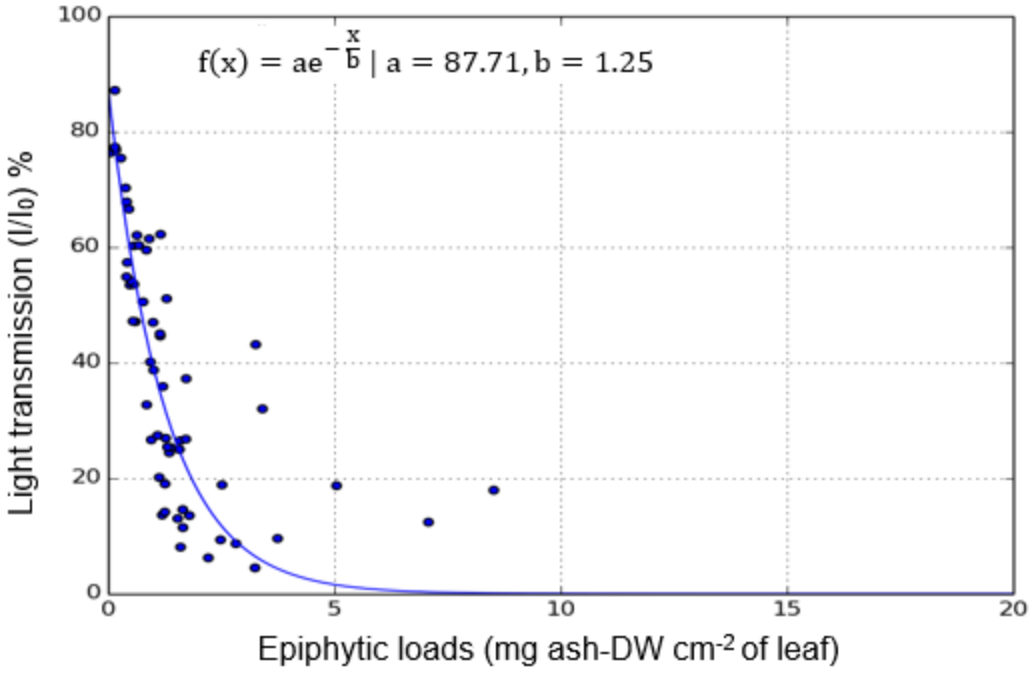

A

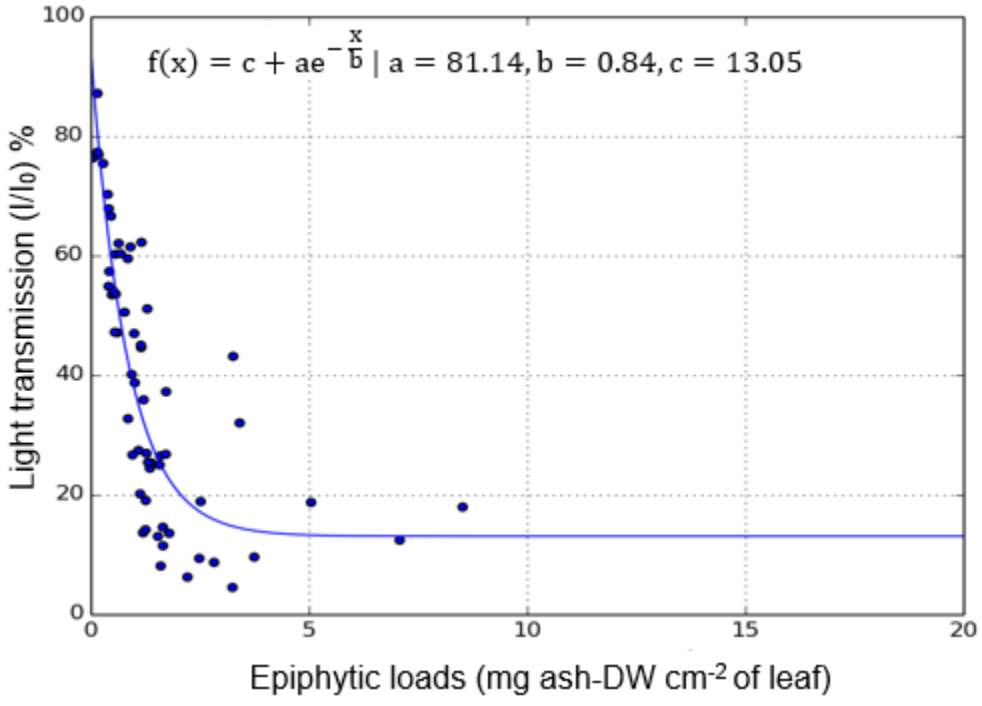

B

Figure 2-10. Decay equations fit to the relationships between total epiphytic loads (mg ash dry weight cm^{-2} of leaf) and light transmission. A) Two-parameter exponential equation. B) Three-parameter exponential equation. C) Two-parameter hyperbolic equation. D) Three-parameter hyperbolic equation. Parameter estimates for regression equations are listed.

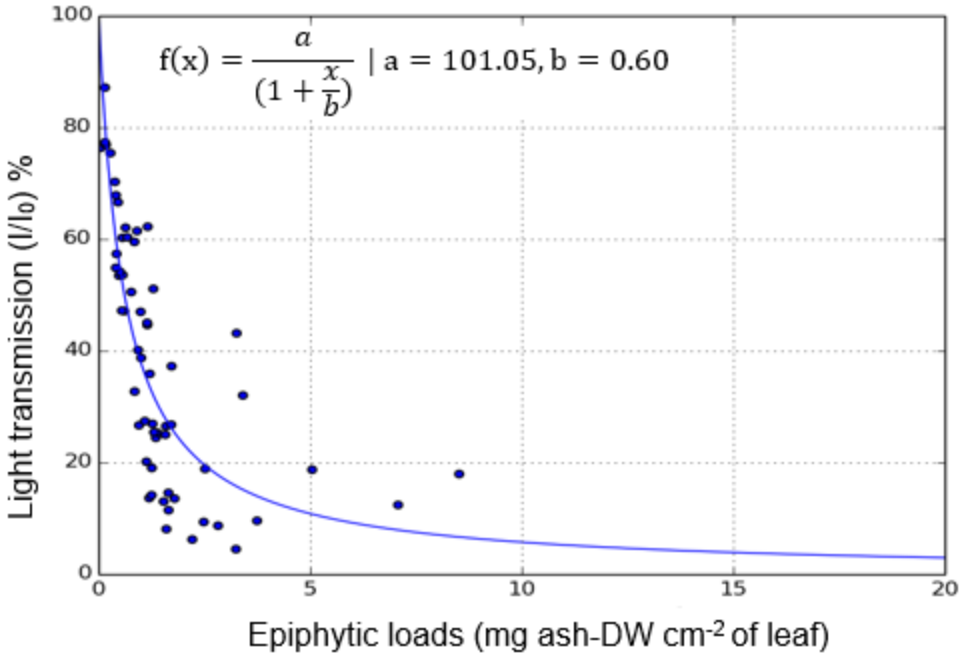

C

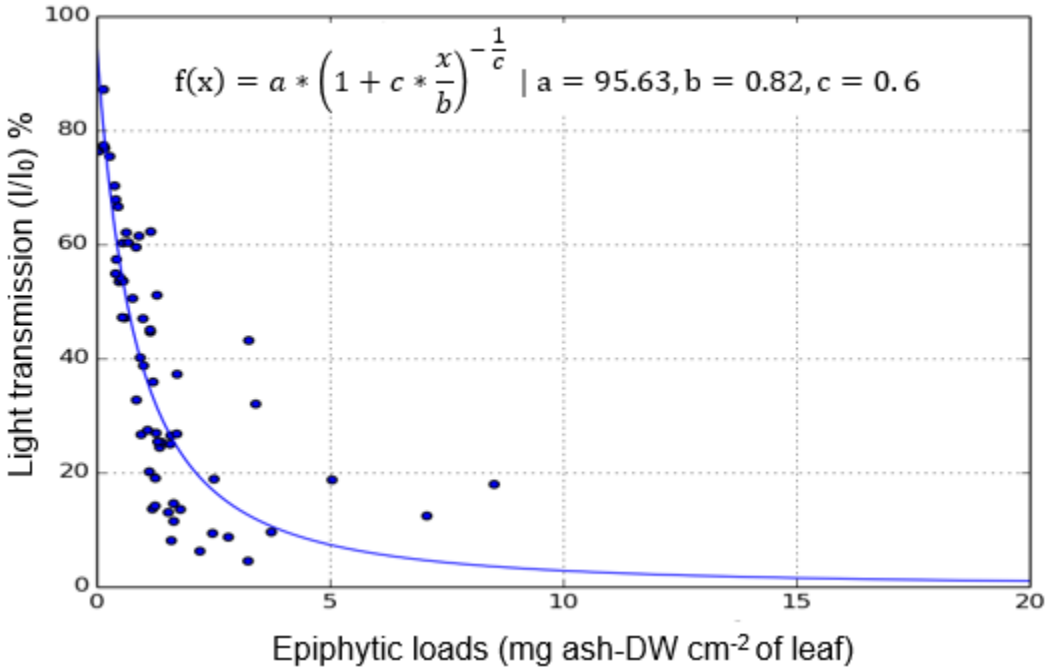

D

Figure 2-10. Countinued.

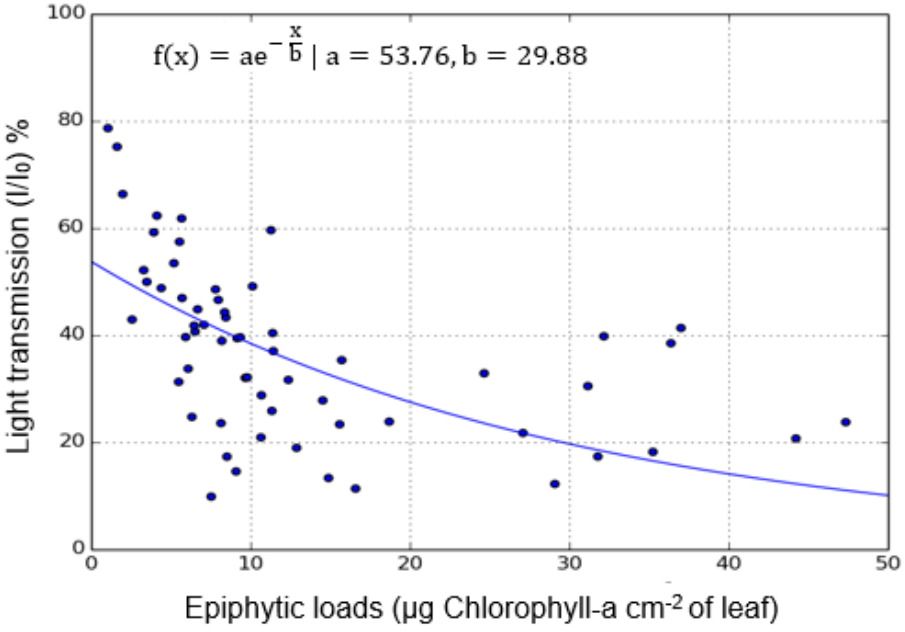

A

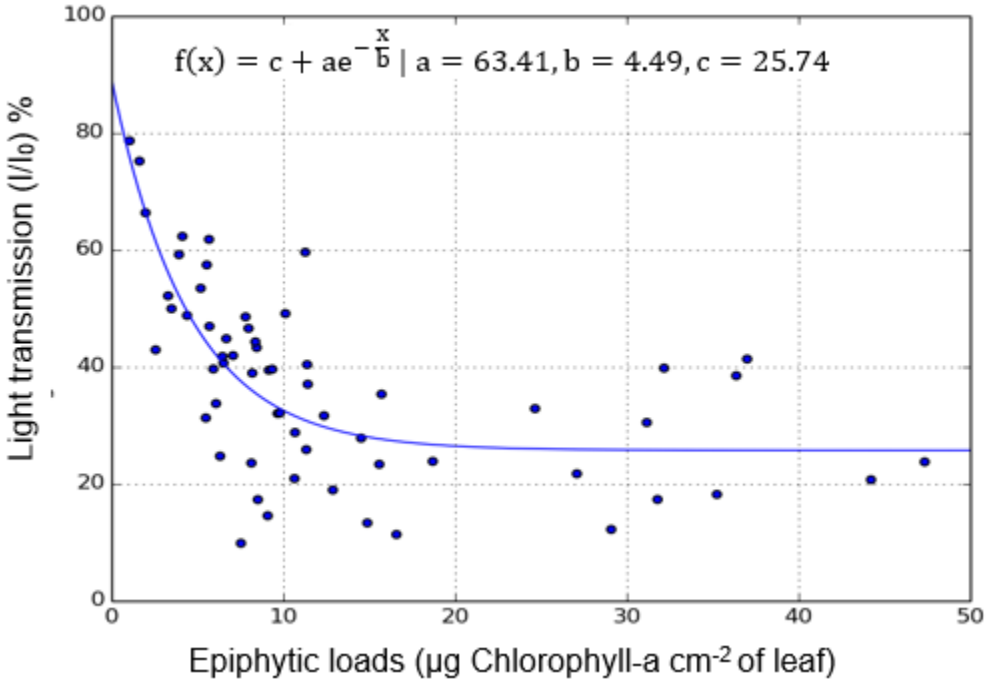

B

Figure 2-11. Decay equations fit to the relationships between total epiphytic loads (µg chlorophyll-a cm^{-2} of leaf) and light transmission. A) Two-parameter exponential equation. B) Three-parameter exponential equation. C) Two-parameter hyperbolic equation. D) Three-parameter hyperbolic equation. Parameter estimates for regression equations are listed.

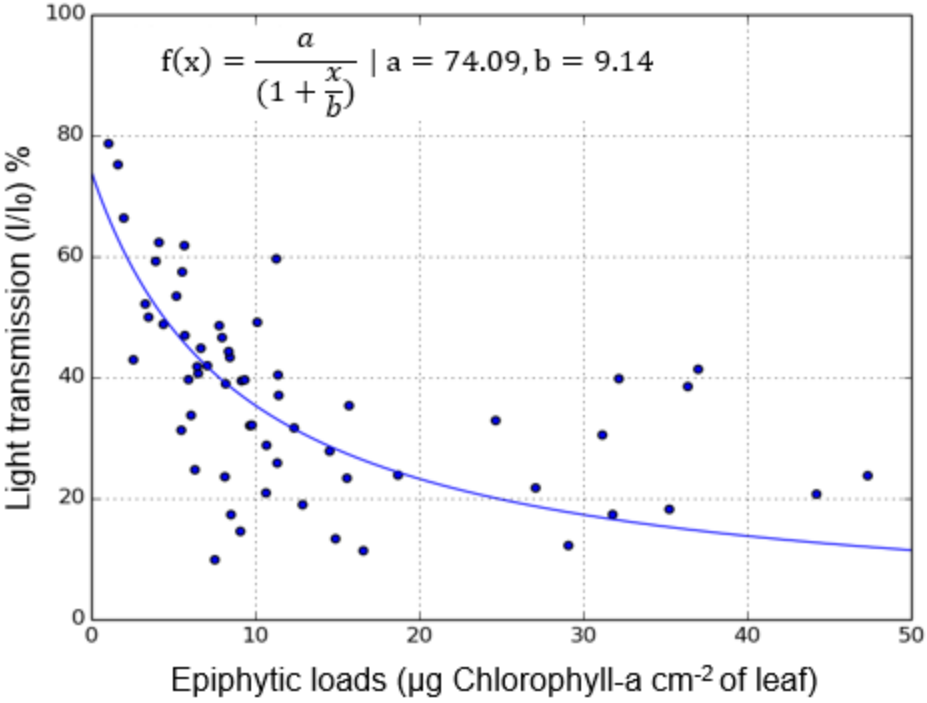

C

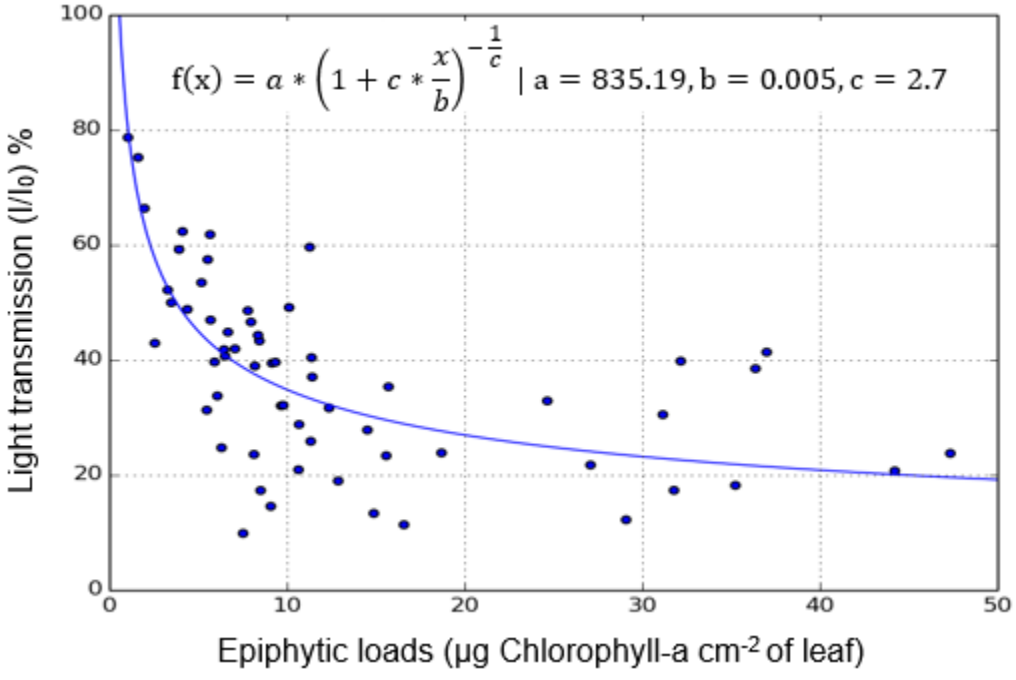

D

Figure 2-11. Continued.

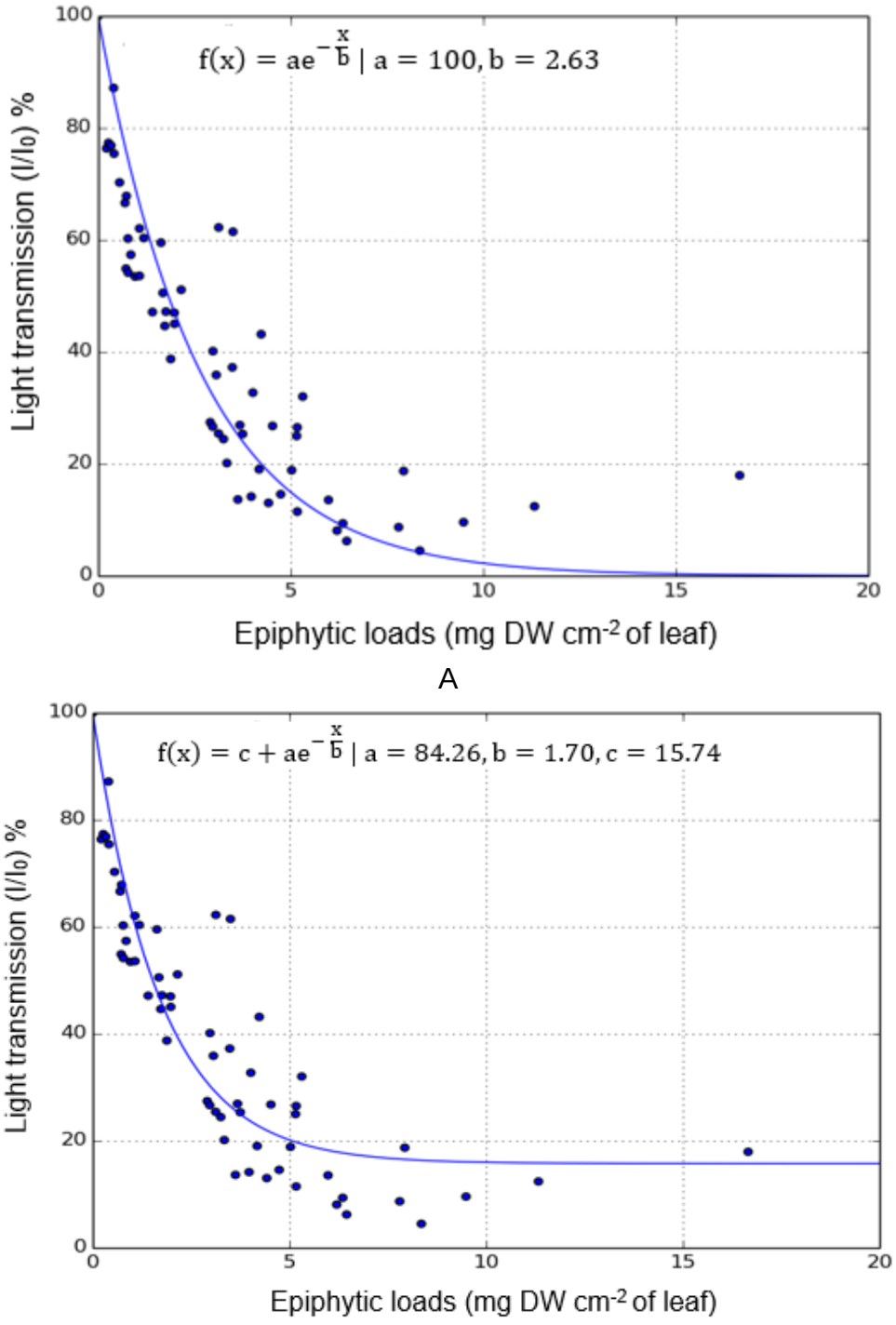

Figure 2-12. Decay equations fit to the relationships between total epiphytic loads (mg dry weight cm^{-2} of leaf) and light transmission that have been constrained to pass through 100% light transmission at epiphytic loads of zero. A) Two-parameter exponential equation. B) Three-parameter exponential equation. C) Two-parameter hyperbolic equation. D) Three-parameter hyperbolic equation. Parameter estimates for regression equations are listed.

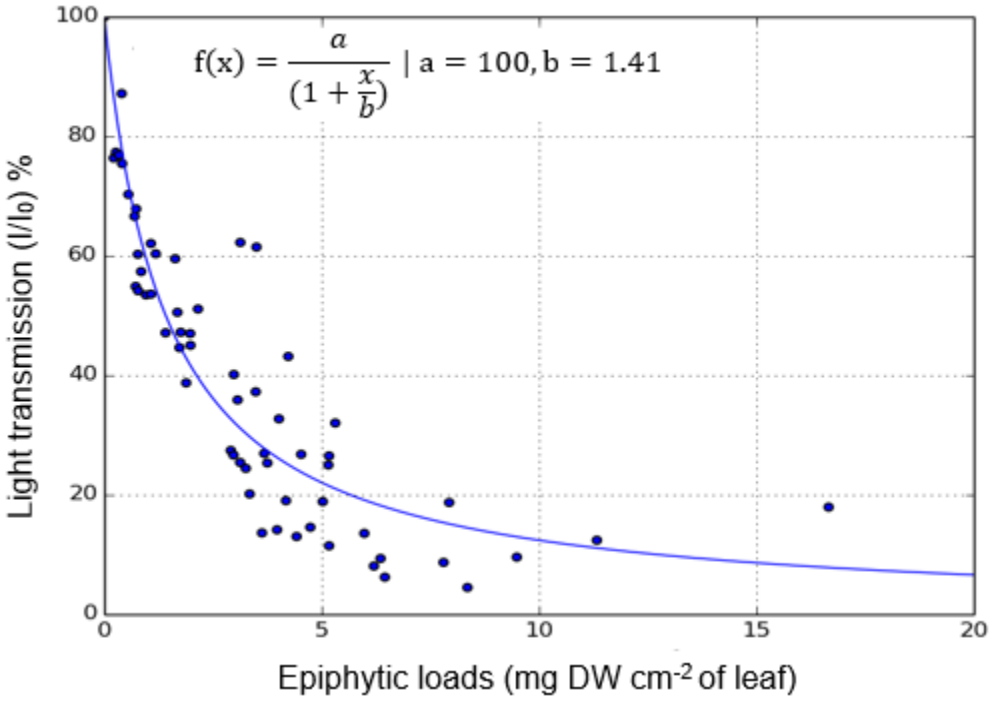

C

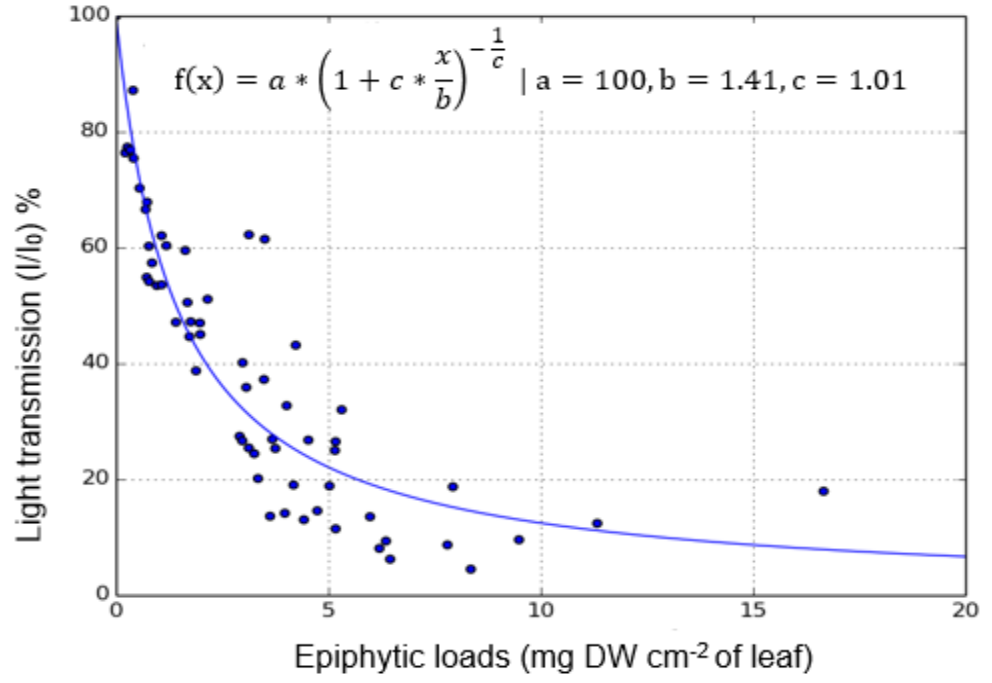

D

Figure 2-12. Continued.

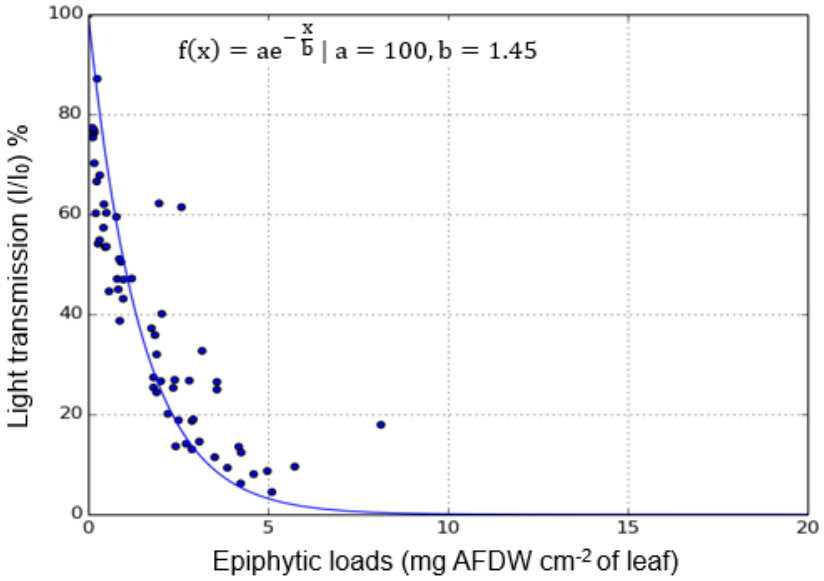

A

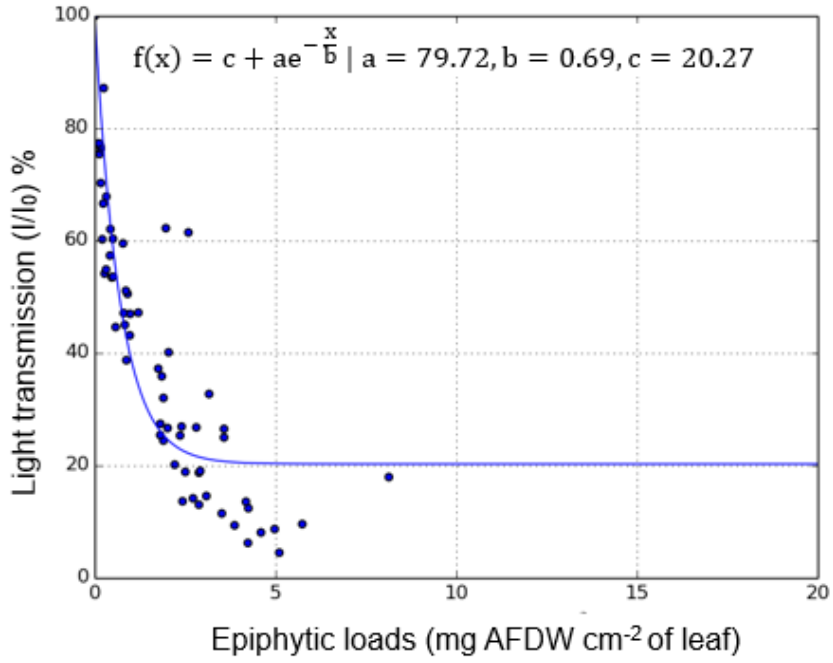

B

Figure 2-13. Decay equations fit to the relationships between total epiphytic loads (mg ash-free dry weight cm^{-2} of leaf) and light transmission that have been constrained to pass through 100% light transmission at epiphytic loads of zero. A) Two-parameter exponential equation. B) Three-parameter exponential equation. C) Two-parameter hyperbolic equation. D) Three-parameter hyperbolic equation. Parameter estimates for regression equations are listed.

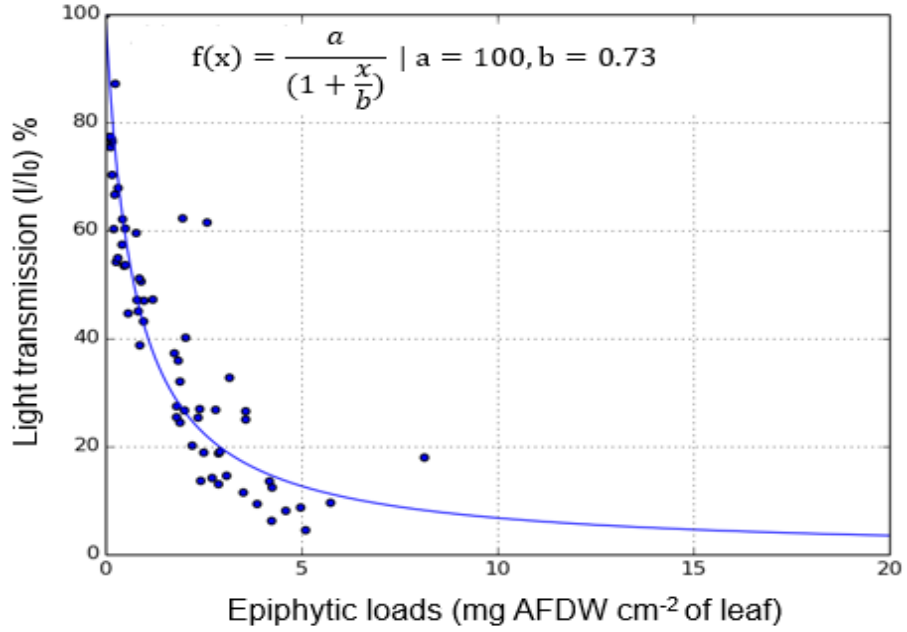

C

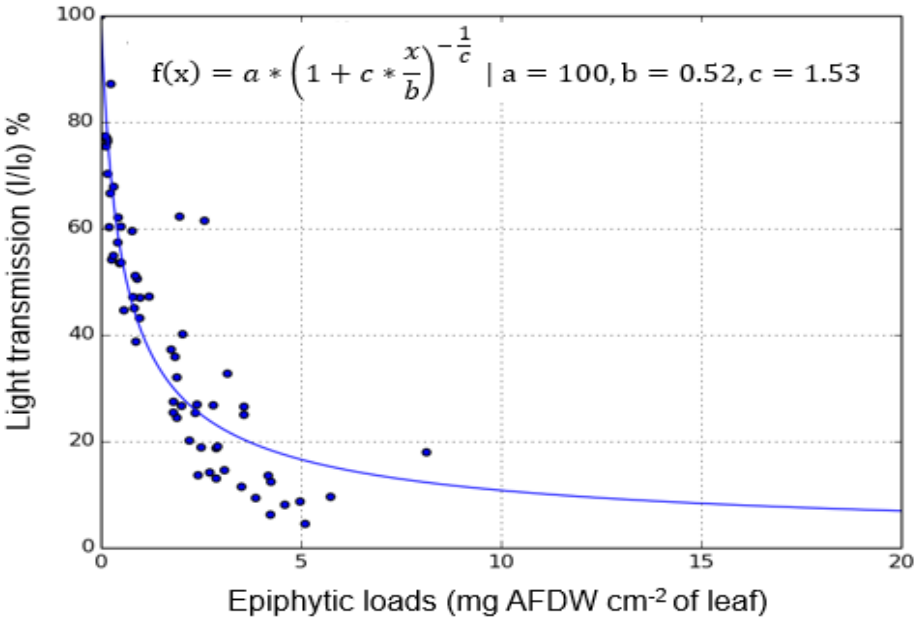

D

Figure 2-13. Continued.

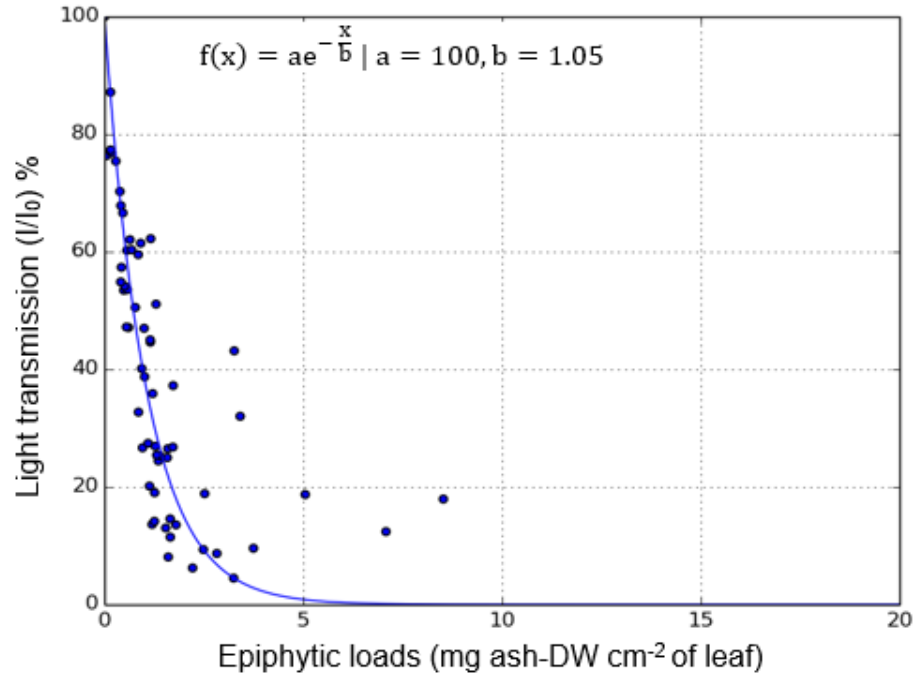

A

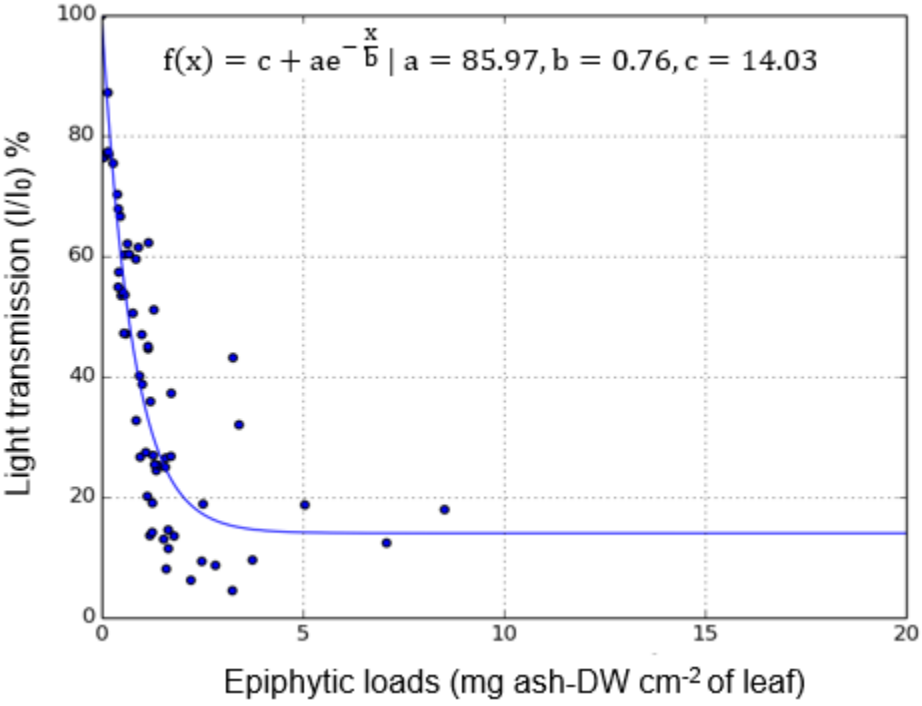

B

Figure 2-14. Decay equations fit to the relationships between total epiphytic loads (mg ash dry weight cm^{-2} of leaf) and light transmission that have been constrained to pass through 100% light transmission at epiphytic loads of zero. A) Two-parameter exponential equation. B) Three-parameter exponential equation. C) Two-parameter hyperbolic equation. D) Three-parameter hyperbolic equation. Parameter estimates for regression equations are listed.

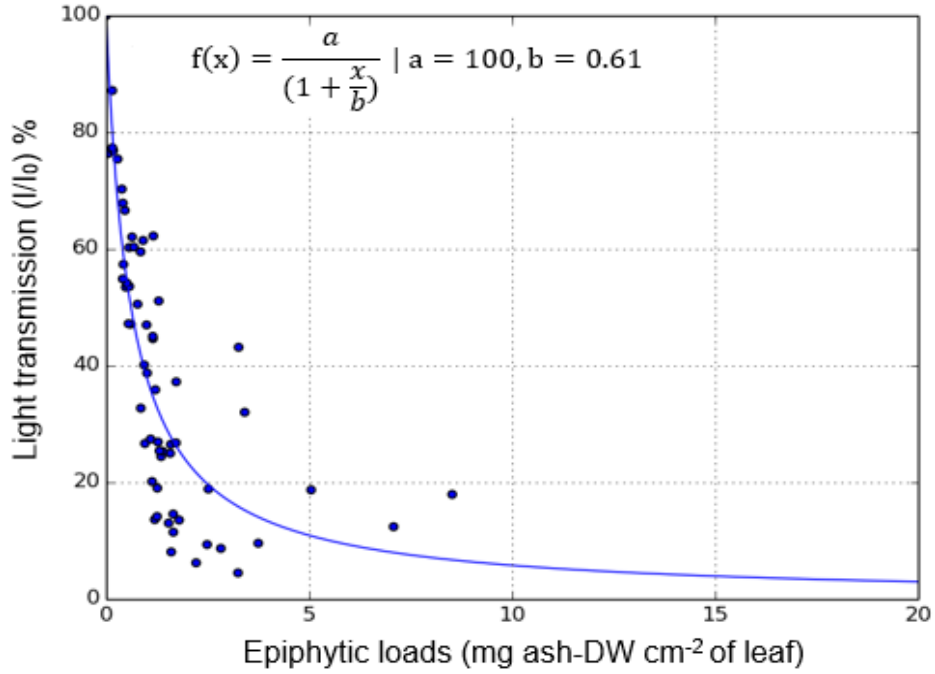

C

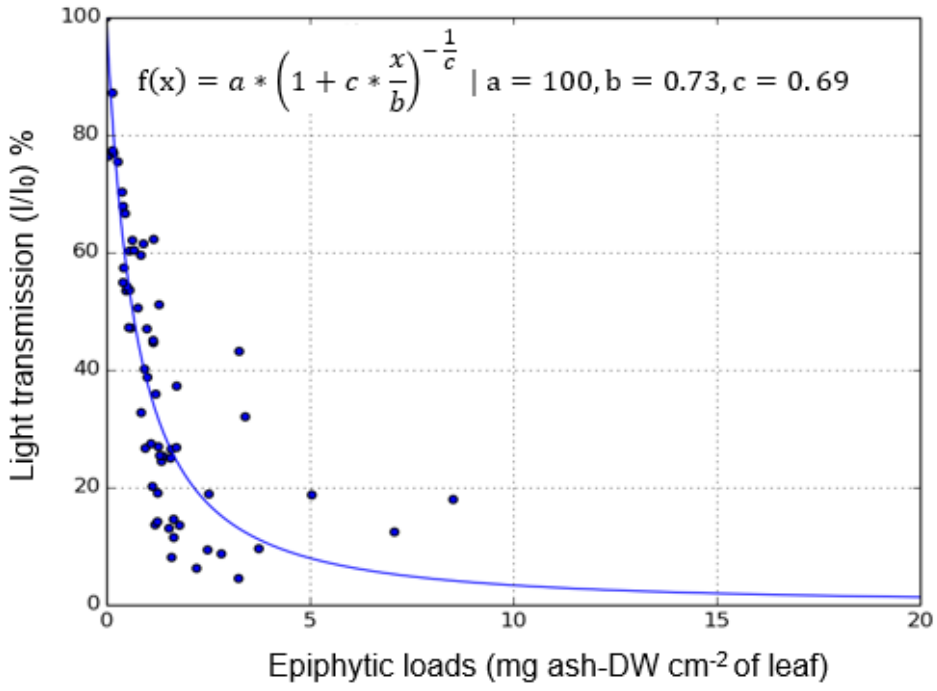

D

Figure 2-14. Continued.

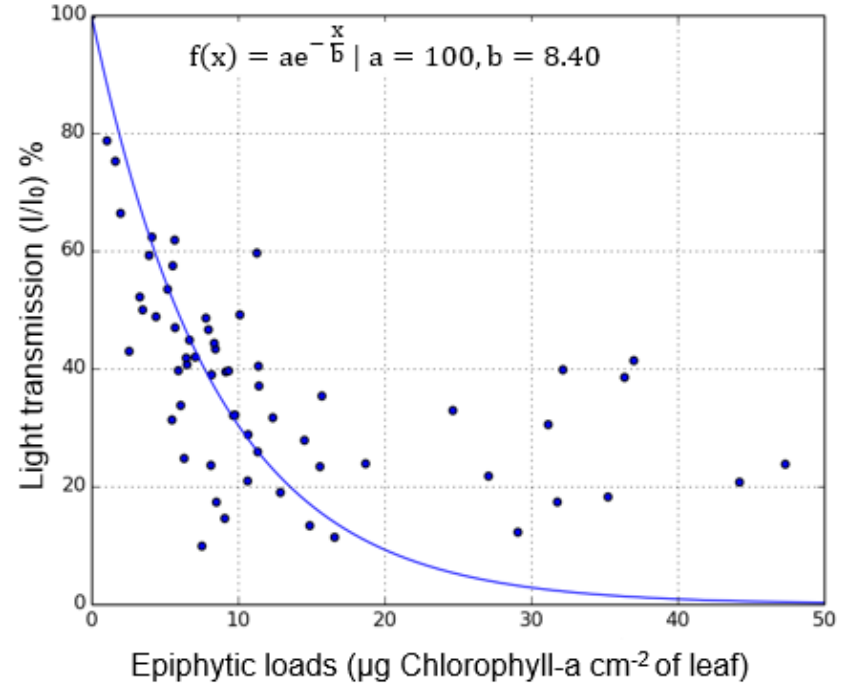

A

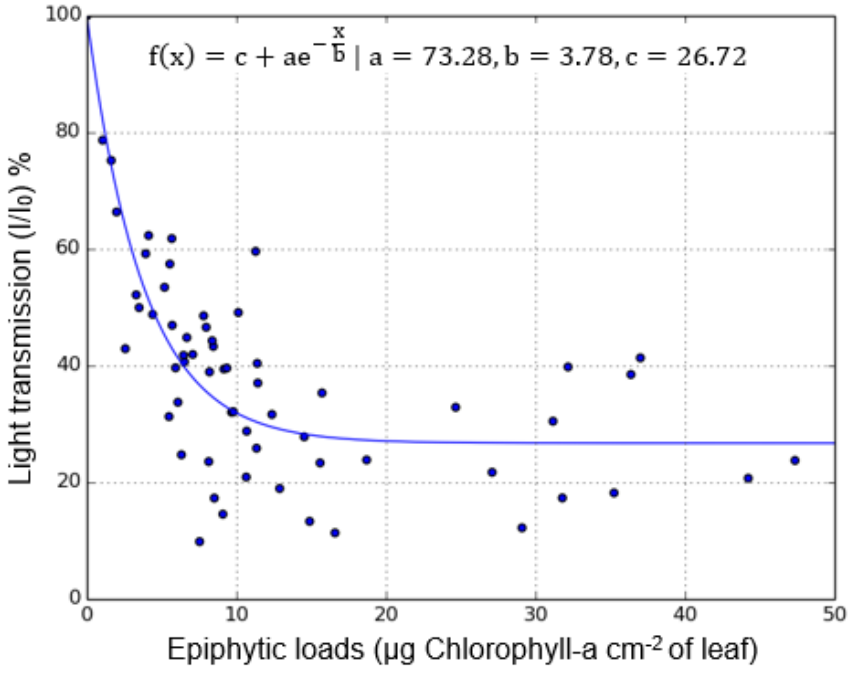

B

Figure 2-15. Decay equations fit to the relationships between total epiphytic loads (µg chlorophyll-a cm^{-2} of leaf) and light transmission that have been constrained to pass through 100% light transmission at epiphytic loads of zero. A) Two-parameter exponential equation. B) Three-parameter exponential equation. C) Two-parameter hyperbolic equation. D) Three-parameter hyperbolic equation. Parameter estimates for regression equations are listed.

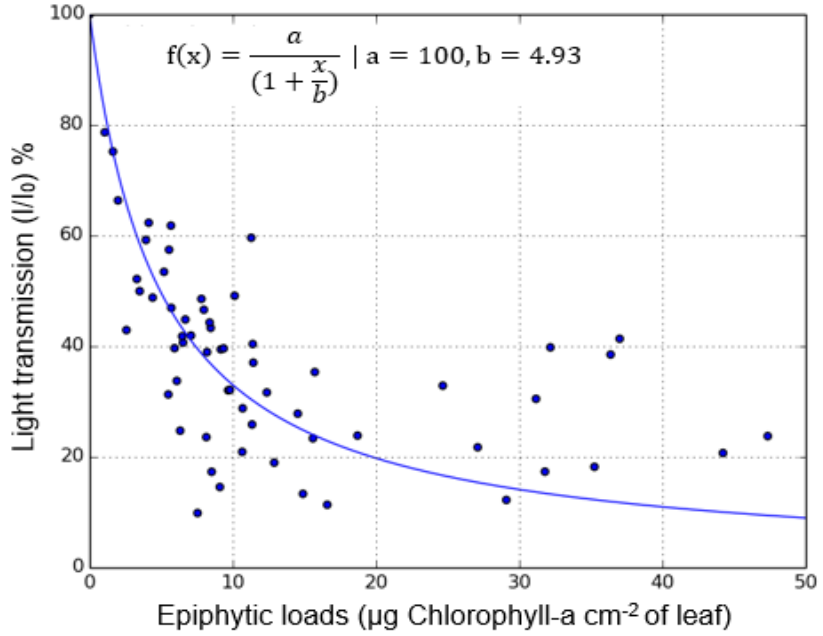

C

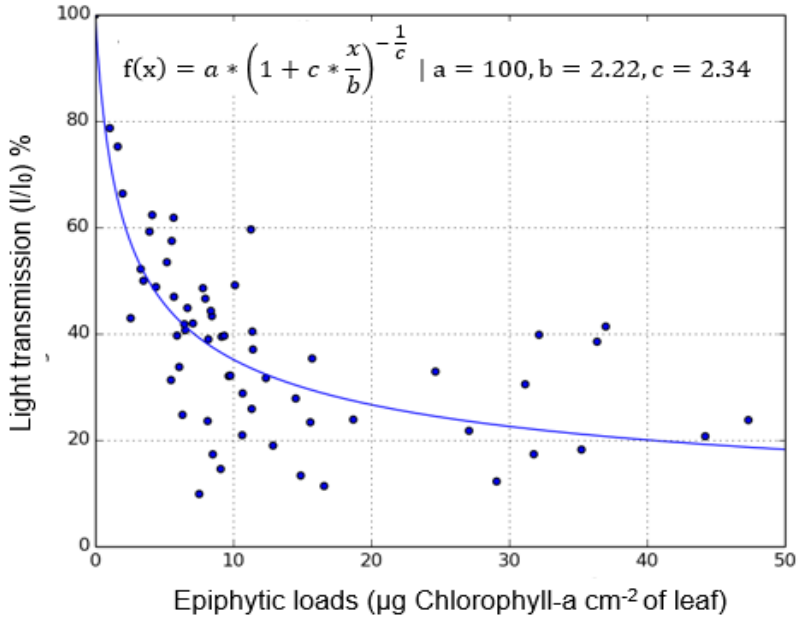

D

Figure 2-15. Continued.

Figure 2-16. Leaf from the Chassahowitzka river showing heterogeneous epiphytic loads on its two sides. Photo courtesy of author.

CHAPTER 3
THE EFFECTS OF EPIPHYTES ON THE GROWTH OF *VALLISNERIA AMERICANA*

Background

Submersed macrophytes are crucial components of aquatic systems because they stabilize sediments and reduce turbidity, absorb and store nutrients, sequester carbon, and provide refuge and foraging habitat for numerous aquatic organisms (Van Donk and van de Bund 2002, Gregg and Rose 1985). However, widespread reduction in the abundance of macrophytes has been observed since the 1900s as a consequence of eutrophication caused by increased nutrient loads, reduced flows, and other factors (Seddon et al. 2000, Waycott et al. 2009). In particular, reductions in available light caused by suspended particles, phytoplankton blooms and growth of epiphytic algae are blamed for losses of macrophytes (Silberstein et al. 1986, Lauridsen et al. 1994).

The influence of epiphytes on macrophytes has been demonstrated in several studies (Sand-Jensen 1977, Bulthuis and Woelkerling 1983, Silberstein et al. 1986). Epiphytes inhibit performance of macrophytes in several ways, including shading leaves, increasing the boundary layer around leaves leading to slower exchange of carbon dioxide (CO_2) and oxygen (O_2), and competing for nutrients (Sand-Jensen et al. 1985, Borowitzka et al. 2006). For example, heavy loads of epiphytes on *Ruppia cirrhosa* caused decreased production and earlier seasonal dieback (Kiørbe 1980). Epiphytic colonization of *Potamogeton pectinatus* was linked to cuticular erosion and peeling (Howard-Williams et al. 1978), and epiphytes on *Potamogeton crispus* caused swelling and disorganization of epidermal cells (Rogers and Breen 1981). Fong et

al. (2000) reported early leaf death and reduction of leaf flexibility in Zosteroids and *Thalassia* under heavy loads of epiphytes.

Epiphytes depress the productivity and reproduction of macrophytes mainly through diminishing the amount of light that reaches the leaves, which decreases photosynthesis (Orth and Van Montfrans 1984, Neckles et al. 1993, Drake et al. 2003). Many studies have confirmed that epiphytes can reduce light availability dramatically (Dennison et al. 1993, Vermaat et al. 1993, Czerny and Dunton 1995, Fitzpatrick and Kirkman 1995, Kurtz et al. 2003), and my measurements of epiphytic light attenuation in Chapter 2 indicated that an epiphytic load of about 7.7 mg DW cm^{-2} can attenuate 90% of incident light.

Most of the literature describing epiphyte-macrophyte interactions has focused on brackish or marine environments. A few studies on relationships in freshwater systems were conducted in lakes (Phillips et al. 1978, Sand-Jensen and Søndergaard 1981, Cattaneo et al. 1998) or in the laboratory (Asaeda et al. 2004). However, the influence of epiphytic loads on the growth and production of macrophytes in Florida's spring systems is poorly understood. To help fill this gap in knowledge, I conducted fieldwork in the spring-fed Chassahowitzka River, where a documented increase in epiphytes on macrophytes was temporally concordant with losses of important macrophytes, including *V. americana* (Notestein 2001).

Vallisneria americana is the dominant macrophyte in the Chassahowitzka River, and it is dioecious and perennial (Notestein 2001). These stoloniferous plants form expansive meadows via clonal extension. They can survive in fresh to mesohaline waters, and they grow in aquatic systems from Central America to Canada (Korschgen

and Green 1988). *Vallisneria americana* has ribbon-like leaves that reach up to 2 m or more in length depending on water movement and depth (Doust and LaPorte 1991). The leaves arise in a cluster from a short vertical stem that sends out rhizomes and stolons from which new shoots develop. Unbranched and fibrous roots are found at the base of each rosette (McFarland 2006).

Knowing how loads of epiphytes affect the growth of macrophytes is important for protecting, restoring and managing Florida's spring systems. For example, identifying the threshold for detrimental epiphytic loads could serve as a valuable index of the health of a system. Toward this end, this investigation measured growth rates for *V. americana* with different loads of epiphytes in the Chassahowitzka River. This study was a further test of the conclusion from Chapter 2, which indicated that epiphytic loads of approximately 6 mg DW cm^{-2} of leaf are sufficient to cause detrimental effects on macrophytes, based on minimum light requirements derived from previous studies (Chamber and Kalff 1985, Duarte 1991).

Materials and Methods

Study Sites

Measurements were made within large, continuous meadows of *V. americana* in Salt Creek (28°43'18" N, 82°35'30" W) and Small Creek (28°43'13" N, 82°35'29" W) that were about 2 km west of the head springs of the Chassahowitzka River (Figure 3-1). These meadows covered about 240 m^2 and 30 m^2 in Salt Creek and Small Creek, respectively (Figures 3-2A and 3-2B). Both meadows consisted of monospecific stands of *V. americana* with epiphytic algae on their leaves and little drift algae. The creeks were too shallow for motor boats and not near the main river, so they were rarely disturbed. In the two areas, seven sets of measurements were collected from

June 2016 to August 2016, with the first four sets occurring in Salt Creek and the last three sets taking place in Small Creek, after manatees grazed the *V. americana* in Salt Creek. Small Creek was shallower, narrower and more shaded by riparian vegetation (Figure 3-2B), with a less dense cover of shorter *V. americana*.

Environmental Measurements

During each visit, depth, water temperature, pH, concentration of dissolved oxygen (DO), salinity, light attenuation and incident solar radiation were measured. Depth was measured to the nearest 0.1 m with a surveyor's pole (Figure 3-3A). Temperature, salinity, pH, and DO were measured with a YSI model 650MDS meter and were recorded to the nearest 0.1ºC, 0.01, 0.01, and 0.1 mg O_2 L^{-1}. To calculate light attenuation coefficients (K_d), two quantum light sensors (Li-Cor Instruments Inc.) were used with a data logger to simultaneously measure photosynthetically active radiation (PAR, µE m^{-2} s^{-1}) at the water's surface and at one or more depths below the surface (Figure 3-3A and B). Values of K_d were calculated using the equation: $K_d = [-\ln(I_z/I_0)]/Z$, where I_0 is the radiation at the surface and I_z is the radiation at depth (Z, Kirk 1994). If the water was deeper than 1 m, measurements were made at three depths (Z = 0.5, 0.75, 1 m), and in shallow water, three replicate measurements were recorded at Z = 0.5 m. Measurements were made at 10 fixed locations uniformly distributed in the meadows and marked with PVC pipes (Figure 3-2), and readings were not corrected for sun angle.

Biomass of *Vallisneria americana* and Epiphytes

Shoot densities and biomass of *V. americana* and biomass of the associated epiphytes within the study meadows were quantified within five, haphazardly tossed quadrats (0.25 m X 0.25 m). A snorkeler counted the number of shoots in the quadrats

and collected six shoots to yield 30 samples for estimates of biomass of *V. americana* and epiphytes. Samples were stored in labeled plastic bags on ice during transport to the laboratory where they were frozen until processing.

In the laboratory, biomasses of shoots and the epiphytic algae on them were measured. After counting the number of leaves per shoot and measuring the heights and maximum widths of leaves, each leaf was placed under a transparent sheet of plastic marked with a 1-cm grid. The number of grid cells within the outline of the leaf were counted to yield the surface area of the leaf, that is, leaf area equaled the number of cells multiplied by 1 cm^2. Leaf area allowed me to express epiphytic biomass per unit area. To account for the heterogeneous distribution of epiphytes on *V*. *americana* leaves, leaves were separated into 10-cm sections before epiphytes were gently scraped off and saved in individual plastic weighing boats that had been pre-weighed and labeled. The clean leaves and the epiphytes were dried at 60°C to a constant weight, as measured to the nearest 0.001 with an electronic balance. Areal biomass (g DW m^{-2}) for *V. americana* and its epiphytes was calculated by multiplying the mean dry weight of *V. americana* shoots or the mean dry weight of epiphytes on shoots by the mean density of shoots.

Measurements of *Vallisneria americana* Growth and Epiphytic Loads

The growth of *V. americana* was documented with a modified leaf-marking technique commonly used for submersed macrophytes with wide leaves and a basal meristem (Figure 3-8, Odum 1957, Zieman 1968, Zieman and Wetzel 1980, Hauxwell et al. 2007). This technique was selected instead of the oxygen-exchange method or incorporation of ^{14}C isotopes because of variation induced by oxygen (O_2) in a plant's lacunal system, recycling of O_2, transport and release of O_2, the theoretical and practical

challenges associated with use of ^{14}C, and the fact that these other techniques would not yield independent estimates of photosynthesis for epiphytes and macrophytes (Westlake 1978, Capone et al. 1979, Kelly et al. 1981, Kremer 1981, Ramus 1981, Lindeboom and De Bree 1982, Sand-Jensen et al. 1982). At the beginning of a sampling period, a quadrat (0.25 m by 0.25 m) was tossed haphazardly five times within the selected meadow and six shoots in each quadrat were identified with a pink flag on a stake and a buoy that marked the area (Figure 3-4). All leaves in each tagged shoot were marked by carefully punching two holes with a syringe needle (18 gauge) approximately 3 cm above the rhizome (Hauxwell et al. 2007). Tagged shoots were retrieved one to two weeks after punching, at which time new shoots were tagged and punched. Shoots and their associated belowground tissue were collected by hand, rinsed in ambient water and placed in labeled plastic bags. All samples were stored on ice in a cooler during transport to the laboratory and frozen until they were processed.

Freezing for 12 h or more made the epiphytes easier to remove. After thawing, each leaf was gently scraped with a scalpel, and the epiphytes were saved. Leaves comprising each shoot were separated and ranked by age from senescent to new before their total lengths and maximum widths were measured (Figure 3-5). Leaf areas also were estimated with a gridded sheet.

For a given shoot, senescent leaves are located at the outside of the bundle, and they bore holes that were at the same height as they were initially punched because these leaves did not grow. These marks served as reference points for measuring growth of younger leaves (Figure 3-6). New growth for younger leaves was identified as the material between their holes and the reference point. All leaves without holes were

considered new growth. Epiphytes, new growth and old leaf tissue were placed in separate pre-weighed, labeled plastic weighing boats and dried at 60°C to a constant weight as determined to the nearest 0.001 g with an electronic balance (Figure 3-7). Growth of *V. americana* shoots (R) was calculated as $\mathrm{R} = \frac{G}{N}$ in cm^2 per day or mg DW per day, where G is the quantity of new material (cm^2 or mg dry weight) and N is the number of days between punching and retrieval (Figure 3-8).

Determination of the Plastochrone Interval (PI) and Leaf Age for *Vallisneria americana*

Age is another influence on the growth of leaves of macrophytes, since many important physiological processes change with age (Cebrian and Duarte 1994), including photosynthesis (Mazzella and Alberte 1986) and synthesis of proteins (Thayer et al. 1984, Zieman et al. 1984). Thus, I sought to estimate the age of leaves. Conventionally, leaf age is expressed as leaf rank (Patriquin 1973, Ott 1980), but Duarte (1991) found that leaves with the same rank may differ in age by 1.1 to 47.2 days. To avoid such errors, leaf age was estimated with the method used by Erickson and Michellini (1957), which converts leaf ranks into absolute age in days using the Plastochrone Interval (PI, Askenasy 1880, Lamoreaux et al. 1978).

Plastochrone intervals (PI, day per leaf) for *V. americana* were derived from observations of newly emerged and unmarked leaves in shoots (Duarte et al. 1994). The interval represents the time between the appearance of two consecutive leaves, and it is calculated as: $\mathrm{PI} = \frac{\text{Time Interval x No.of marked shoots}}{\text{No. of newly emerged leaves in marked shoots}}$; where Time Interval is the number of days between punching and retrieval for shoots with at least one new leaf.

Once the plastochrone interval for *V. americana* was known, estimates of leaf age in days could be calculated for all leaves (Erickson and Michellini 1957). These calculations involved a Plastochrone Index (PI Index): $\mathrm{PI\ Index} = \mathrm{R} - 1 + \frac{\mathrm{lnL_1} - \mathrm{lnL_r}}{\mathrm{lnL_2} - \mathrm{lnL_1}}$; where R is the rank of a given leaf among all the leaves in a shoot arranged from youngest to oldest, $\frac{\mathrm{lnL_1} - \mathrm{lnL_r}}{\mathrm{lnL_2} - \mathrm{lnL_1}}$ represents the fractional age of the youngest leaf (which is < 1), $\mathrm{L_1}$ and $\mathrm{L_2}$ are the lengths of the two youngest leaves in the shoot (ranks 1 and 2), and $\mathrm{L_r}$ is the reference length or the length at which a new leaf can be detected. Estimates of leaf age in days were made by multiplying the PI Index by the Plastochrone Interval.

Statistical Analyses

Regression analyses were used to examine the relationships between new growth per shoot per week and epiphytic loads expressed as total loads per shoot or loads per unit area. These analyses were performed using Microsoft Excel.

A boundary analysis was employed to identify epiphytic loads that impeded the growth of *V. americana* (Ludwig and Tongway 1995). The analysis involved (1) ranking growth rates according to epiphytic loads from highest to lowest, (2) bracketing contiguous sets of growth rates in a window of preassigned width (w = 4 for Salt Creek and 6 for Small Creek), (3) splitting each window into two equal groups ($\frac{1}{2}w = 2\ or\ 3$), (4) averaging the growth rates in the two groups (H_1 and H_2), (5) computing a dissimilarity index as squared Euclidean distance (SED) = $[(Mean\ H_1) - (Mean\ H_2)]^2$, (6) moving the window one position further along the ordered series of growth rates, (7) computing another dissimilarity index, (8) repeating this process for the entire dataset (Figure 3-9), and (9) plotting the dissimilarity indices against loads of epiphytes.

Thresholds for the effect of epiphytic loads were identified as the first large increase in the dissimilarity indices. As a test of the thresholds, growth rates below the threshold were compared to growth rates above the threshold with Welch's t-test.

Results

Environmental Data

The environmental conditions at these study sites were similar to those documented in Chapter 2, which was about 294 m away. During my sampling, water temperatures ranged from 25.9°C to 31.1°C. Average daytime dissolved oxygen concentrations (DO) were 8.84 mg L^{-1}, pH averaged 7.89 and mean salinity was 3.55‰. The tide and runoff from the land's surface led to variation in attenuation coefficients (K_d), with the mean K_d being 3.27. Incident light at the two sites differed, with the mean and maximum in Small Creek 26.43% and 53.57%, respectively, of values in Salt Creek at noon.

In situ Biomass of *Vallisneria americana* and Epiphytes

In Salt Creek, the areal biomass of *V. americana* was 143 g DW m^{-2} as estimated from mean shoot dry weight and mean shoot density (182 shoots m^{-2}). The areal biomass in Small Creek was 37.35 g DW m^{-2}, with a mean shoot density of 86 shoots m^{-2}. New leaves appeared in shoots every 5.25 ± 0.63 days, i.e., about every 5 days.

Loads of epiphytes per shoot varied, with a range of 10.9 to 15,211 mg DW per plant (0.08 to 32.37 mg DW cm^{-2}), and an overall mean ± standard deviation of 1,735 (± 2,556) mg DW per plant (6.66 ± 7.26 mg DW cm^{-2}). Epiphytic loads accumulated near the tips of leaves, and sections between the base of the shoots and 7 cm were free of epiphytes (Figure 3-10). Mean epiphytic loads per leaf differed with leaf age, with an increase to a maximum value of 6.86 mg DW cm^{-2} on 40-day-old

leaves and a decrease on older leaves (Figure 3-11). Epiphytes were not present on all leaves younger than 3 days, 85.71% of leaves aged 3 to 9 days, and 22.63% of leaves aged 9 to 15 days (Figure 3-11).

Effect of Leaf Age on Growth of *Vallisneria americana*

The reference length (L_r) was set as 1.8 cm because it was the length of the shortest new leaf. Based on estimated ages, leaves were grouped into four age classes: young (< 20 days), early (20-29 days), mature (30-39 days), and senescent (≥ 40 days). Of all leaves sampled in Small Creek and Salt Creek, respectively, young leaves represented 26.46% and 35.11%, early leaves represented 17.95% and 25.29%, mature leaves represented 17.95% and 21.96%, and senescent leaves represented 37.64% and 17.64% (Figure 3-12).

New growth was reduced in leaves older than 30 days and essentially absent in the few leaves older than 40 days (Figure 3-13). The largest amounts of growth were 22.92 cm^2 per week in Small Creek and 30.24 cm^2 per week in Salt Creek, which were recorded for leaves that were 15 days old (Figure 3-13). Maximum values for new growth increased up to 15 days and reached approximately zero after 40 days (Figure 3-14).

Effect of Epiphytic Load on growth of *Vallisneria americana*

Fieldwork provided seven sets of measurements representing a total of 134 shoots and 1236 leaves. Linear regressions yielded low coefficients of determination (R^2), regardless of whether epiphytic loads were standardized to unit area (Figures 3-15 and 3-16). Nevertheless, growth expressed as gain in dry weight or surface area was negatively correlated with epiphytic loads in Salt Creek and positively correlated with epiphytic loads in Small Creek.

Given the variation in growth related to the age of leaves, multiple regressions were employed to examine relationships of growth to leaf age (X_1), epiphytic load (X_2), and the interaction of leaf age and epiphytic load ($X_1 \times X_2$). Growth was negatively correlated with both leaf age and epiphytic load in both Salt and Small creeks (Tables 3-1 and 3-2).

Estimation of a Threshold for Detrimental Epiphytic Load

Threshold epiphytic loads that inhibited growth of *V. americana* were estimated for leaves in different age classes in Salt Creek and Small Creek. Lack of epiphytes on young leaves or lack of growth for mature leaves restricted these analyses to two age classes in each creek (Figures 3-17 and 3-18). For Small Creek, boundary analysis using a window of six datapoints indicated thresholds at ~ 0.4 mg DW cm^{-2} for early leaves (20-29 days) and between 0.85 and 0.79 mg DW cm^{-2} for mature leaves (30-39 days, Figures 3-17A and 3-17B). For Salt Creek, boundary analysis using a window of four datapoints indicated thresholds between 3.84 and 4.76 mg DW cm^{-2} for young leaves (< 20 days) and between 4.92 and 5.23 mg DW cm^{-2} for early leaves (20-29 days, Figures 3-18A and 3-18B). These thresholds were confirmed by significant differences in Welch's t-tests (Table 3-3).

Discussion

My environmental data (temperature, DO, salinity, and K_d) fell within the ranges of data from two transects (5 and 6) that were surveyed from 1998 to 2005 (Frazer 2000, Frazer et al. 2001, Frazer et al. 2006). My temperatures, salinities and K_d values were above the average values because my sampling always occurred during low tides.

My measures of biomass for *V. americana* and its epiphytes illustrated changes in the Chassahowitzka system since previous sampling (Frazer 2000, Frazer et al. 2001, Frazer et al. 2006). During my sampling, maximum biomass of *V. americana* (143 g DW m^{-2}) was about 10% of the historic average (1295.53 ± 189.68 g DW m^{-2}) and close to the historic low. In contrast, my mean epiphytic biomass was twice that of the historic average (2.25 ± 0.21 µg Chl-a g^{-1} DW host plant), and my maximum epiphyte load was 26.06 µg Chl-a g^{-1} DW host plant as compared to the historic maximum of 6.53 µg Chl-a g^{-1} DW host plant. These differences suggest degradation of *V. americana* due to increased epiphytic loads.

Furthermore, average shoot biomass in Salt Creek was higher than values recorded in Small Creek. This difference probably arises from differences in incident solar radiation, which was 75% lower in Small Creek. Similar differences were reported for *V. americana* by Blanch et al. (1998) in the River Murray in South Australia where light regimes were affected by turbidity, and in a shading experiment conducted in Perdido Bay, at the border between Alabama and Florida (Kurtz et al. 2003).

Numbers of new leaves per shoot and total leaves per shoot in Small Creek were higher than values in Salt Creek. This result supports the conclusion that low light availability leads to production of new leaves in *V. americana*, which was reported by Kimber et al. (1995) and Muenscher (1936). Additional leaves per shoot increase photosynthetic production in Small Creek, where less light is available.

Epiphytic loads were higher in Salt Creek, and it has been shown that light has a strong positive effect on the growth of epiphytes (Burnell et al. 2014). Epiphytic loads on *V. americana* initially increased with leaf age and then declined after 40 days

(Figure 3-11), which agrees with observations for seagrass species (Borum 1987, Hootsmans and Vermaat 1991). The increase in epiphytic biomass indicates that epiphytic growth exceeds losses from grazing or sloughing, and the presence of a maximum load points to a balance between growth and loss at about 40 days (Borum 1987), with the subsequent decrease likely caused by loss of older and more heavily epiphytized sections. Epiphytes tend to increase near the tips of leaves (Figure 3-10), which are older and exposed to colonization and growth for a longer time. Borowitzka et al. (1990) found similar results for the seagrass *Amphibolis griffithii*.

Growth rates for leaves varied between Salt Creek and Small Creek primarily as a consequence of the amount of incident light, but leaf age and epiphytic loads influenced growth rates at both sites. Leaf age appears to limit overall growth potential, and epiphytic loads above a certain threshold essentially reduce growth to zero, with thresholds varying according to the age of leaves. Young leaves (< 20 days) in Salt Creek stopped growing at epiphytic loads of ~ 4.3 mg DW cm^{-2}, and substituting this load into the unconstrained two-parameter exponential decay equation from Chapter 2 ($\text{Light transmision } \% = 79.61 * e^{\frac{-\text{epiphytic loads}}{3.63}}$) indicated that the leaves were receiving 24.35% of incident light. Growth of early leaves (20-29 days) in Salt Creek ceased at ~ 5.08 mg DW cm^{-2}, which equates to 19.67% of incident light. In Small Creek, where incident light was 75% less, thresholds for early leaves (20 days < leaf age < 30 days) and mature leaves (30 days < leaf age< 40 days) were 0.4 and 0.8 mg DW cm^{-2}, respectively, which equates to 17.83% and 15.97% of available incident light. Overall, the threshold epiphytic load that limited growth of *V. americana* in the Chassahowitzka River was between 4 and 5 mg DW cm^{-2}. In other words, the minimum

light requirement was about 22% of incident light at the leaf's surface. In Chapter 2, the critical threshold for epiphytic loads was estimated to be 6 mg DW cm^{-2} based on values for light requirements drawn from the literature. Results based on measurements of growth in the field were < 6 mg DW cm^{-2} in part because of light attenuation by the overlying water column. My results were similar to previous reports for seagrasses near the Homosassa and Weeki Wachee rivers, where sites that had a median light penetration > 20% of incident light supported the most abundant and diverse beds of seagrass (Choice et al. 2014).

To my knowledge, this is the first study to quantify a threshold for the influence of epiphytes on growth of freshwater macrophytes using in-situ measurements. The results can be applied to improve management of water quality, light attenuation and the health of macrophytes, which are critical components of Florida's spring-fed aquatic systems.

Table 3-1. Statistics for multiple regression involving epiphytic loads, leaf ages and their interaction for Salt Creek.

ANOVA	df	SS	MS	F	Significance F	R^2	Adjusted R^2	Term	Coefficient	t-value	P-value
Regression	3	9038	3013	128	7.32E-64	0.39	0.39	Intercept	10.57	25.08	2.47E-95
Residual	597	14096	24					Epiphytic load	-0.23	-14.64	1.03E-41
Total	600	23133						Leaf age	-0.57	-8.93	5.11E-18
								Interaction	0.01	7.43	3.75E-13

Table 3-2. Statistics for multiple regression involving epiphytic loads, leaf ages and their interaction for Small Creek.

ANOVA	df	SS	MS	F	Significance F	R^2	Adjusted R^2	Term	Coefficient	t-value	P-value
Regression	3	5727	1909	134	4.26E-67	0.39	0.39	Intercept	8.41	26.58	5.19E-105
Residual	631	9001	14					Epiphytic load	-0.15	-15.84	7.71E-48
Total	634	14727						Leaf age	-4.58	-6.63	7.33E-11
								Interaction	0.08	6.58	1.02E-10

Table 3-3. Estimated threshold of epiphytic loads that prevent the growth of *Vallisneria americana*. Welch's t-tests assessed differences in mean epiphytic loads below and above each threshold.

Creek	Age	Epiphytic loads (mg dry weight cm^{-2})				
		Threshold	Values versus threshold	Mean	SE	P-value
Small	Early	0.40-0.41	below	0.34	0.00	2.08E-03
			above	0.61	0.04	
	Mature	0.79-0.85	below	0.57	0.01	1.14E-07
			above	1.32	0.25	
Salt	Young	3.84-4.76	below	1.27	0.06	8.07E-03
			above	13.83	52.28	
	Early	4.92-5.23	below	2.74	1.35	1.06E-18
			above	16.13	70.20	

Figure 3-1. Location of study areas in Salt Creek (28°43’18” N, 82°35’30” W) and Small Creek (28°43’13” N, 82°35’29” W). Both areas were about 2 km west of head springs of the Chassahowitzka River, Florida. Reprinted with permission from Google Earth, https://www.google.com/earth/ (November 18, 2017).

A B

Figure 3-2. Study areas in the Chassahowitzka River. A) The area in Salt Creek was wide (about 32 m) with less shade from riparian vegetation. B) The area in Small Creek was shallow, narrow (about 5 m) and shaded by riparian vegetation. Anchored PVC bars evenly distributed in the two areas as fixed spots for measurements of irradiation and light attenuation. Photos courtesy of author.

A B

Figure 3-3. Equipment used to take measurements in the field. A) A surveyor's pole with an underwater quantum light sensor to measure water depth and light attenuation coefficient (K_d). B) An underwater quantum light sensor with a data logger for measuring and recording photosynthetically active radiation (PAR, µE m^{-2} s^{-1}). Photos courtesy of author.

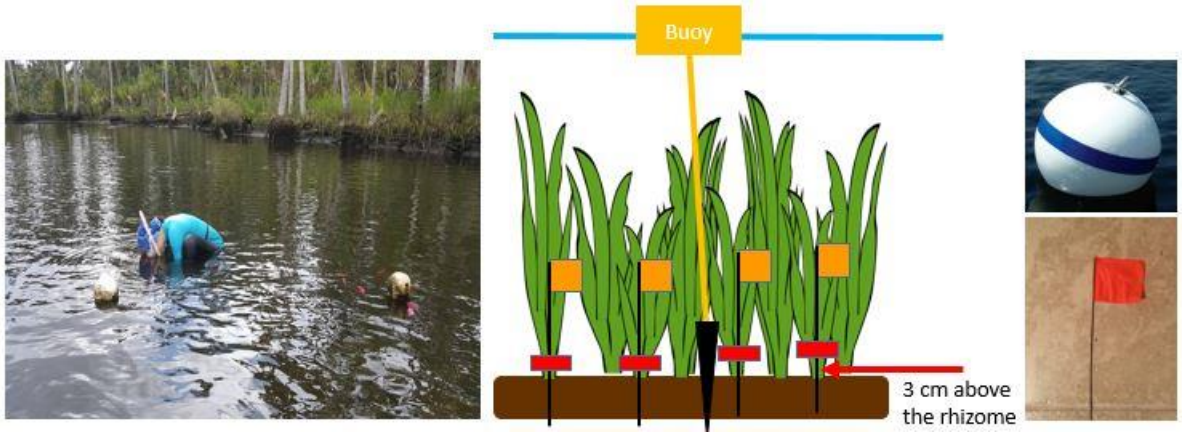

Figure 3-4. Depiction of sampling events. During each sampling event, a snorkeler punched two holes through the leaves of 30 shoots of *Vallisneria americana* approximately 3 cm above their rhizomes, and they were marked with pink flags and a buoy. Photos courtesy of author.

Figure 3-5. Typical *Vallisneria americana* shoot during processing. Leaves on each shoot were separated and ranked by age from senescent leaves (right) to new leaves (left) before their total lengths and widths of leaves were measured. Photo courtesy of author.

Figure 3-6. Holes in leaves used to measure growth. The scars on senescent leaves served as reference points for measuring growth of younger leaves. Photos courtesy of author.

Figure 3-7. Labeled, pre-weighed boats containing samples for processing. Dry weights were determined for epiphytes, new growth and original material. Photo courtesy of author.

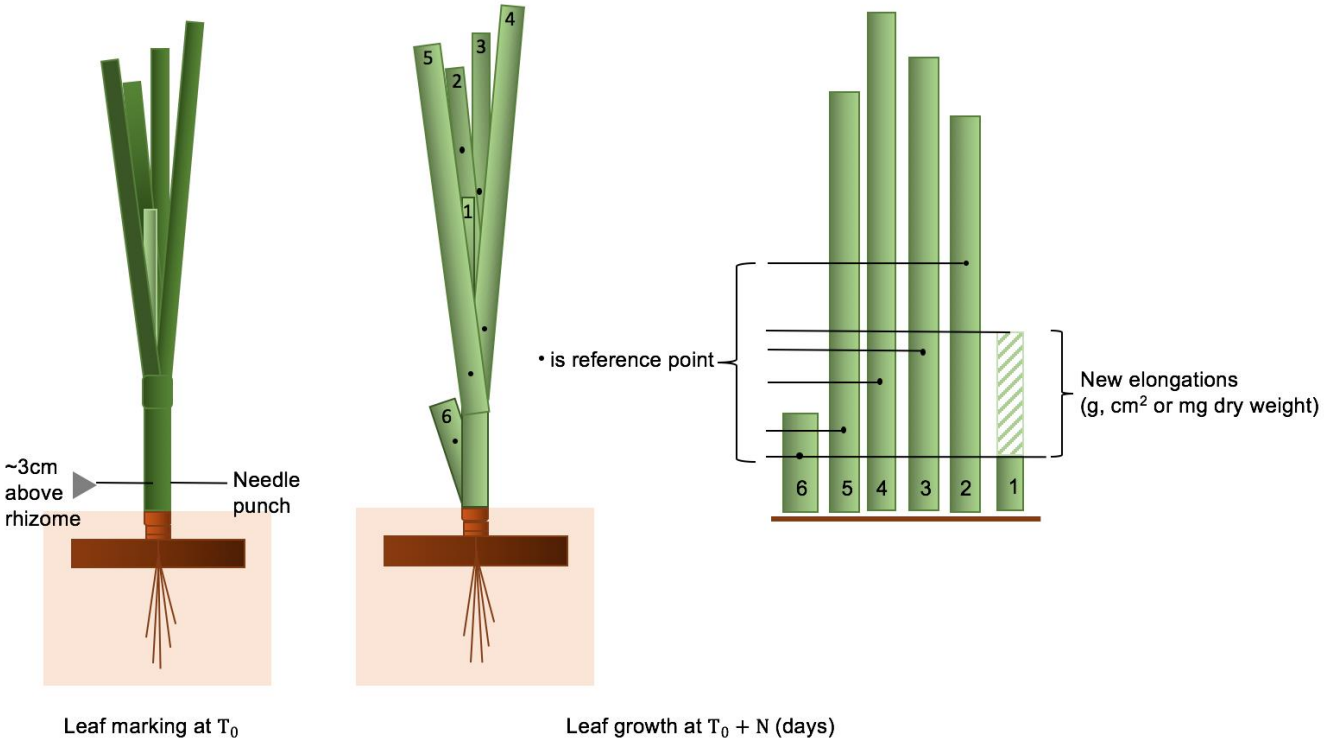

Figure 3-8. Schematic of modified leaf-marking technique. Modified from Short and Duarte (2001).

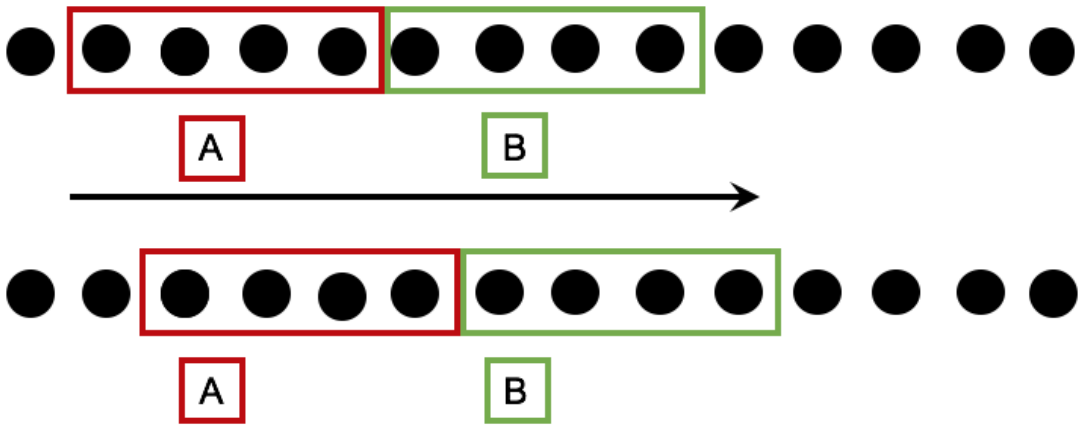

Figure 3-9. Schematic of the moving-split window technique. In a window eight datapoints wide, a dissimilarity value was calculated using the means of the four datapoints in the red and green frames before the window was moved one datapoint and a new index was calculated.

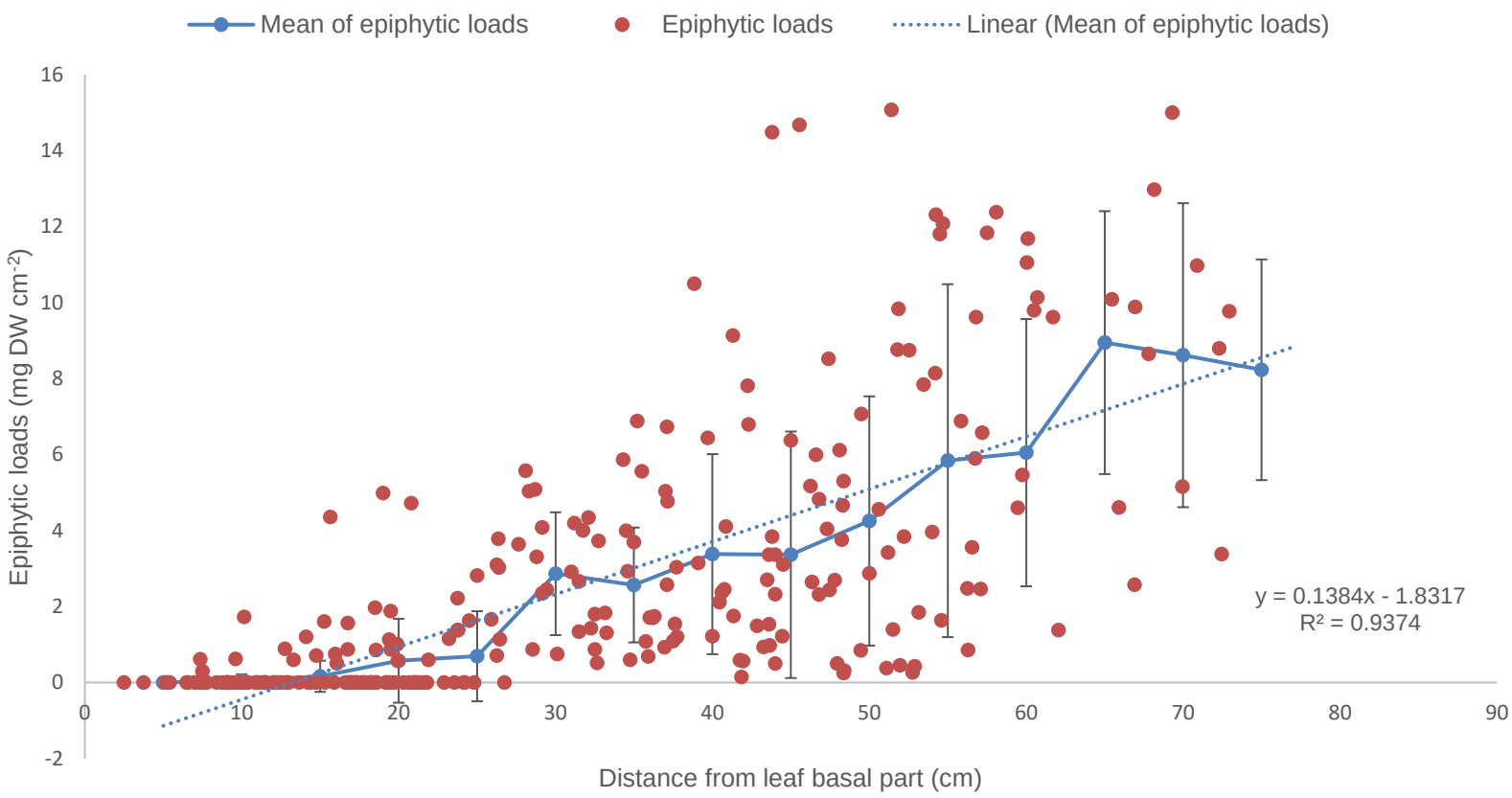

Figure 3-10. Distribution of epiphytic loads along the leaves of *Vallisneria americana*. Orange points represent the epiphytic loads on different sections of leaves, blue points and bars represent the means and standard errors for epiphytic loads on consecutive 5-cm-long leaf sections. Blue dotted line depicts the trend.

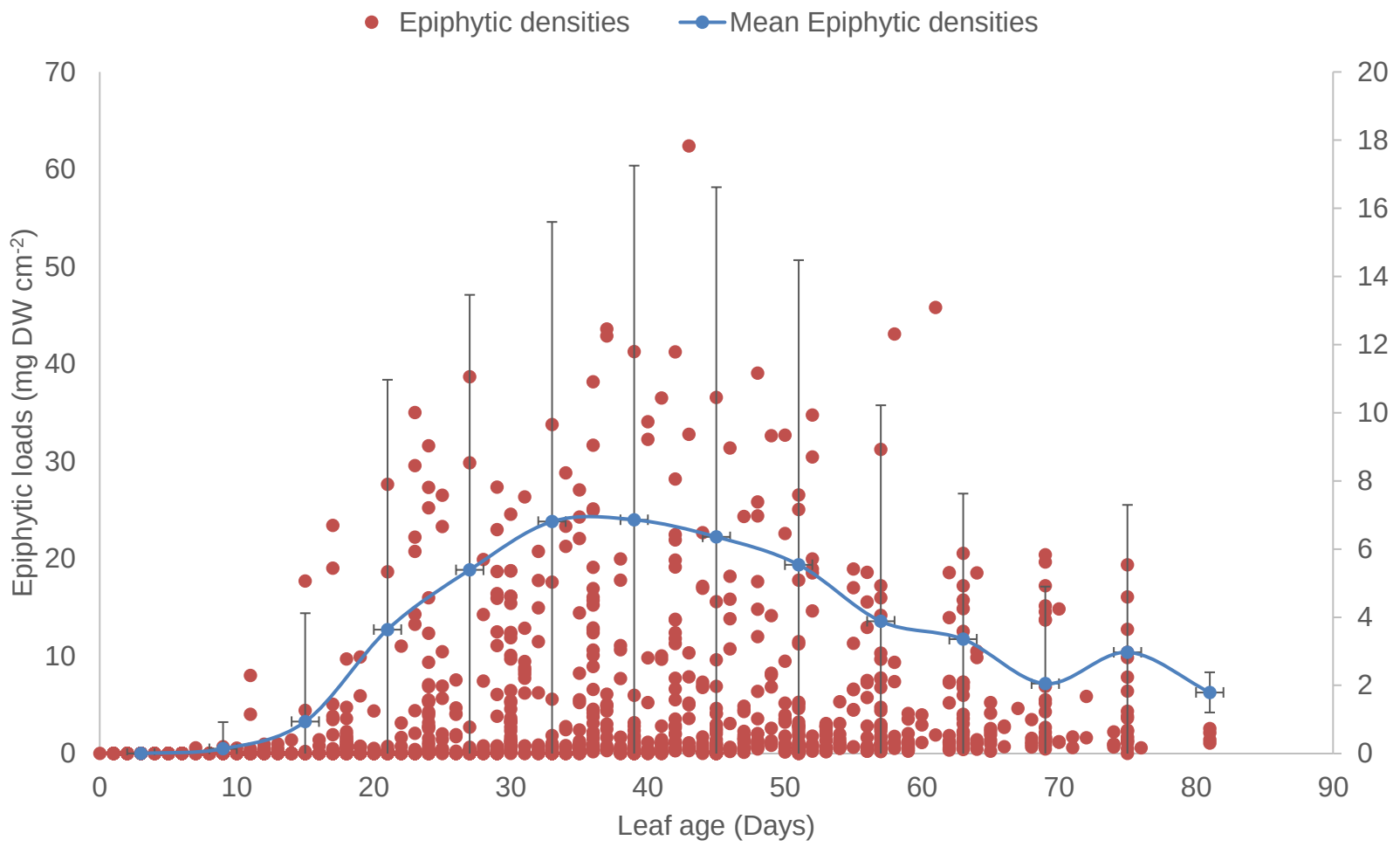

Figure 3-11. The relationship between epiphytic load and leaf age for *Vallisneria americana*. Orange points represent the epiphytic loads on leaves with different ages, blue points and bars represent the means and standard errors for epiphytic loads. Blue line depicts the trend.

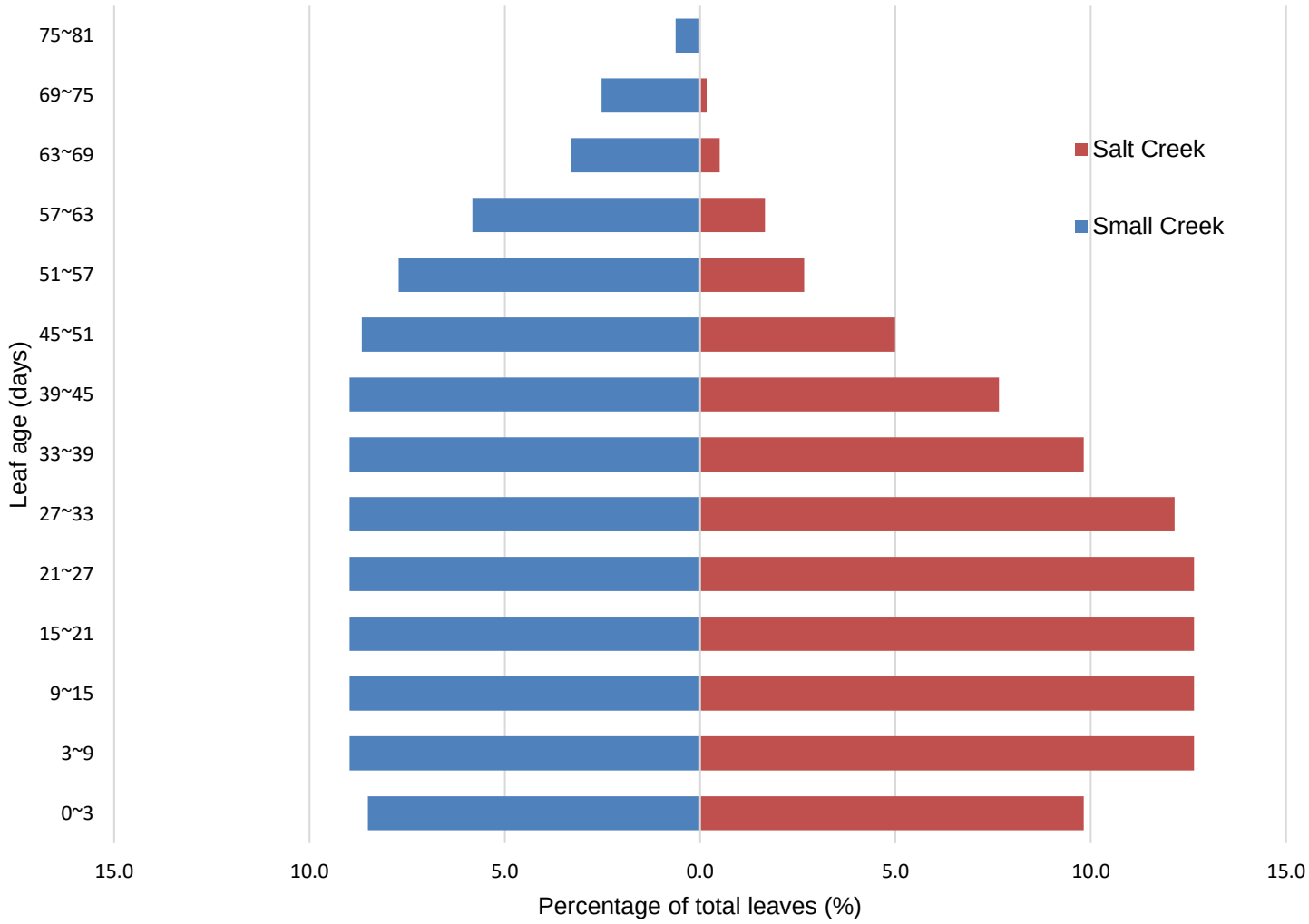

Figure 3-12. Percentage of *Vallisneria americana* leaves in different age classes (days) in Small Creek (left) and Salt Creek (right).

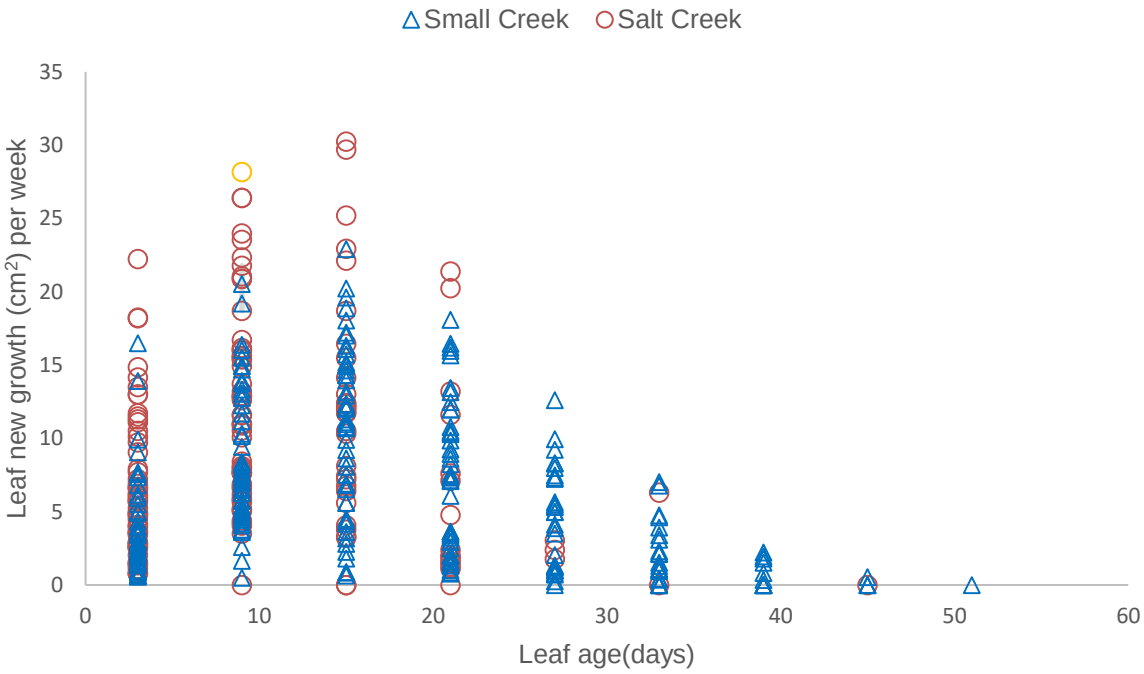

Figure 3-13. Growth of leaves of *Vallisneria americana* (cm^2 per week) of different ages (days), in Small Creek (blue triangles) and Salt Creek (orange circles).

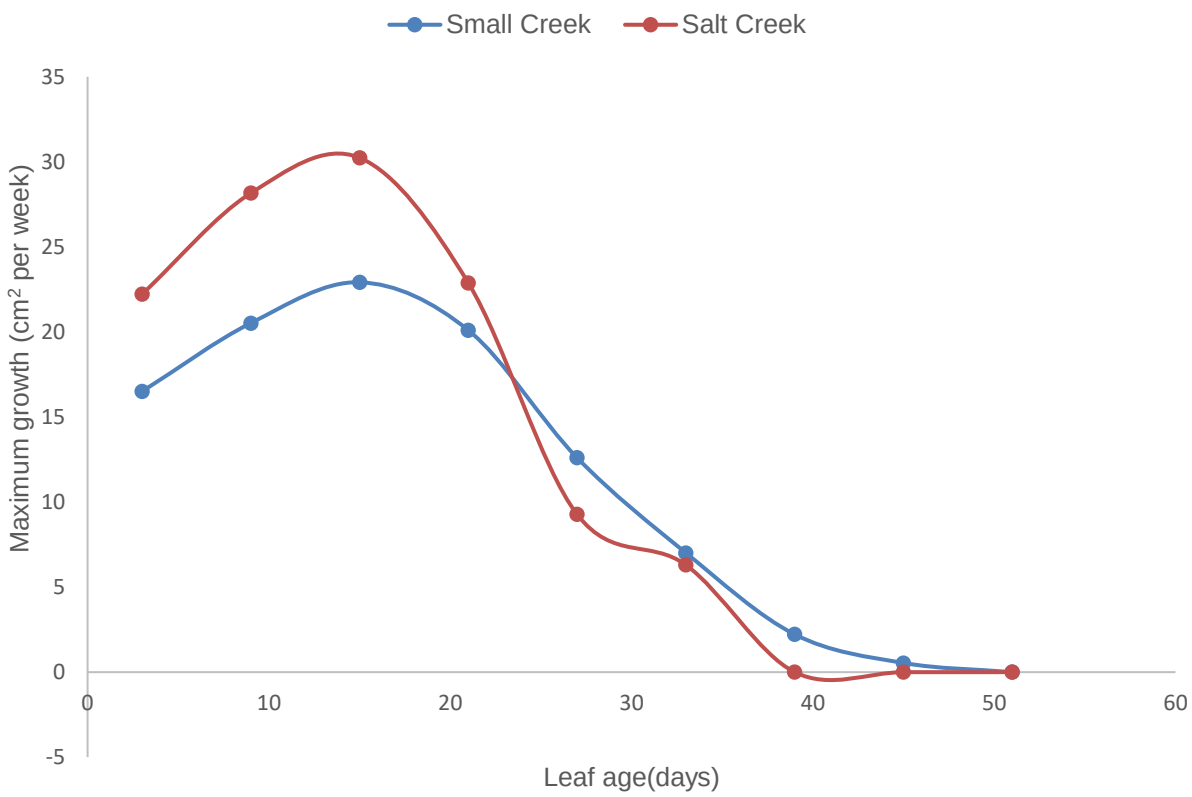

Figure 3-14. Maximum growth of *Vallisneria americana* leaves (cm^2 per week) of different ages (days) in Small Creek (blue) and Salt Creek (orange).

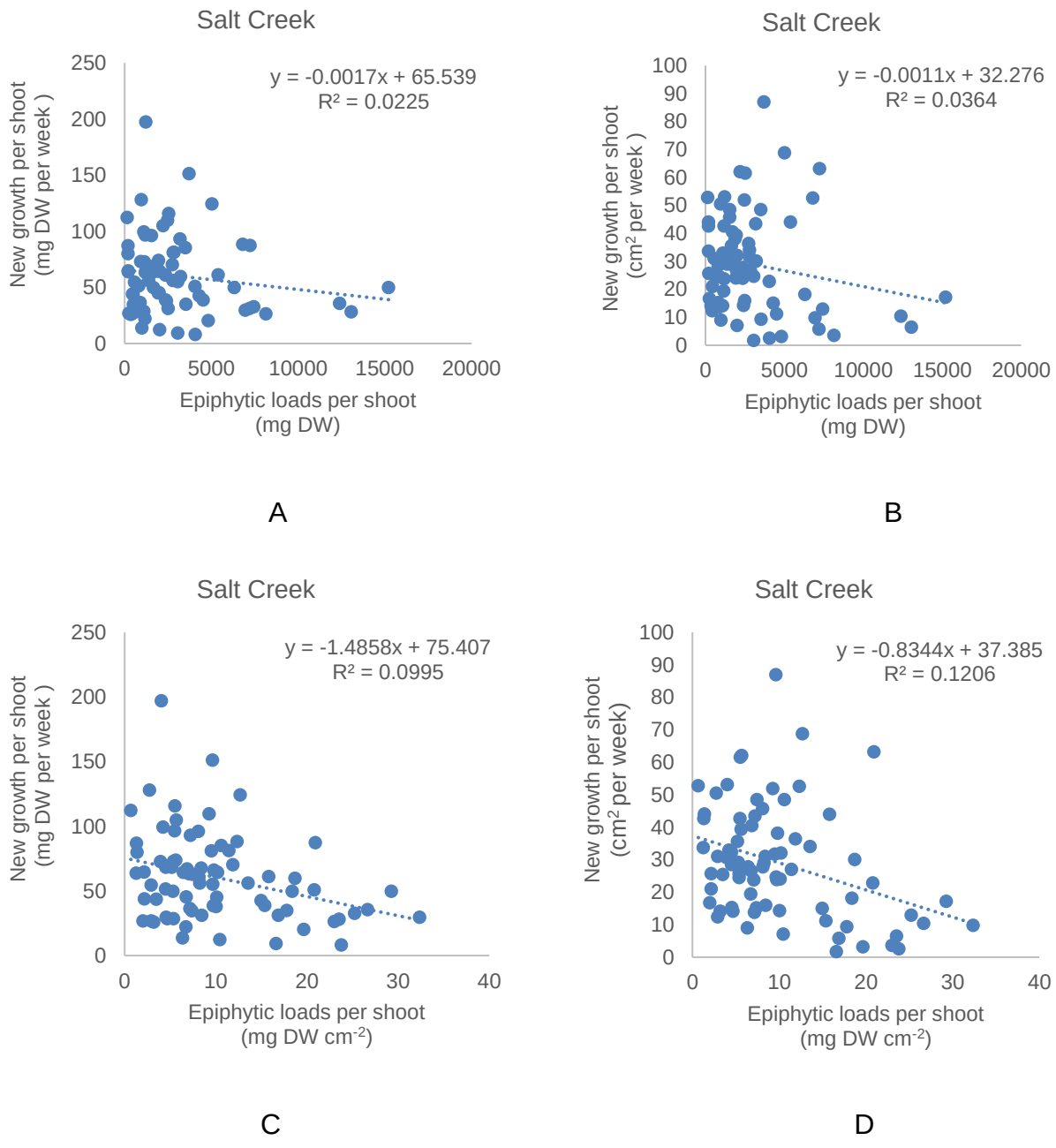

Figure 3-15. Relationships and trends for epiphytic loads and growth of *Vallisneria americana* shoots in Salt Creek. A) and B) Epiphytic loads expressed as mg dry weight (DW). C) and (D) Epiphytic loads expressed as mg DW cm^{-2}. A) and C) Growth expressed as mg DW per week. B) and D) Growth expressed as cm^2 per week.

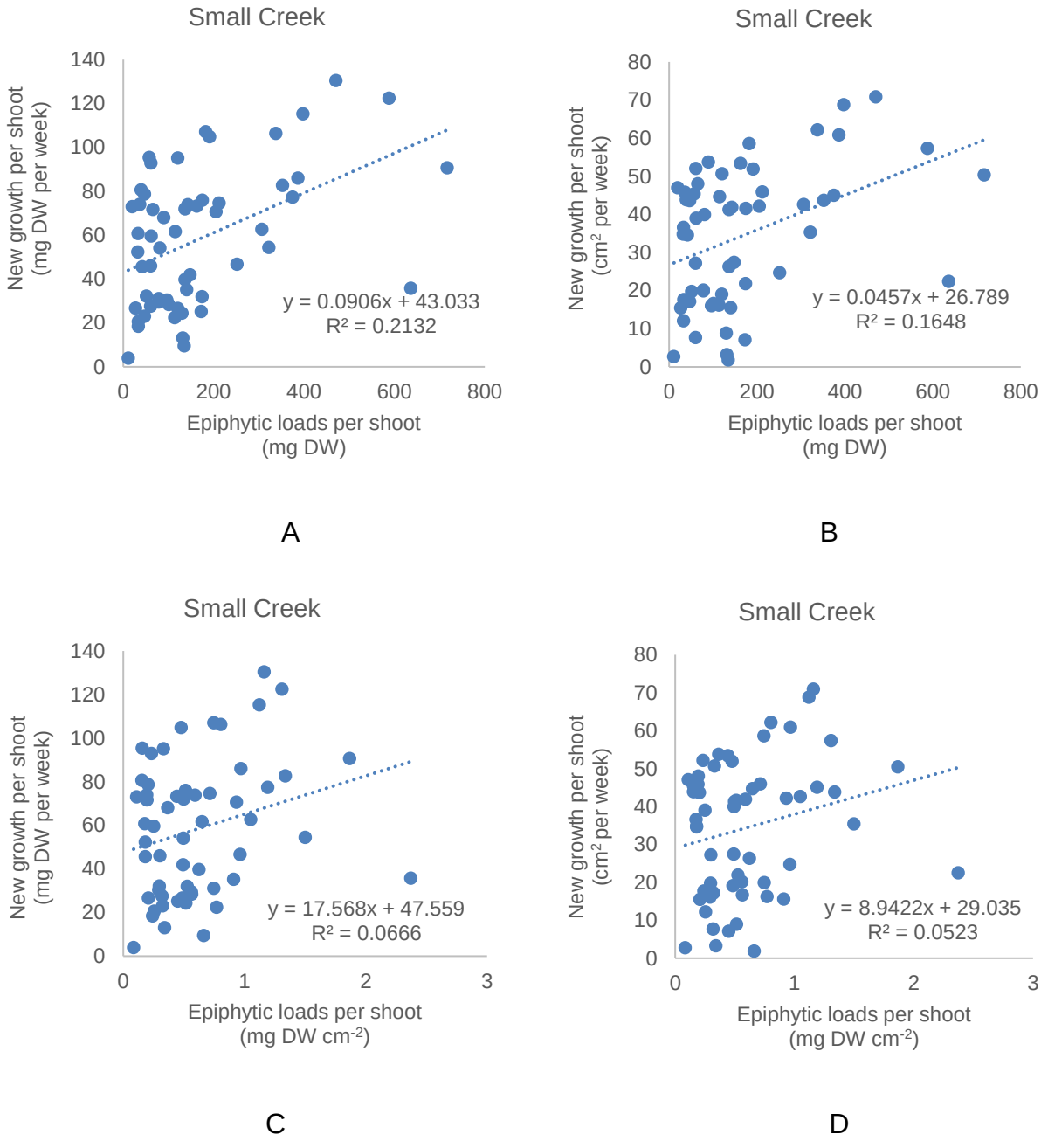

Figure 3-16. Relationships and trends for epiphytic loads and growth of *Vallisneria americana* shoots in Small Creek. A) and B) Epiphytic loads expressed as mg dry weight (DW). C) and D) Epiphytic loads expressed as mg DW cm^{-2}. A) and C) Growth expressed as mg DW per week. B) and D) Growth expressed as cm^2 per week.

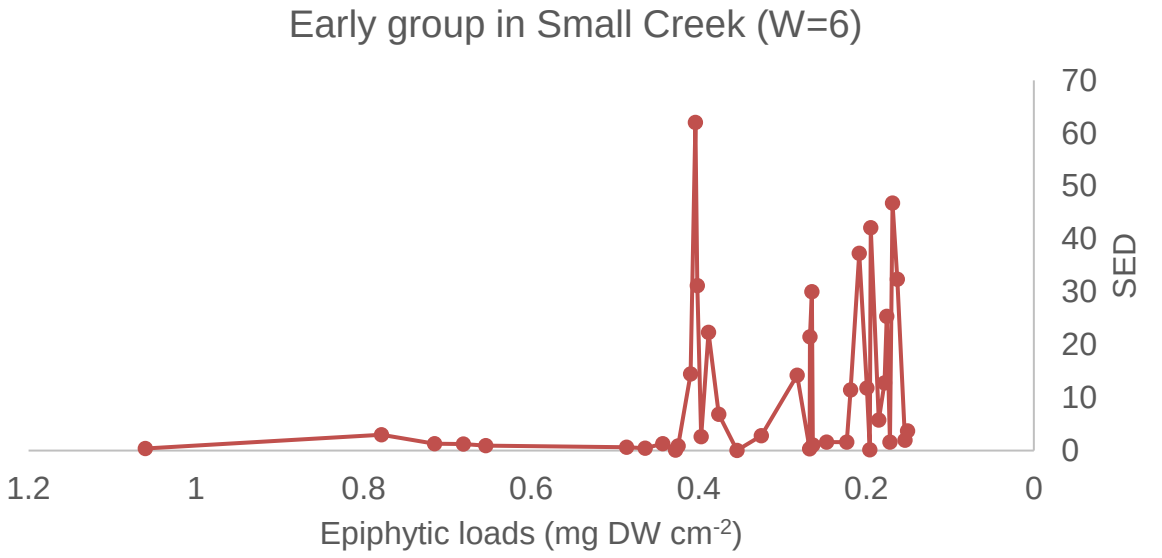

A

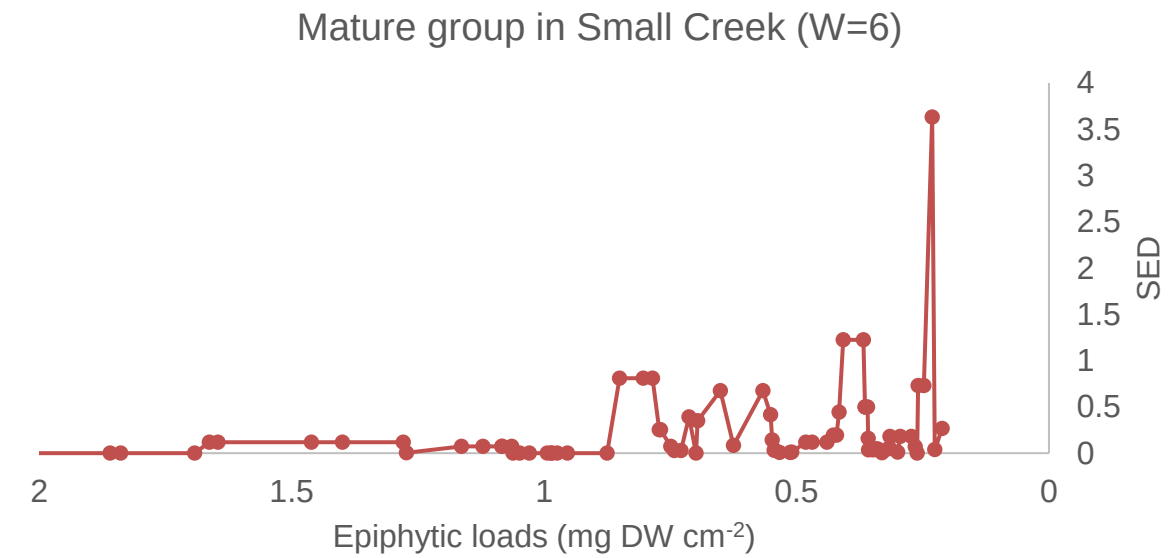

B

Figure 3-17. Squared Euclidean distances (SED) versus epiphytic loads in Small Creek. A) Plants in the early age class. B) Plants in the mature age class. Moving window (W) included six datapoints.

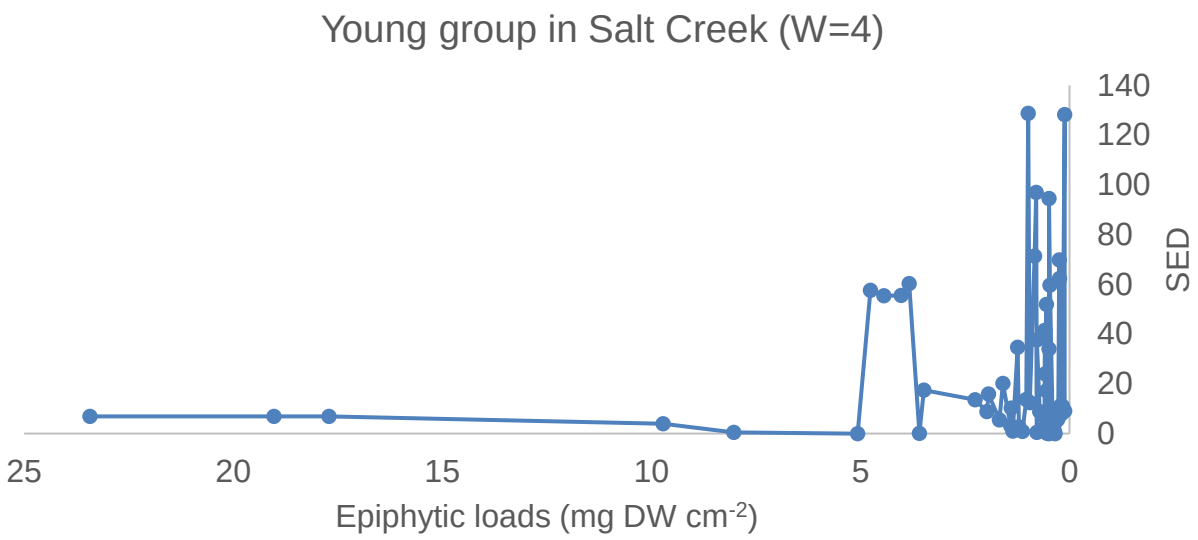

A

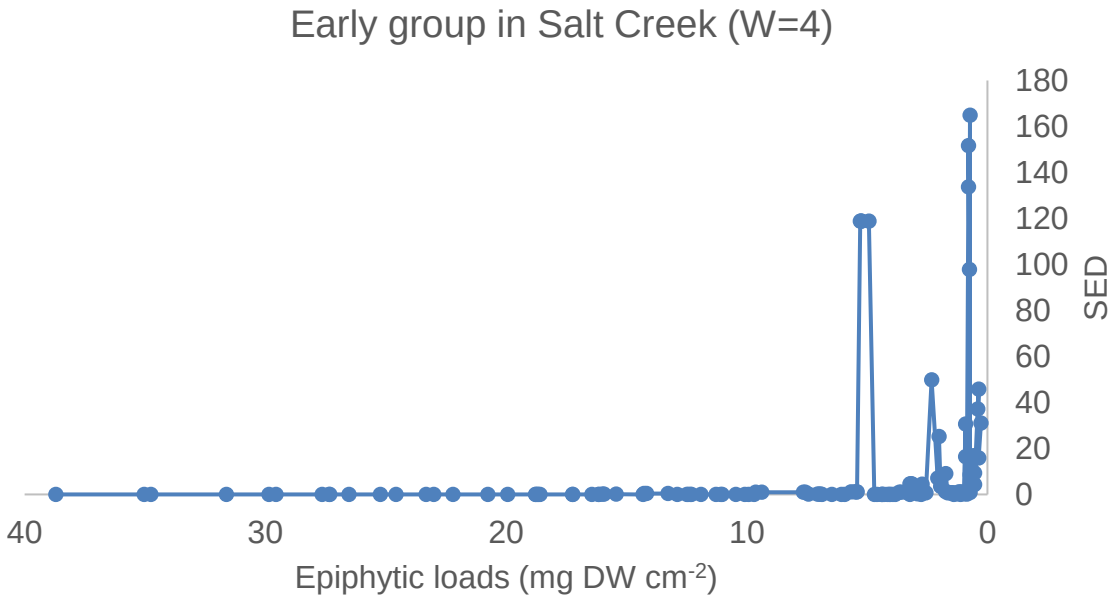

B

Figure 3-18. Squared Euclidean distances (SED) versus epiphytic loads in Salt Creek. A) Plants in the young age class. B) Plants in the early age class. Moving window (W) included four datapoints.

CHAPTER 4
A MODEL OF *VALLISNERIA AMERICANA* GROWTH UNDER DIFFERENT EPIPHYTIC LOADS

Background

Meadows of submersed macrophytes are found in many aquatic systems around the world. They are major contributors to primary production, provide nursery habitats for aquatic organisms (Orth and Van Montfrans 1984), stabilize sediments, and assimilate and store nutrients (Oshima et al. 1999). In recent decades, proliferation of nuisance algae has seriously threatened the survival of macrophytes (Silberstein et al. 1986). In Florida's spring-fed systems, temporal concordance between increased epiphytic loads and loss of submersed macrophytes has been widely observed, with the Chassahowitzka River being a prime example (Notestein 2001).

In the Chassahowitzka River, *Vallisneria americana* meadows represent an important and formerly extensive habitat (Frazer et al. 2001). The leaves of *V. americana* support many epiphytes, which can be responsible for up to 20-30% of the total primary production (Notestein 2001). Evidence suggests that epiphytic loads have several detrimental impacts on the productivity and growth of the host plant, especially through competition for available light and nutrients (Mazzella and Ott 1984, Dunn et al. 2008, Frankovich and Zieman 2005, Orth and Moore 1983). In addition, epiphytes can increase drag on leaves of macrophytes, causing shear stress and loss of biomass (Doyle 2001).

A primary limitation on the distribution and productivity of macrophytes, and other photosynthetic organisms, is the amount of light available to support metabolism and growth (Spence 1976, Chambers and Kalff 1987, Duarte 1991, Lorenti et al. 1995, Pirc 1985). In some aquatic systems, strong seasonal variations in sunlight,

temperature, and precipitation produce seasonality in the growth of macrophytes (Zimmerman et al. 1994). In Florida's spring-fed systems, however, the major influence is sunlight, a consequence of the stabilizing effect of the groundwater that maintains a relatively constant temperature, volume, and quality of water (Odum 1957). In addition to seasonal variation caused by changes in insolation, the amount of incident light reaching the photosynthetic tissues of macrophytes is affected by attenuation caused by material in the water column and epiphytes growing on their leaves (Kirk 1994). In particular, results in Chapter 2 and 3 indicate that epiphytes cause dramatic reductions in light available to macrophytes, and thereby their productivity. Hence, light availability, which varies across waterbodies, represents an essential factor modulating the productivity of macrophytes (Nelson and Waaland 1997, Buia and Mazzella 1991, Zupo et al. 1997). In this study, light availability controlled gross photosynthetic productivity of *V. americana*, with the relationship between available light and productivity being strong regardless of season and latitude.

One way to make such relationships useful is to develop a simulation model of macrophytic production (Elkalay et al. 2003, Plus et al. 2003, Short 1980, Zimmerman et al. 1994, Madden and Kemp 1996, Bocci et al. 1997, Coffaro and Sfriso 1997, Best and Boyd 2001). The majority of such models have been generated for coastal areas (e.g., Elkalay et al. 2003, Plus et al. 2003) and do not take into account loss of biomass caused by the release or transfer of dissolved organic carbon (DOC). In addition, past models measured growth for whole plants (Elkalay et al. 2003) over time steps of one day (Plus et al. 2003), which may compromise their accuracy. Besides the effects of light, most of these models included nutrient concentrations in the water column (e.g.,

nitrogen or phosphorus) as factors limiting production. There are, however, few substantiated reports of growth of submersed plants in natural freshwater systems being limited by nutrient concentrations (Sytsma and Anderson 1993). In many of Florida's springs, increased nutrient concentrations in the water column are not positively correlated with algal blooms or reductions of macrophytes (Heffernan et al. 2010). In addition, macrophytes can absorb nutrients both through their leaves and their roots, so they can grow under oligotrophic concentrations (Iizumi and Hattori 1982). As a result, Florida's springs can be considered to have ample nutrients for macrophytes. In addition, few models focus on *V*. *americana* (e.g., Best and Boyd 2001), and to the best of my knowledge, no model has been developed for submersed macrophytes in Florida's spring systems. Consequently, I chose to develop a new model, which fills a gap in knowledge of Florida's spring systems.

I constructed a simulation model relating the ability of *V. americana* to convert available light to biomass under the negative influence of epiphytic loads (a V-E model). This model employed a 15-min time step and focused on production by 1-cm sections of leaves. The preliminary model was tested by comparing the results of simulations with field observations from Chapter 3. Furthermore, the influence of epiphytic loads on growth of *V. americana* growth was assessed with scenarios involving plants with no loads of epiphytes. In two other scenarios, plants were considered to have epiphytic loads of 4 and 5 mg DW cm^{-2} of leaf to verify the proposed threshold for epiphytic loads that affect the survival of *V. americana*. In addition, the contribution to photosynthetic production for the youngest sections of leaves were differentiated, given a heterogeneous distribution of epiphytes. The ultimate aim of this modeling is to provide

water resource managers with an objective tool to assess the vulnerability of *V. americana* to epiphytic loads. For example, managers can use an upper threshold for non-detrimental loads of epiphytes as an early warning indicator for the need to protect existing macrophytes from additional epiphytization.

Description of the Model

The model is composed of four main ecological elements, Water, Epiphytic Algae, Light, and *V. americana*, the latter treated hierarchically as Section, Leaf, and Plant (Figure 4-1). In the Chassahowitzka River, Light is the limiting factor for photosynthesis and addition of biomass by *V. americana*. Light availability is influenced by conditions in the Water and by loads of Epiphytic Algae, with both the water column and epiphytes on *V. americana* attenuating incident light. Whatever light reaches the leaves of *V. americana* is used to convert inorganic matter, which is not considered to be limiting, into organic matter that generates addition of biomass (growth) if production exceeds the requirements associated with maintenance of existing biomass, which includes respiration, a loss term associated with the epiphytic load, and a loss term associated with the age of the leaves.

Thus, in the model, the growth of *V. americana* is a result of an interaction between a key extrinsic environmental factor, i.e., light, and key intrinsic characteristics associated with maintenance. The linkages among extrinsic and intrinsic factors are codified via mathematical expressions and statistical relationships related to light attenuation, photosynthesis, respiration, and losses of biomass associated with epiphytic loads and senescence of sections of leaves (Table 4-1).

Growth of *Vallisneria americana*

In its simplest form, growth of leaves of *V. americana* is calculated on the basis of the amount of net photosynthetic production allocated to aboveground biomass, which is expressed as the net photosynthetic production of a section of a leaf multiplied by a factor that determines the quota of production allocated to new leaf biomass (Q_l, Table 4-2). Based on field observations in Chapter 3, the potential for growth varies with leaf age (Figure 4-2). In this model, leaves of *V. americana* are divided into 1-cm sections, with the number of sections (n, Table 4-1) depending on the length of each leaf. The overall net photosynthetic production per leaf is given by the sum of the net production in all sections ($B_{sec,j}$, Table 4-1). Similarly, the net production per shoot (B_s, Table 4-1) is the sum of the net photosynthetic production for all leaves (B_{li}) in that shoot.

The net photosynthetic production for a section ($B_{sec,j}$, Table 4-1) is calculated by subtracting degradative processes that consume photosynthetic product from gross photosynthetic production. In this model, respiration, excretion of dissolved organic carbon (DOC) and senescence and dehiscence induced by epiphytes are the main degradative processes. Therefore, variation in net photosynthetic acquisition ($\frac{dB_{sec,j}}{dt}$, Table 4-1) by *V. americana* can be described by the differential equation: $\frac{dB_{sec,j}}{dt} = \left(P_{sec} - R - L_{DOC} - L_{epi}\right) * A$; where P_{sec} is the photosynthetic rate per 15-min time step for sections of leaves, R is the respiration rate per section and time step, L_{DOC} is the loss of photosynthetic product from DOC excretion, L_{epi} is the loss of product induced by epiphytes, which varies with epiphytic load, and A (cm^2) is the area of a 1-cm^2 section of leaf.

Photosynthesis of *Vallisneria americana*

Since light is the main factor that determines production of *V. americana* biomass in the Chassahowitzka River, gross photosynthetic production is estimated through a Photosynthesis-Irradiance relationship, which is the most commonly used tool to estimate biological productivity in aquatic systems (Kirk 1994). The Photosynthesis-Irradiance relationship is an empirical relationship between light radiation (I_{sec}, Table 4-1) and photosynthetic rate (P_{sec}, Table 4-1), generally expressed as $P_{sec} = \frac{P_{max}*[I_{sec}]}{K_m+[I_{sec}]}$; where P_{sec} is the specific photosynthetic rate per 15-min time step for leaves receiving a given amount of photosynthetically active radiation (PAR), P_{max} is the maximum potential photosynthetic rate, $[I_{sec}]$ is a given amount of incident PAR, and K_m is the irradiance half saturation constant or the amount of PAR needed for photosynthesis to proceed at ½ P_{max}. The values of P_{max}, K_m, I_c (Table 4-2), the light intensity at the compensation point, and I_s (Table 4-2), the light intensity at the saturation point, are taken from the literature. Light availability $[I_{sec}]$ is a crucial factor in estimating photosynthetic production, and it is generated by the light availability module.

Available Light for *Vallisneria americana*

The amount of light reaching the surface of leaves is a function of the light measured at the water surface, and it decreases because of extinction in the water column caused by water molecules, turbidity, and dissolved color, and extinction due to shading by epiphytes. In the water column, incident light decreases exponentially with increasing depth, and increasing epiphytic biomass generates a similar exponential decrease in available light (Kemp et al. 2004). The equation for transmission of light through the water column is given by the Lambert-Beer Law: $I_D = I_0 * e^{-(K_d)(D_{sec})}$

(Kirk 1994); where I_D is the irradiance at depth D_{sec}, I_0 is the amount of incident light, K_d is the extinction coefficient, and D_{sec} is the depth of the leaf section in question. A similar equation describing transmission of light through epiphytes is derived from the results in Chapter 2, and it is expressed as: $I_e = I_0 * a * e^{\frac{-E_{sec}}{b}}$ (Kirk 1994); where I_e is the amount of light that reaches the surface of the leaf after penetrating the epiphytic load, I_0 is the amount of incident light reaching the epiphytes, a and b are constants that can vary among macrophytes and epiphytic communities, and E_{sec} is the epiphytic load on the section in question. The equations can be combined to calculate the amount of light available for photosynthesis as: $I_{sec} = I_0 * e^{-(K_d)(D_{sec})} * a * e^{-E_{sec}/b}$ (Batiuk et al. 1992). The values of constants are derived from fieldwork in Chapters 2 and 3.

Loss of Photosynthetic Product

Respiration, excretion of DOC and loss of biomass caused by epiphytization reduce gains of biomass through photosynthesis in this model. A fraction of the gross photosynthetic production generated by *V. americana* is used to satisfy the metabolic demands of existing biomass, i.e., respiration (Best and Boyd 1999). In general, respiration (R) is influenced by temperature, but I applied a constant respiration rate because groundwater discharges into the Chassahowitzka River create a relatively constant, year-round water temperature of about 25°C (Frazer et al. 2001, Figure 4-4C). The respiration rate (R) is the sum of losses associated with above-ground and below-ground tissues.

The excretion of dissolved organic carbon (L_{DOC}, Table 4-1) represents another non-negligible component of the loss of biomass from macrophytes (Demarty and Prairies 2009, Duarte et al. 2010). In the model, it is described as: $L_{DOC} = ß_{DOC} * P_{sec}$;

where ß$_{DOC}$ is the rate of DOC excretion and P_{sec} is the amount of carbon fixed in photosynthesis.

In addition, epiphytic loads not only reduce the amount of light reaching leaves, their colonization enhances senescence and dehiscence of leaves, which represent additional factors that reduce growth. In the model, these losses are calculated as: $L_{epi} = ß_{epi} * E_{sec} * P_{sec}$, which assumes that a given epiphytic load (E_{sec}) generates a loss (L_{epi}) that is proportional to the amount of gross photosynthetic production (P_{sec}) scaled by a coefficient (ß$_{epi}$) estimated during calibration (Elkalay et al. 2003).

Distribution of Epiphytic Biomass

Loads of epiphytes are generally low on young, fast-growing leaves, whereas older, slower growing leaves are largely colonized; therefore, epiphytic biomass on sections of leaves (E_{sec}) is calculated using a linear function:

$$E_{sec} = r_{epi} * (j - 7) * A$$

$$r_{epi} = \frac{E_l}{(1 * W_l) * \frac{(n-7) * (n-7+1)}{2}}$$

where j is the rank of the section in question (from youngest to oldest), r_{epi} is a scaling coefficient for epiphytic biomass, A, E_l, and n are the area of a section, epiphytic biomass found on the whole leaf, and the total number of sections comprising the leaf in question, respectively. The coefficients in these two equations are derived from the results in Chapter 3 (Figure 3-10) that indicated that epiphytic biomass increased linearly with distance above a bottommost 7-cm section that was generally free of epiphytes.

Simulations

In this simplified model, the *V. americana* meadows were assumed to exist in an environment free of pests, diseases, and competitors, with suitable weather and an ample supply of nutrients. Intraspecific competition for light (self-shading) is not considered because water currents move the leaves constantly, keeping exposure to available light fairly even.

In addition to these extrinsic factors, the growth of *V. americana* relies on the intrinsic factors as well (Ott 1979). All plants are assumed to be at the same developmental phase, and substantial transfers of organic matter do not occur between leaves and non-photosynthetic rhizomes and roots. Moreover, losses through herbivory, sloughing of leaves and fragmentation were not included in this model, given the focus on a short time interval (~7 days).

All calculations were performed for 1-cm-long sections of leaves at 15-min time steps using the Python programing language. Simulations were run from 13 June 2016 to 22 August 2016 (62 days), which was the period when meadows in the Chassahowitzka River were sampled (Chapter 3). This approach allowed comparisons between simulated and measured data. These measurements of growth (mg DW per week) as a function of epiphytic load (mg DW cm^{-2} of leaf) displayed a marked exponential decline, with scattered values below this boundary (Figure 4-3). Transmission of light through epiphytes displayed a similar relationship (Chapter 2), which suggests a cause-and-effect relationship. Thus, I believe that data constituting the upper boundary of the growth versus epiphytic load curve represent those leaves influenced primarily by epiphytic loads, whereas data under the boundary represent those leaves influenced by epiphytes and other factors (e.g., grazers, substrates, and

nutrients). The model was calibrated initially using data on the boundary to establish parameters related to epiphytic loads, and then run for the rest of data without changing any parameters. The estimated values of some parameters were similar to values reported in the literature (Table 4-2), which gives me confidence in my ability to estimate other parameters. Other data related to *V*. *americana* (e.g. ages of leaves, lengths and widths of leaves, dry weights of leaves, epiphytic loads on leaves, and areas and dry weights of new growth were taken from the results of field experiments in Chapter 3.

Values for relevant driving variables were obtained from several sources (Figure 4-4). Photosynthetically active radiation (PAR) reaching the water surface was obtained from the Florida Automated Weather Network (FAWN) Lecanto station (N28°49'44", W82°29'56", ~14.25 km from study area). Water depth and water temperature were obtained from the USGS station at the head-spring of the Chassahowitzka River (No. 02310650, N28°42'54", W82°34'37). These data were calibrated to match *in situ* measurements recorded during each sampling event (Chapter 3) that were proportional to the *in situ* measurements scaled by a coefficient. The discrepancy was computed between the *in situ* measurements and the calibrated data on the temporal period of *in situ* measurements. The calibrated data for PAR and water depth can capture 84.58% and 69.48% of *in situ* measurements.

Sensitivity Analysis

A sensitivity analysis investigated the impact of variation in parameters on the model's outputs. Each parameter was modified by $\pm$20%, and the model was run using one modified parameter at a time. Then, results of the series of runs were analyzed with a sensitivity index (SI, Chapelle et al. 2000):

$$SI = \frac{100}{p * n} * \sum_{i=1}^{n} \frac{\left|X_i - X_i^{ref}\right|}{X_i^{ref}}$$

where p is the percentage of variation applied to a parameter ($\pm$20%), n is the number of simulated plants (60), X_i is the new state value generated with the new parameter value, and X_i^{ref} is the reference state value derived using the original calibrated parameters. Afterwards, mean SI values were calculated for of +20% and -20%.

Results and Discussion

The model supports different simulations. I focused on representative scenarios that exemplify insights that can be derived using this model.

Use of Boundary Data to Estimate Detrimental Effects of Epiphytes

The set of data bounding measurements of growth for leaves with differing epiphytic biomass was used to calibrate the model (Figure 4-3), with the resulting predictions showing good agreement with field measurement (R^2= 85%, Figures 4-5A and 4-5B). The steep slopes of the initial declines imply that epiphytes on *V. americana* strongly influence growth of leaves (Figure 4-5A). Growth was near zero at loads of approximately 300 mg DW per leaf (~4.6 mg DW cm^{-2} of leaf).

Given these results, a method to estimate the vulnerability of *V. americana* to epiphytic loads involves application of the negative exponential curve that fits the data on the boundary (Figure 4-3). The equation $y = 47 * e^{-\frac{x}{1.07}}$ describes the growth of *V. americana* leaves (y) as a function of epiphytic loads (x). This empirical model provides an estimate of growth potential given a stipulated epiphytic load, based on an assumption that epiphytes are the only environmental influence. Thus, the estimates do

not account for influences of other factors (e.g., light and leaf age). Nonetheless, the approach can provide managers with useful information regarding the health of macrophytes.

Comparative Modeling for Salt Creek and Small Creek

To test the model's applicability and universality, it was applied separately to data from Salt Creek and Small Creek. A total of 63 *V. americana* plants (607 leaves) from Salt Creek and 47 plants (524 leaves) from Small Creek yielded inputs for the model. Predicted values showed good concordance with field observations from both creeks, with R^2 = 67% and R^2 = 62%, respectively (Figure 4-6). The root mean square deviation (RMSD) assesses how well a model describes a system, and the values were 19.14 and 39.23 for Salt Creek and Small Creek, respectively (Figures 4-6A and 4-6B). The higher RMSD for Small Creek (Figure 4-6B) highlights a more scattered distribution than that for Salt Creek (Figure 4-6A). One potential reason for this scatter may be the more complex light regime in Small Creek caused by shading from riparian vegetation. For example, the degree of shade changed with sun angle, but the model did not account for this variation. The maximum predicted growth per week is 154 and 256 g DW per shoot for Salt Creek and Small Creek, respectively (Figure 4-6). More growth in Small Creek can be attributed to lower epiphytic densities (Chapter 3).

To differentiate the contributions to net photosynthetic production by 1-cm sections of leaves, plants were separated into a Salt Creek batch and a Small Creek batch, and the net photosynthetic production of each section of leaf was calculated (Table 4-4). For Salt Creek, positive (+) net photosynthetic production disappeared above the section at 15 cm from the base or (0 cm), which implied that sections from 15 cm to the apex of the leaf (87 cm) did not contribute to accumulation of energy

by a plant, but rather those sections consumed energy. For Small Creek, where epiphytic loads were lower (Chapter 3), the negative (-) net photosynthetic production began at 36 cm to 48 cm from the leaf base. The reason Salt Creek exhibited larger negative net photosynthetic production is because higher light levels generated heavier loads of epiphytes on younger sections of leaves (Mazzella and Ott 1984, Dunn et al. 2008, Frankovich and Zieman 2005, Orth and Moore 1983, Doyle 2001).

Thus, the model suggests that younger photosynthetic tissues near the base of *V. americana* leaves serve as the most important contributors to the energy needed to support growth. This conclusion contrasts with results from other studies (Titus et al. 1975, Elkalay et al. 2003) and contradicts the intuitive hypothesis that the optimum photosynthetic tissues for submersed macrophytes are near the water surface, where there is greater light availability. Evidence also suggests that *V. americana* can survive and grow with low levels of available light because of its efficient use of light (Best and Boyd 2001), and in my study area, shallow, clear water may ensure sufficient light reaches the base of shoots.

Modeling Growth in the Absence of Epiphyte Loads

The negative impacts of epiphytic loads were evaluated with a comparison of the predictions from a scenario with no epiphytic loads and one using observed epiphytic loads. Without impacts from loads of epiphytes, all sections had positive net photosynthetic production (Table 4-4). The basal sections (0-10 cm) remained the most important areas for photosynthesis, generating +30.55% and +40.43% of the net photosynthetic production in Salt Creek and Small Creek, respectively. Although positive net photosynthetic production was generated by every section, less total

production was generated by older sections near the tips of leaves, which is probably a consequence of a decrease in the number of sections contributing.

Two methods were used to assess the degree of impact generated by epiphytes: $\Delta y = P_{net}^{epi=0} - P_{net}^{field\ epi}$ and $R = \frac{P_{net}^{epi=0} - P_{net}^{field\ epi}}{P_{net}^{epi=0}}$; where $P_{net}^{epi=0}$ and $P_{net}^{field\ epi}$ represent the net photosynthetic production of plants with no epiphytic loads and those with the observed epiphytic loads, respectively. The equations generate values for Δy, the absolute difference between net photosynthetic production under different epiphytic loads, and R, which represents a relative difference scaled to the scenario with no epiphytes.

The absolute differences in net photosynthetic production increased linearly with intensity of epiphytization in Small Creek (Figure 4-7A and 4-7B), and the relative differences displayed a positive, logarithmic relationship to increasing epiphytic loads (Figures 4-7C and 4-7D). Epiphytic loads of 10.9 to 716.8 mg DW per plant (0.085 to 2.37 mg DW cm^{-2} of leaf) led to the losses of 14.26 to 311.13 mg DW, which equate to 0.0096 to 3.88 times the net photosynthetic production achieved by *V. americana* in Small Creek.

Compared to Small Creek, the differences in net photosynthetic production (Δy and R) in Salt Creek did not exhibit an obvious relationship to increasing epiphytic loads (145 to 15211 mg DW per plant or 0.67 to 32.37 mg DW cm^{-2} of leaf, Figures 4-8A, 4-8B, 4-8C and 4-8D). The higher epiphytic loads generated larger decreases in net photosynthetic production, with maximum Δy reaching 704.92 mg DW, which is 15 times higher than the net photosynthetic production achieved by *V. americana* in Salt Creek. At lower epiphytic loads (< 6 mg DW cm^{-2}), relative differences in net

photosynthetic production exhibited a certain degree of linearity (R^2 = 0.45) as epiphytic loads increased (Figure 4-8E).

Stratifying Epiphytic Loads

When studying the influence of epiphytic loads on growth of *V. americana*, it is important to express density of epiphytes in a useful way. In this chapter, epiphytic loads were expressed in mg DW per plant and mg DW cm^{-2} of leaf; however, these two methods do not describe the characteristic distribution of epiphytes on plants. Some larger plants have larger surface area that, in total, carries more epiphytic biomass, but weights of epiphytes do not translate directly into cover on leaves. Leaf area is an important variable for most ecophysiological processes, including absorbtion of light, respiration, photosynthetic efficiency, absorption of nutrients, and plant growth (Blanco and Folegatti 2005); therefore, standardized epiphytic loads per unit area of leaves was employed. This method effectively eliminates the influence of plant size, but it cannot reflect the heterogeneous distribution of epiphytic biomass in the real world.

I used field data to stratify epiphytic loads (mg DW cm^{-2} of section) for 1-cm sections because they should experience similar depths, incident light intensities, and macrophyte architecture (Gosselain et al. 2005). Epiphytic loads for sections varied from algal-free in sections 1-7, through a linear increase to 35 mg DW cm^{-2} for sections 8-50, and then stabilization until section 84, with a few sections beyond this point having up to 50 mg DW cm^{-2} of section (Figure 4-9A).

Using the stratified method to express epiphytic loads, I evaluated absolute and relative differences in net photosynthetic production caused by different epiphytic loads (Figures 4-9B and 4-9C). At low epiphytic loads (< 6 mg DW cm^{-2} of layer), the impacts on net photosynthetic production increased rapidly with increased epiphytic loads

(Figures 4-9B and 4-9C). After this point, absolute differences declined with increasing epiphytic loads (Figure 4-9B), mainly because fewer sections contribute to the total decrease (Table 4-4). Relative differences reach an asymptote at about 1.1 mg DW cm^{-2} of section (Figure 4-9C). These phenomena imply that epiphytic loads in the Chassahowitzka River make a maximum impact on growth, in large part because the filamentous epiphytic algae add biomass by extending away from the leaf surface without covering more surface area. Some relative difference values (R) are greater than 1 is because layers with higher epiphytic loads (>8 mg DW cm^{-2} of section) have negative net photosynthetic production, which makes $P_{net}^{epi=0} - P_{net}^{field\ epi} > P_{net}^{epi=0}$.

Scenarios with Epiphytic Loads of 4 mg DW cm^{-2} and 5 mg DW cm^{-2}

To test for a threshold epiphytic load that prevents growth of *V. americana*, simulations were performed with total epiphytic loads of 4 mg DW cm^{-2} of leaf and 5 mg DW cm^{-2} of leaf for fourteen *V. americana* plants. Loads of epiphytes were assumed to increase linearly from the base of the leaves to their tip. With epiphytic loads of 4 mg DW cm^{-2} of leaf, two of the fourteen plants generated positive net photosynthetic production, and the others exhibited no net photosynthetic accumulation. Furthermore, no net photosynthetic production was achieved by any of the 14 plants with epiphytic loads of 5 mg DW cm^{-2} of leaf. To a certain extent, these results indicate that the threshold for detrimental epiphytic loads for *V. americana* is between 4 and 5 mg DW cm^{-2} of leaf. This conclusion agrees with results in Chapters 2 and 3.

Based on this critical threshold, I calculated that, in the Chassahowitzka River, the minimum light required to support growth of *V. americana* is 20-26% of incident

surface irradiance, which is a value that is in agreement with the 21% proposed by Chambers and Kalff (1985).

Sensitivity Analysis

To test the sensitivity of the model to variation in its component parameters, I increased and decreased each of the main parameters by 20%. The model is sensitive ($\overline{SI}$ ≥ 0.25) to variation in: the fraction of net photosynthetic production allocated to increasing leaf tissue (Q_l), the maximum potential rate of photosynthetic production (P_{max}), respiration rate (R), coefficient of epiphytic light attenuation, and coefficient of epiphyte-induced biomass loss ($ß_{epi}$, Figure 4-10). The model based on the photosynthesis-irradiation curve is most sensitive to P_{max}. The sensitivity analyses highlighted the need for accurate estimates of parameters that influence production and link production to epiphytic loads. Other parameters, such as the coefficient for light attenuation in the water column (K_d), the half saturation constant (K_m), and saturating light intensity (I_s) have only minor effects on results (0.05 ≤ $\overline{SI}$ <0.25), probably because the shallow water at my study sites attenuates only a small amount of light and incident light is always sufficient for maximum growth of submersed macrophytes like *V. americana*, a shade-tolerant plant. Further evidence that light is not limiting comes from the fact that the model is not sensitive to variation in the compensation point (I_c, $\overline{SI}$ <0.05).

Summary

The model produced predictions that agreed well with *in situ* measurements (R^2= 67%), and it supported useful simulations of growth of *V. americana* subject to different epiphytic loads in the Chassahowitzka River. The inclusion of light, water

depth, and epiphytic biomass, seemed to capture the most important influences on the growth of *V. americana*. Moreover, the importance of epiphytic loads has been confirmed by the model, particularly regarding competition for light.

The model considers 1-cm sections of leaves and a 15-min time step, which was meant to increase the accuracy of predictions relative to previous studies (Elkalay et al. 2003, Plus et al. 2003). In particular, the importance of the basal part of the leaves of *V. americana* in generating a substantial portion of the total photosynthetic production of a whole plant is indicated clearly by this model, but seldom considered in other physiological or ecological studies. In addition, DOC excretion appears to be a non-negligible loss of biomass (Demarty and Prairies, 2009), so it is important to include this component in models of growth for *V. americana*.

Various scenarios highlighted the processes incorporated into the model and provided insights into potentially important ecological effects. The scenario with no epiphytic load indicated that the detrimental effect of epiphytes on growth occurs at a relatively low biomass. When the effect reaches a certain level, adding filamentous algae adds biomass, but it does not shade more tissue or reduce growth of the macrophyte substantially. In addition, scenarios demonstrated that epiphytic loads of 4 to 5 mg DW cm^{-2} of leaf represent a likely threshold beyond which leaves of *V*. *americana* do not grow.

Because of the sensitivity of *V. americana* growth to increasing epiphytic loads, epiphytes can be used key bioindicators for monitoring the health of spring-fed systems. The model presented here serves as a tool for simulating the effects of epiphytic loads

on *V. americana*, and it provides support for water resource managers to improve management of these important systems.

Table 4-1. Equations comprising the growth and production model for *Vallisneria americana*.

Parameter	Process	Equation	References
B_s	Shoot growth (mg DW per week)	$B_s = \sum_{i=1}^{N} B_{li}$	
B_{li}	Leaf growth (mg DW per week)	$B_{li} = \begin{cases} Q_l * \sum_{j=1}^{n} dB_{sec,j} \\ 0, if \sum_{j=1}^{n} dB_{sec,j} < 0 \end{cases}$	Best and Boyd (2001)
$B_{sec,j}$	Net production per section (mg DW per 15min)	$\frac{dB_{sec,j}}{dt} = \left(P_{sec} - R - L_{DOC} - L_{epi}\right) * A$	Elkalay et al. (2003)
P_{sec}	Gross photosynthetic production per section (mg CO_2 m^{-2} per 15 min)	$P_{sec} = \begin{cases} P_{max}, if\ I_{sec} \geq I_s \\ \frac{P_{max} * [I_{sec}]}{K_m + [I_{sec}]}, if I_c \leq I_{sec} \leq I_s \\ 0, if\ I_{sec} \leq I_c \end{cases}$	Kirk (1994)
I_{sec}	Available light for section j (µE m^{-2} s^{-1})	$I_{sec} = \begin{cases} I_0 * e^{-(K_d)(D_{sec})} * a * e^{\frac{-E_{sec}}{b}}, if E_{sec} > 0 \\ I_0 * e^{-(K_d)(D_{sec})} * 1, if E_{sec} = 0 \end{cases}$	Batiuk (1992)
L_{epi}	Biomass loss induced by epiphytes (mg CO_2 m^{-2} per 15 min)	$L_{epi} = ß_{epi} * E_{sec} * P_{sec}$	Elkalay et al. (2003)
L_{DOC}	Biomass loss for DOC excretion	$L_{DOC} = ß_{DOC} * P_{sec}$	Penhale and Smith (1977)
E_{sec}	Epiphytic biomass (mg DW cm^{-2} of leaf) of section j	$E_{sec} = \begin{cases} r_{epi} * (j-7) * A \\ 0, if\ j \leq 7 \end{cases}$	This study
D_{sec}	Water depth (m) of section j	$D_{s□c} = \begin{cases} \frac{D - j + 0.5}{100} \\ 0, \quad if\ D < j \end{cases}$	This study
r_{epi}	Epiphytic biomass ration per leaf (mg DW cm^{-2} of leaf)	$r_{epi} = \begin{cases} \frac{E_l}{A * \frac{(n-7)*(n-7+1)}{2}}, if\ n > 7 \\ 0 \end{cases}$	This study
A	Section area (cm^2)	$A = 1\text{cm} * \text{W}$	
n	Number of layers	$n = ing□ter\ of\ (\frac{L}{1cm})$	

Table 4-2. Parameters comprising the growth and production model for *Vallisneria americana*.

Parameter	Description	Value	References
Q_l	Fraction of net photosynthetic production allocated to leaf	0.8	Best and Boyd (2001)
R	Respiration Rate (mg CO_2 m^{-2} per 15 min)	2.57	Penning de Vries and Van Laar (1982)
P_{max}	The maximum potential photosynthetic production (mg CO_2 m^{-2} s^{-1})	0.12	Titus and Adams (1979)
K_m	The irradiance half saturation constant (µE $m^{-2}s^{-1}$)	123.08	Titus and Adams (1979)
I_c	The light intensity at compensation point (µE $m^{-2}s^{-1}$)	9.4	Titus and Adams (1979)
I_s	The light intensity at saturation point (µE $m^{-2}s^{-1}$)	846.15	Titus and Adams (1979)
K_d	Water column light attenuation coefficient ($1/m$)	1.56	Measurements
a	Epiphytic load light attenuation constant 1	0.3	This study
b	Epiphytic loads light attenuation constant 2	2	This study
ß$_{epi}$	Coefficient of epiphyte-induced biomass loss (cm^2 of leaf/mg DW)	0.2-0.75	This study
ß$_{DOC}$	Coefficient of biomass loss for DOC excretion	0.4	Penhale and Smith (1977)
N	Number of leaves per shoot		Measurements
j	Section number		
L	Length of leaf (cm)		Measurements
W	Width of leaf (cm)		Measurements
D	Water depth (cm)		Calibrated with data from USGS
I_0	Incident light radiation (µE m^{-2} s^{-1})		Calibrated with data from FAWN
E_l	Leaf epiphytic biomass (mg DW cm^{-2} of leaf)		Measurements
dt	Time step (min)	15	Fixed
T	Temperature (℃)	25	Fixed

Table 4-3. Conversions used in the growth and production model for *Vallisneria americana*.

Description	Units conversion rate	References
Solar radiation unit conversion	$1W/m^2 = 2.04\mu E/(m^2 * s)$	Environmental Growth Chambers
Leaf dry weight and area unit conversion	Old leaves: $1\ cm^2 = 3.28g\ DW$ New leaves: $1\ cm^2 = 1.68mg\ DW$	This study
Metabolite unit conversion	$1\frac{gCH_2O}{gDW * d} = 256.86\frac{mgC0_2}{m^2 * 15min}$	This study
Synthetic product unit conversion	$1\ mg\ CO_2 = 0.68\ mg\ DW$	Duarte (1992)

Table 4-4. Percentages of net photosynthetic production for sections of *Vallisneria americana* leaves. “+” represents positive net photosynthetic production, which implies biomass accumulation; “-” represents negative net photosynthetic production, which implies loss of biomass.

Stratified leaves (cm)	Salt Creek			Small Creek		
	Section count	Field observed epiphytic loads	Epiphytic load = 0	Section count	Field observed epiphytic loads	Epiphytic load = 0
81-90(Apex)	21	-0.24%	+0.11%			
71-80	75	-0.77%	+0.44%			
61-70	288	-0.98%	+1.65%			
51-60	719	-2.56%	+4.06%			
40-50	1393	-4.67%	+7.98%	97	-0.16%	+0.56%
31-40	2147	-6.98%	+12.21%	524	+0.5%	+5.80%
21-30	3226	-8.44%	+18.08%	1873	+7.27%	+20.41%
11-20	4654	-1.77%	+24.91%	3343	+25.91%	+32.81%
0-10(Base)	6126	+125.72%	+30.55%	4621	+66.49%	+40.43%

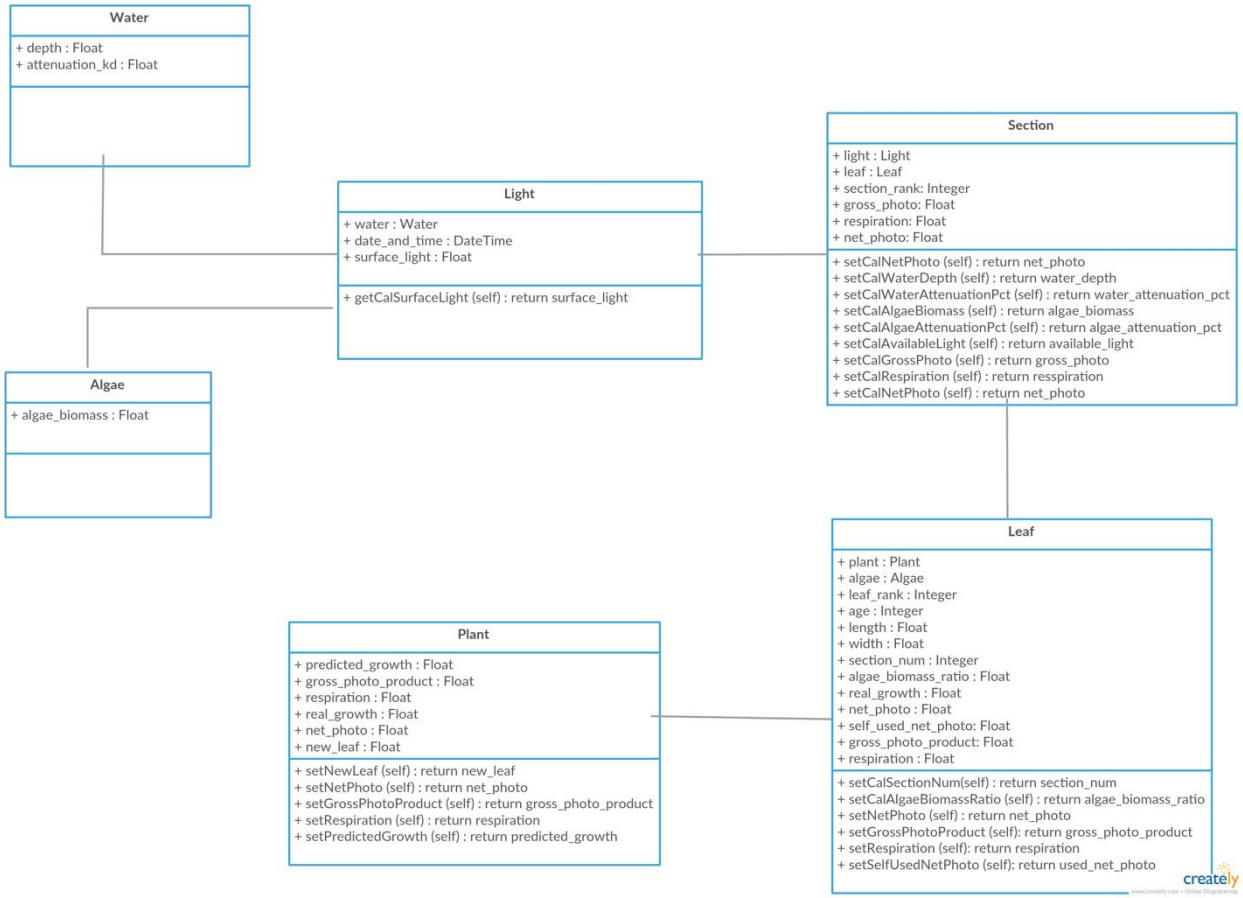

Figure 4-1. Unified modeling language diagram for the Chassahowitzka Spring system. Diagram shows the structure and dynamic behavior among: Water, Epiphytic Algae, Light Irradiation, and *Vallisneria americana* (hierarchically expressed as Section, Leaf, and Plant). The objects in the ecosystem are represented by compartments and interactions are represented by the links.

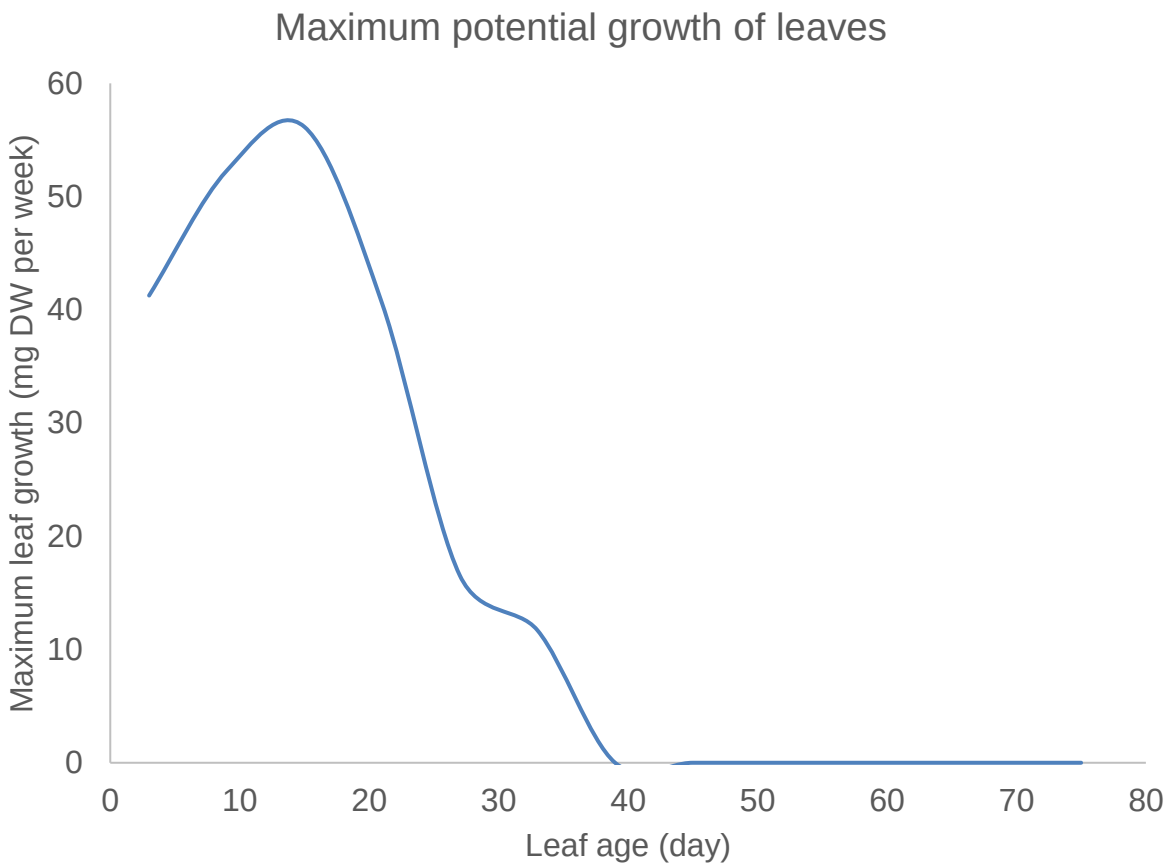

Figure 4-2. Maximum potential growth (mg dry weight [DW] per week) for *Vallisneria americana* leaves of different ages.

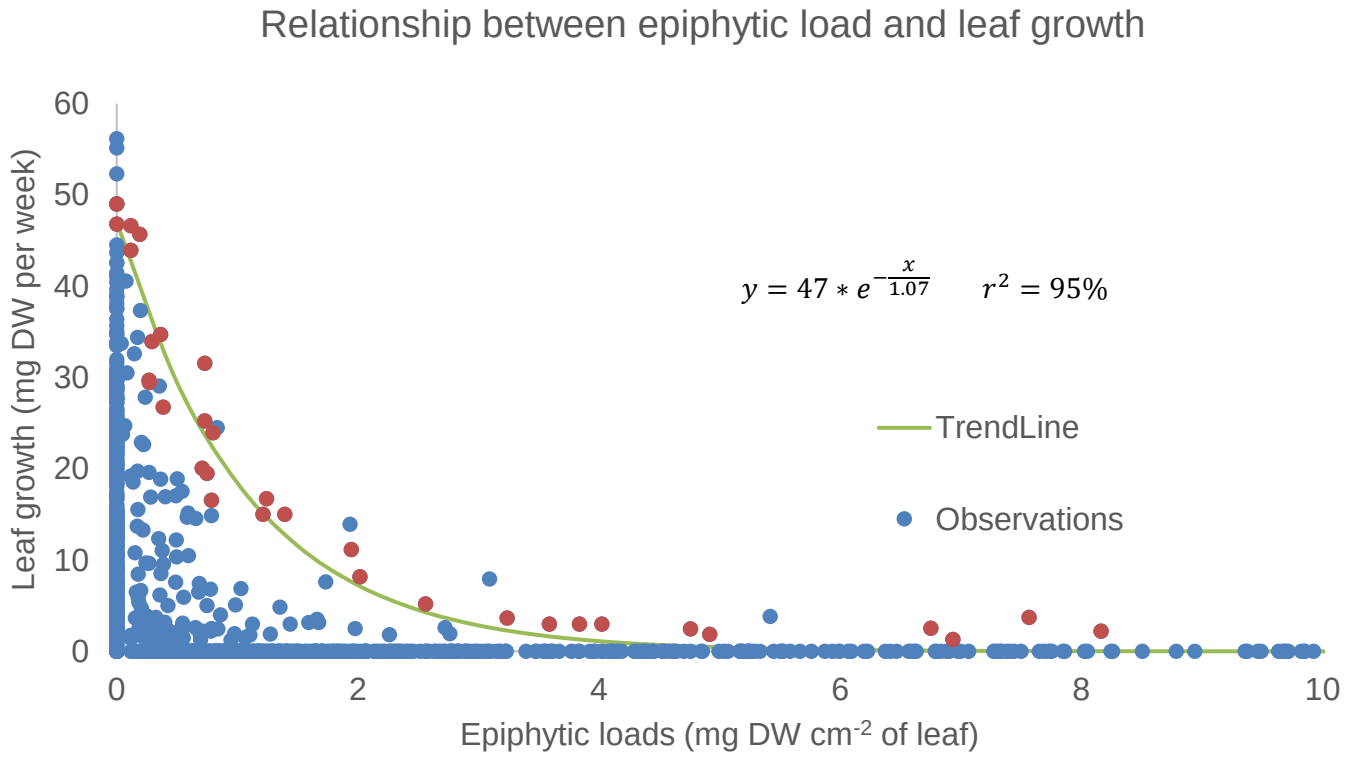

Figure 4-3. Observed growth of *Vallisneria americana* leaves (mg DW per week) as a function of epiphytic load (mg DW cm^{-2} of leaf). Observations on the boundary (orange dots) display an exponential decline (green line) of the form $y = 47e^{-\frac{x}{1.07}}$, with $r^2 = 95\%$.

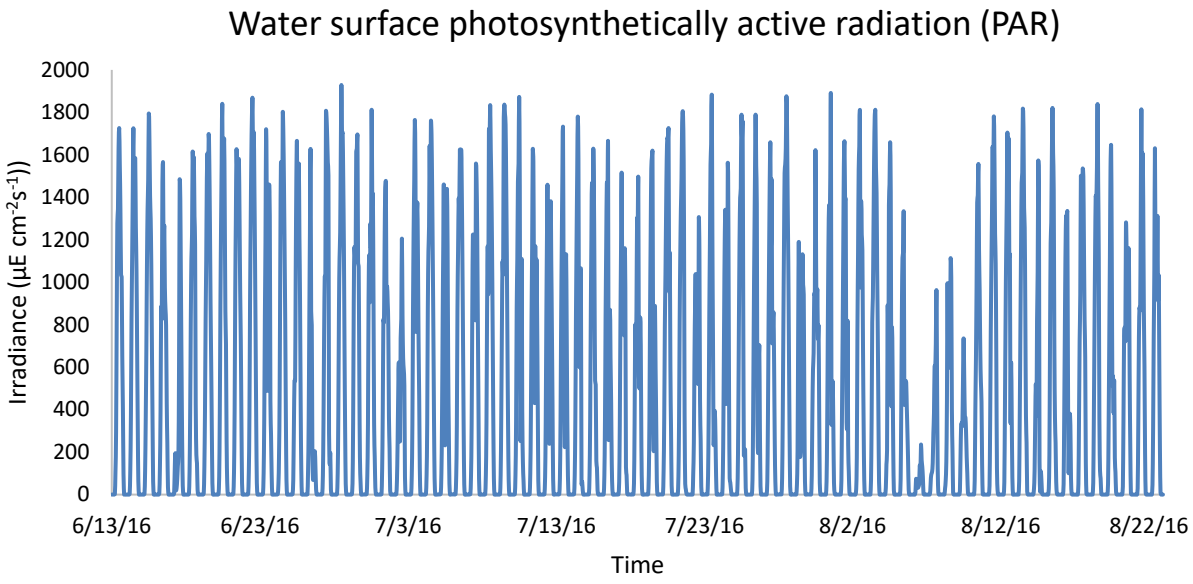
Water surface photosynthetically active radiation (PAR)
Irradiance (µE cm-2s-1))
2000
1800
1600
1400
1200
1000
800
600
400
200
0
6/13/16
6/23/16
7/3/16
7/13/16
7/23/16
8/2/16
8/12/16
8/22/16
Time

A

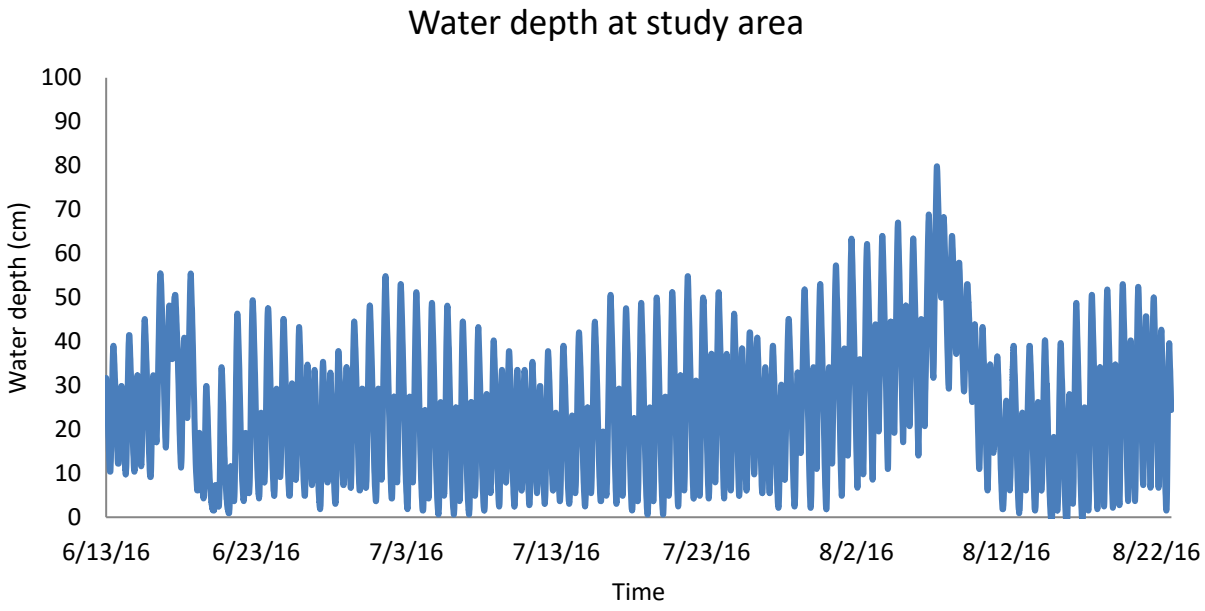
Water depth at study area
Water depth (cm)
100
90
80
70
60
50
40
30
20
10
0
6/13/16
6/23/16
7/3/16
7/13/16
7/23/16
8/2/16
8/12/16
8/22/16
Time

B

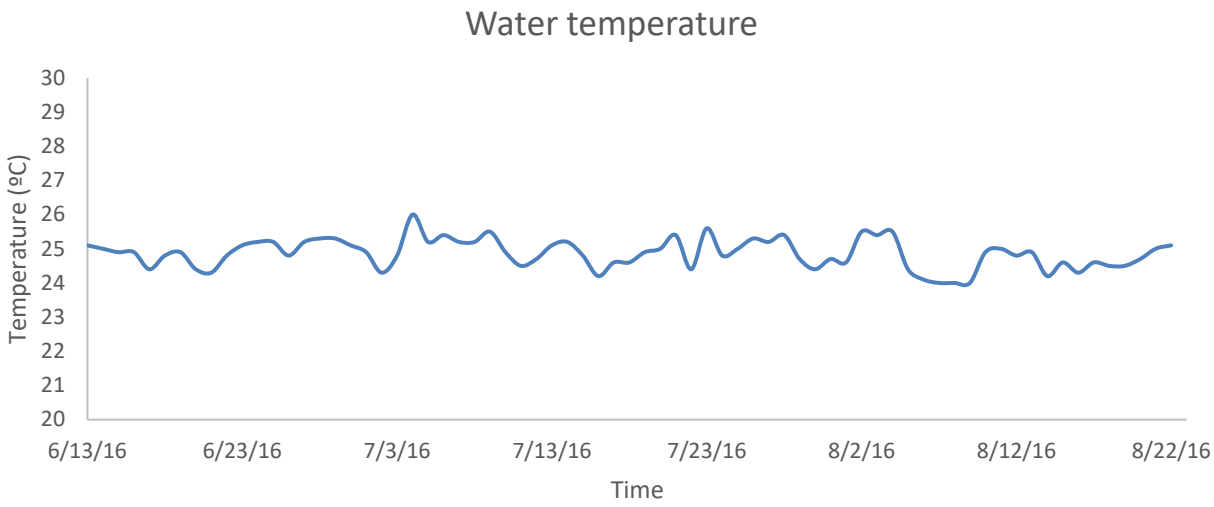

C

Figure 4-4. Variables used in the growth and production model for *Vallisneria americana*. A) Photosynthetically active radiation (PAR) at the surface of the water. B) Water depth. C) Water temperature.

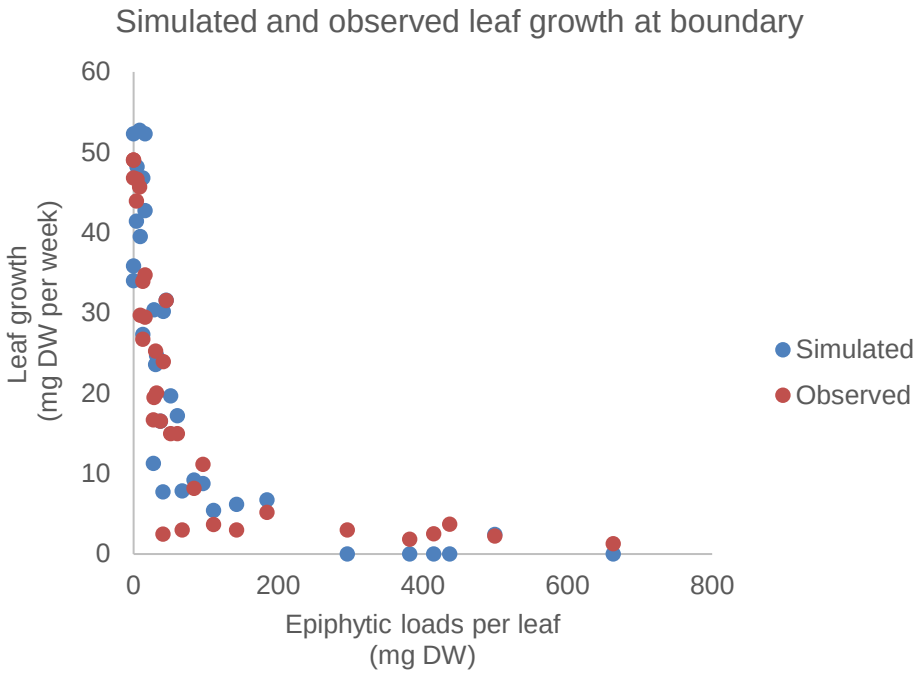

A

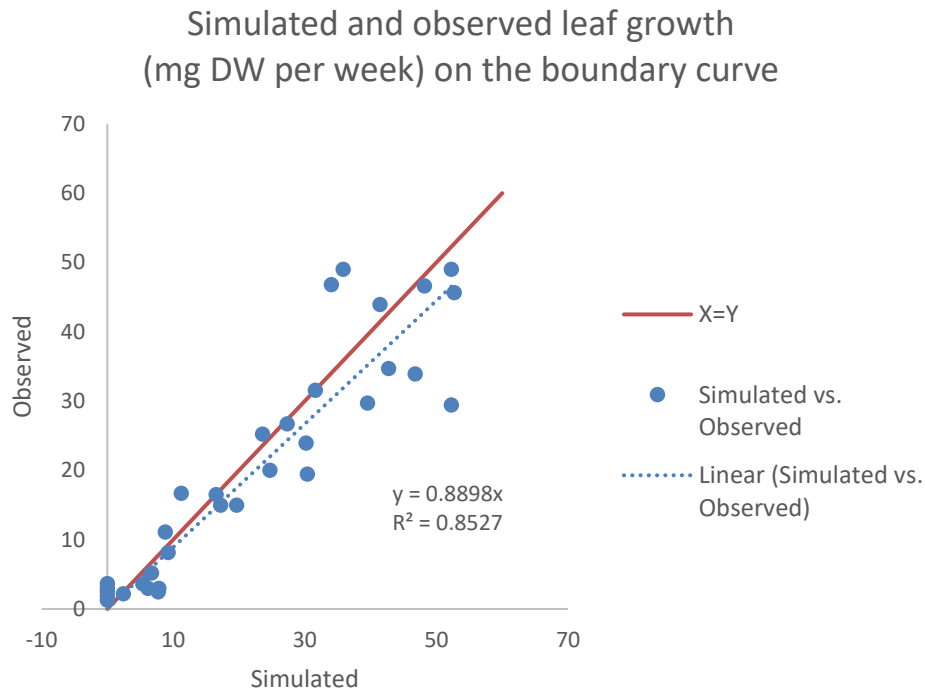

B

Figure 4-5. Comparison of simulated and maximum observed growth of *Vallisneria americana* leaves with different epiphytic loads. A) Actual growth (mg dry weight [DW] per week). B) Model predictions versus *in situ* measurements (n=33).

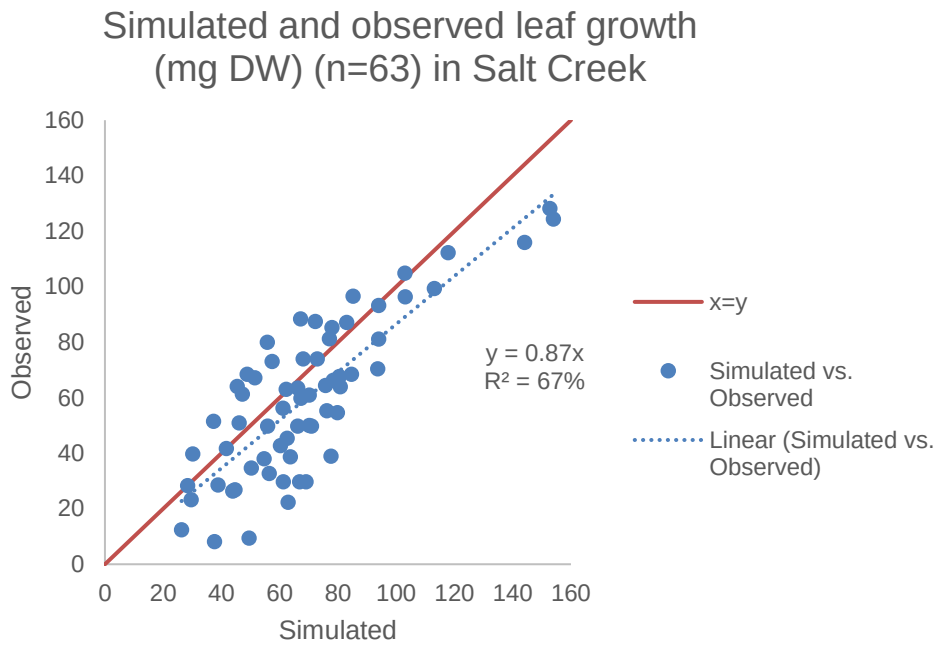

A

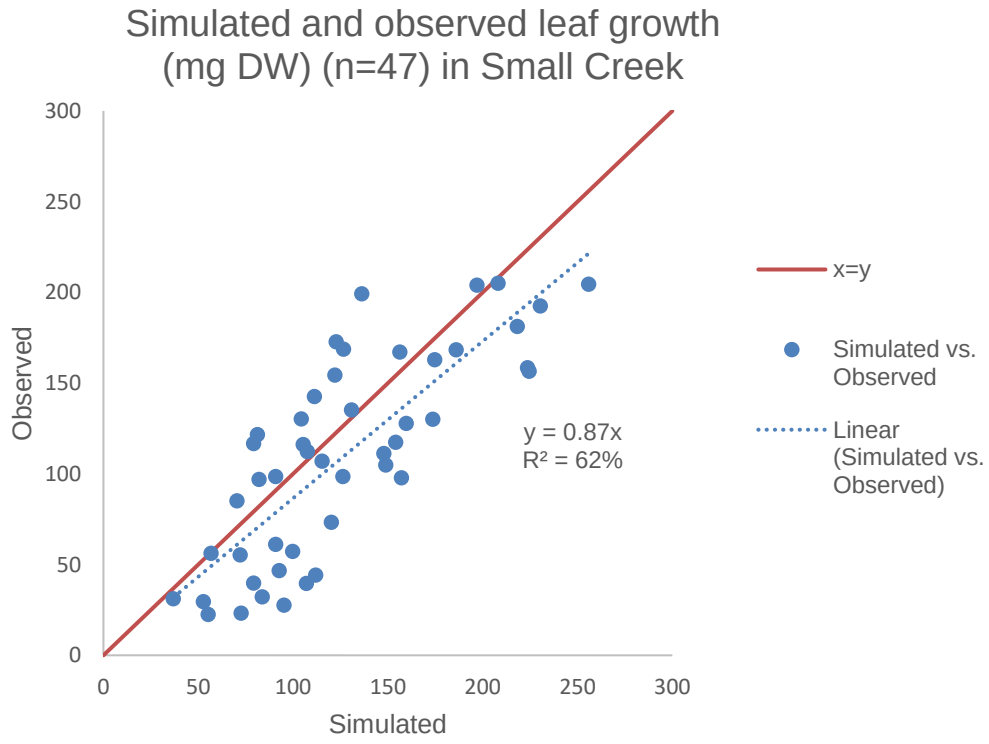

B

Figure 4-6. Comparison of model predictions with *in situ* measurements of growth for leaves of *Vallisneria americana*. A) Plots are for leaves from Salt Creek with R^2= 67% (n=63). B) Plots are for leaves from Small Creek with R^2= 62% (n=47).

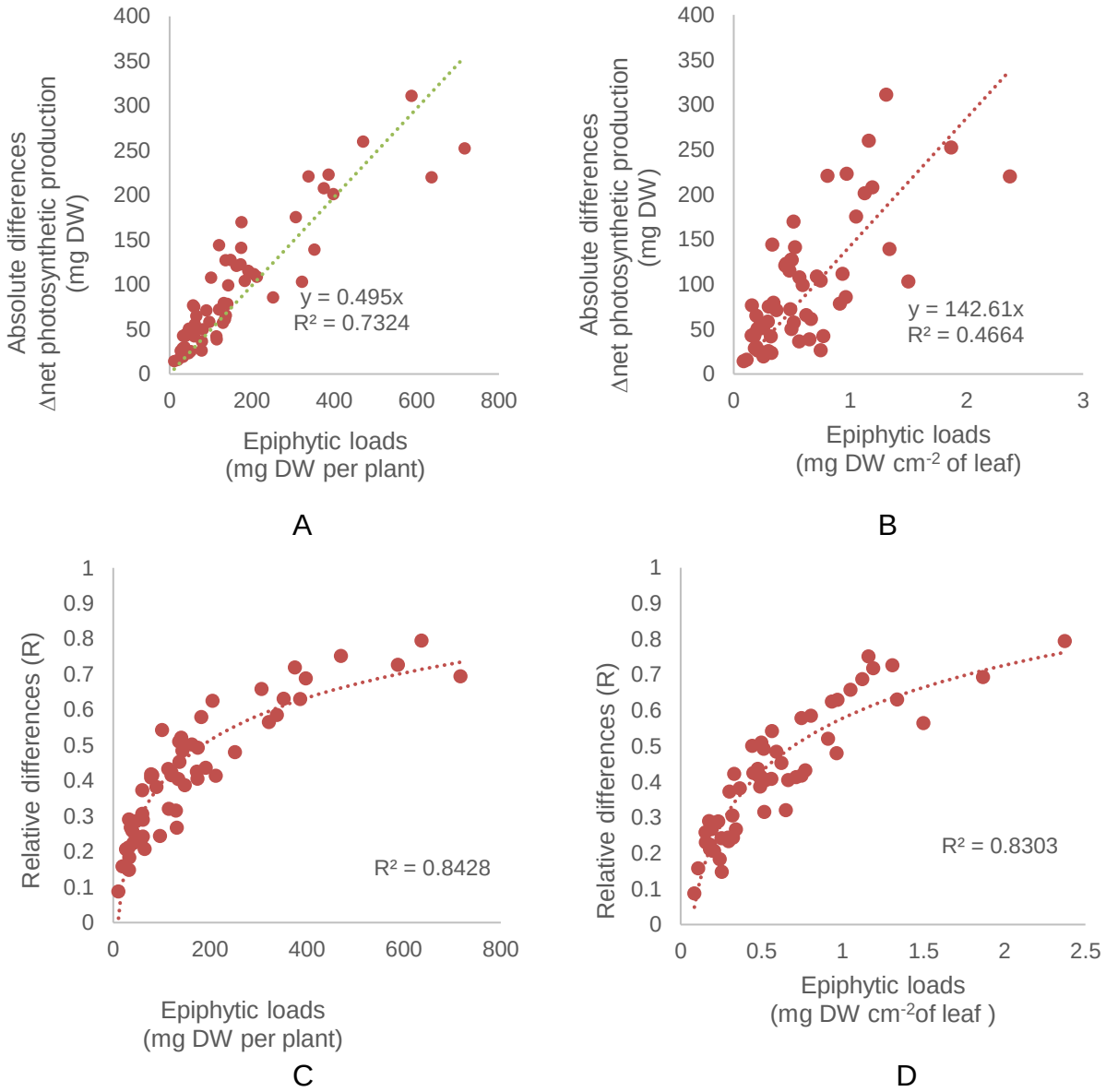

Figure 4-7. Differences in net photosynthetic production for leaves of *Vallisneria americana* with different epiphytic loads from Small Creek. A) and B) Plots show absolute differences (Δ net photosynthetic production). C) and D) Plots show relative differences (R).

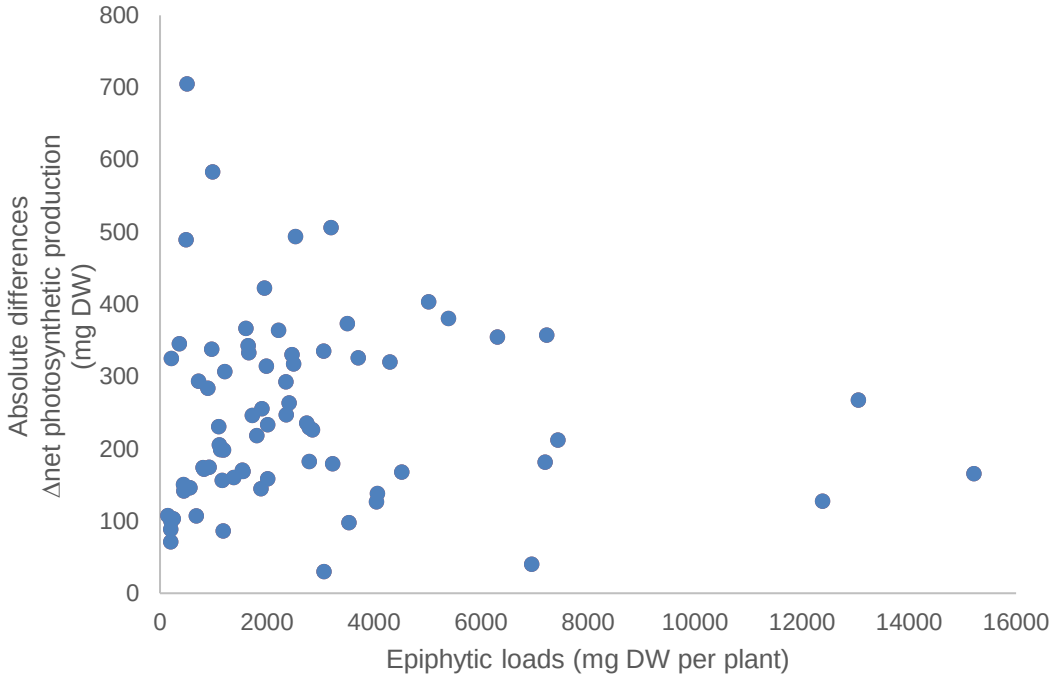

A

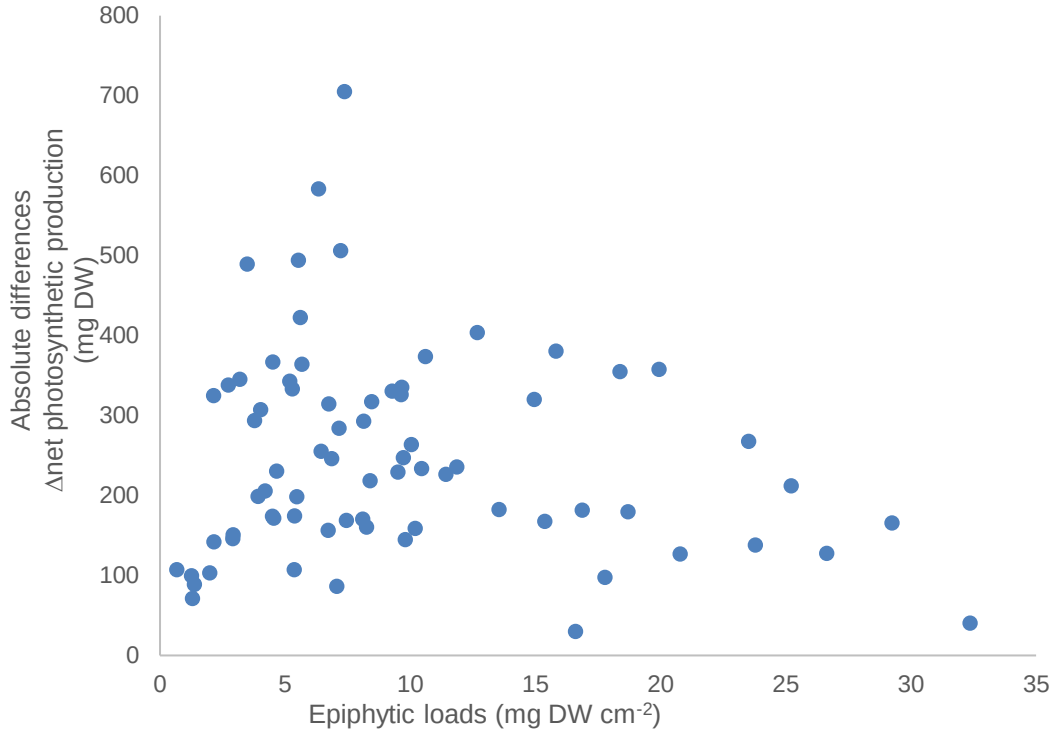

B

Figure 4-8. Differences in net photosynthetic production for leaves of *Vallisneria americana* with different epiphytic loads from Salt Creek. A) and B) Plots show absolute differences (Δ net photosynthetic production). C), D) and E) Plots show relative differences (R).

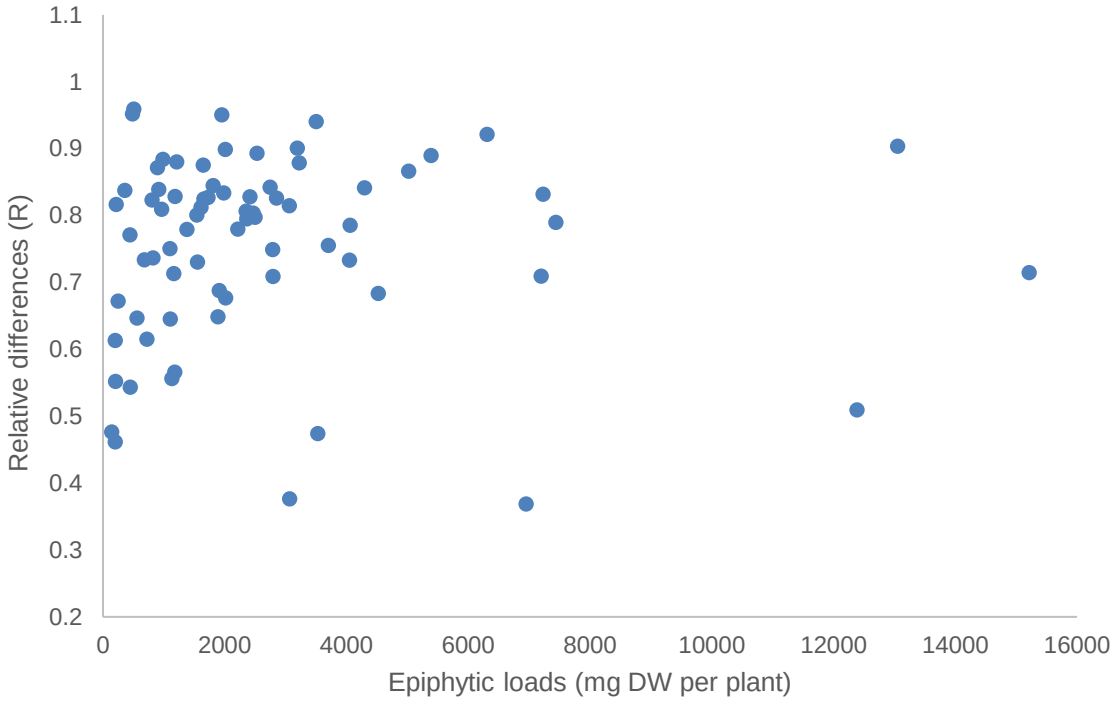

C

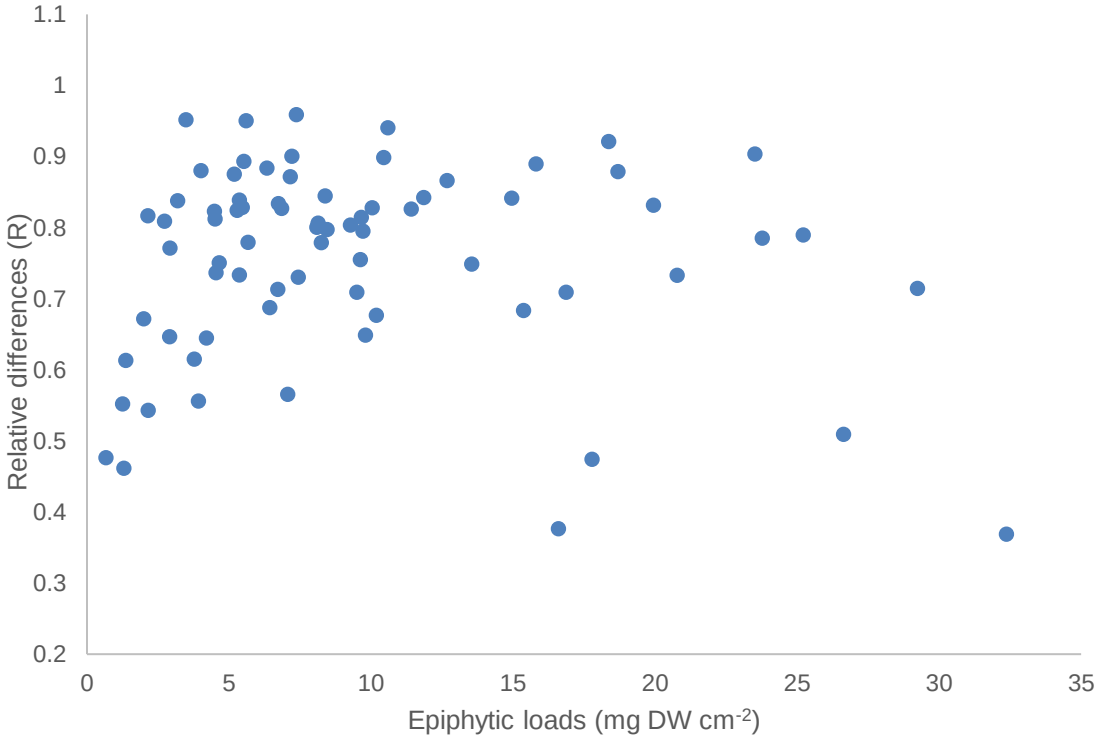

D

Figure 4-8. Continued.

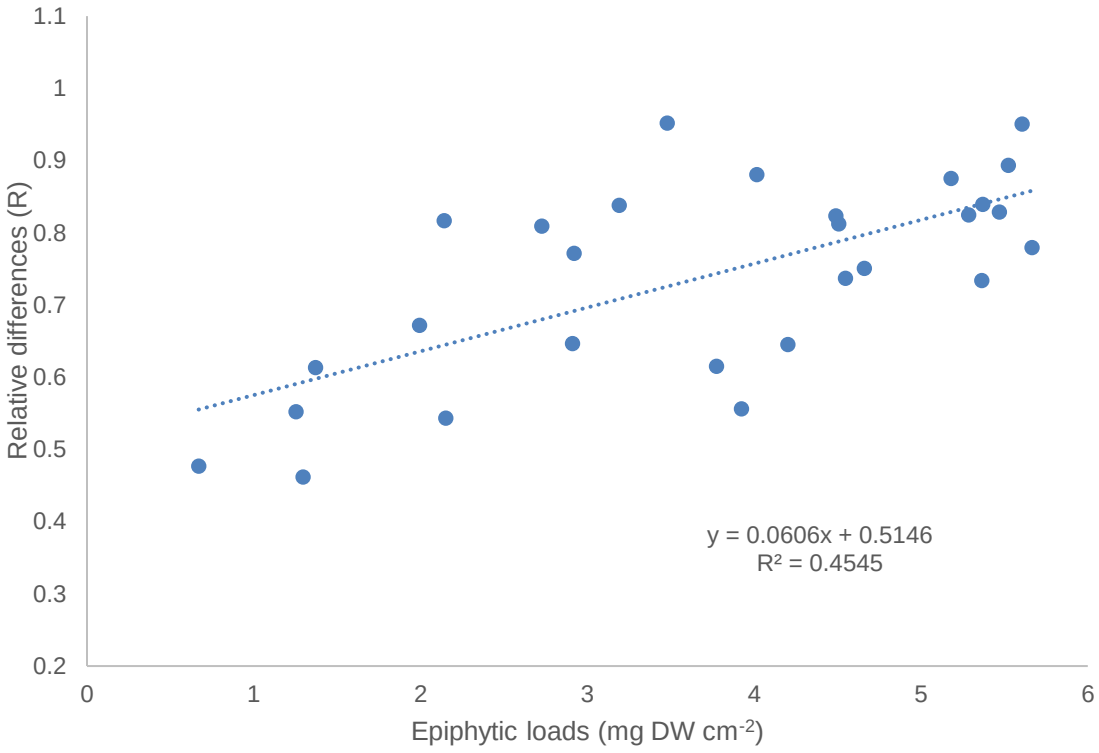

E

Figure 4-8. Continued.

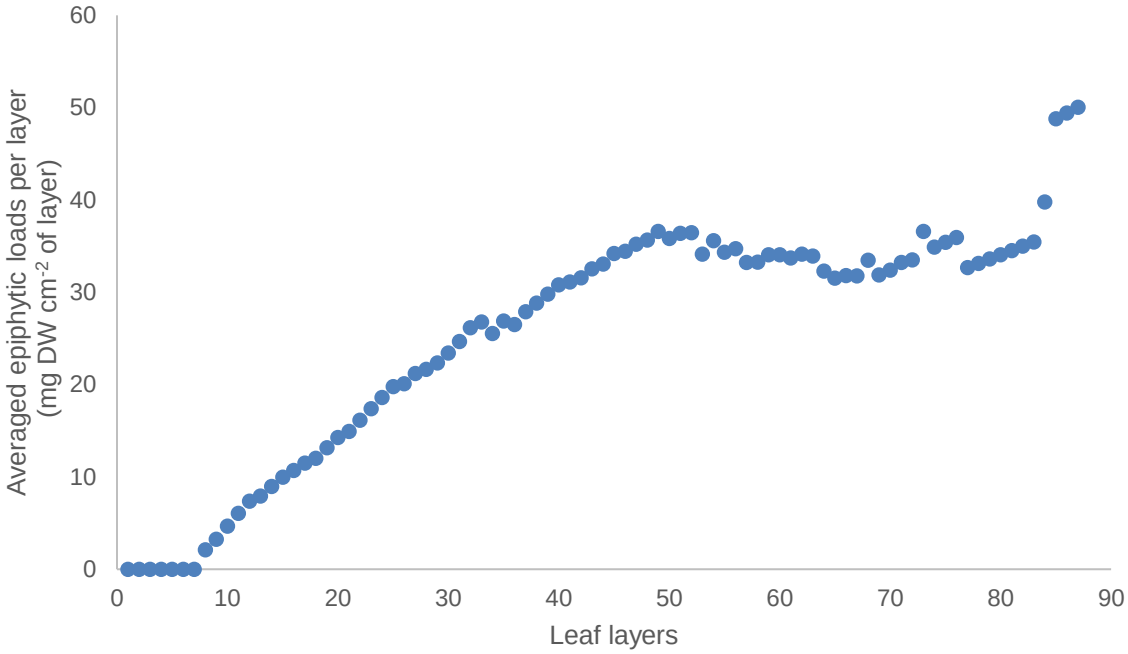

A

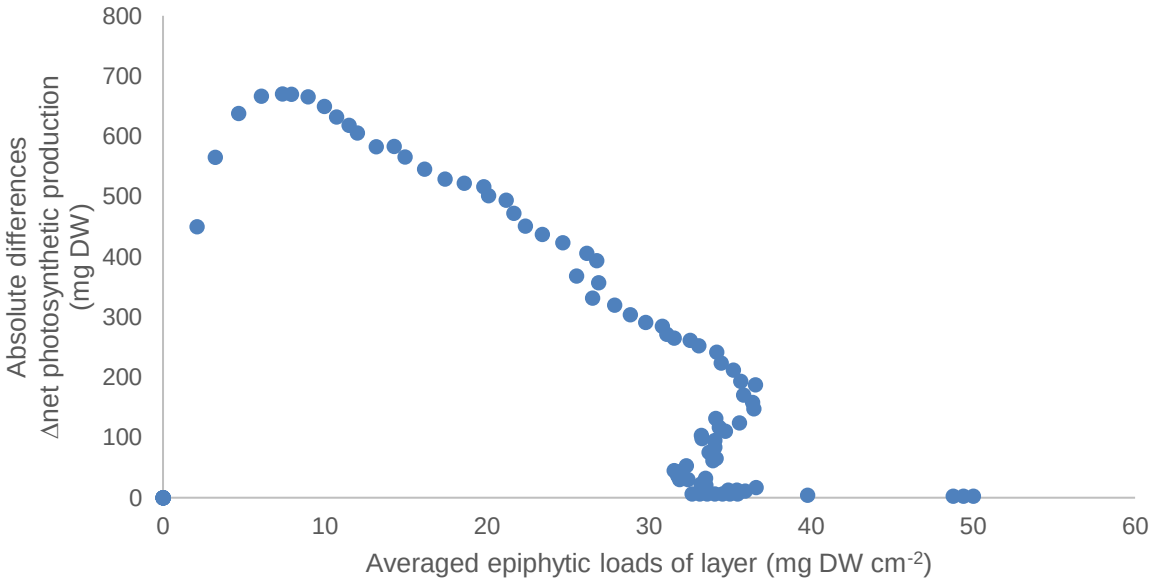

B

Figure 4-9. Distribution of epiphytic loads and differences in net photosynthetic production for sections of leaves of *Vallisneria americana* with different epiphytic loads from Salt Creek. A) Plots show heterogeneous distribution of epiphytes along the lengths of leaves. B) Plots show absolute differences (Δ net photosynthetic production). C) Plots show relative differences (R).

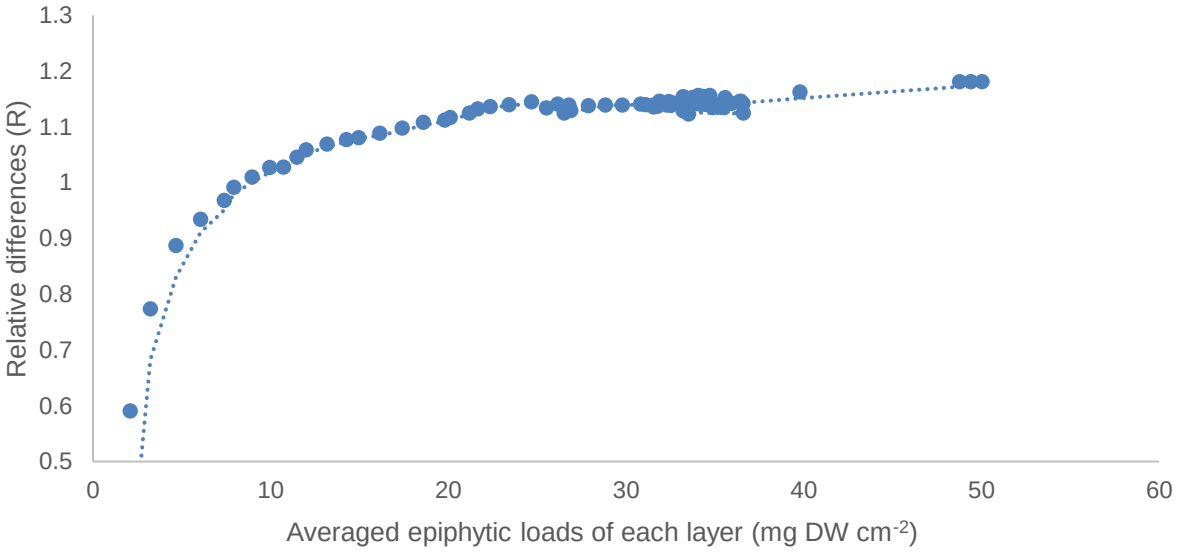

C

Figure 4-9. Continued.

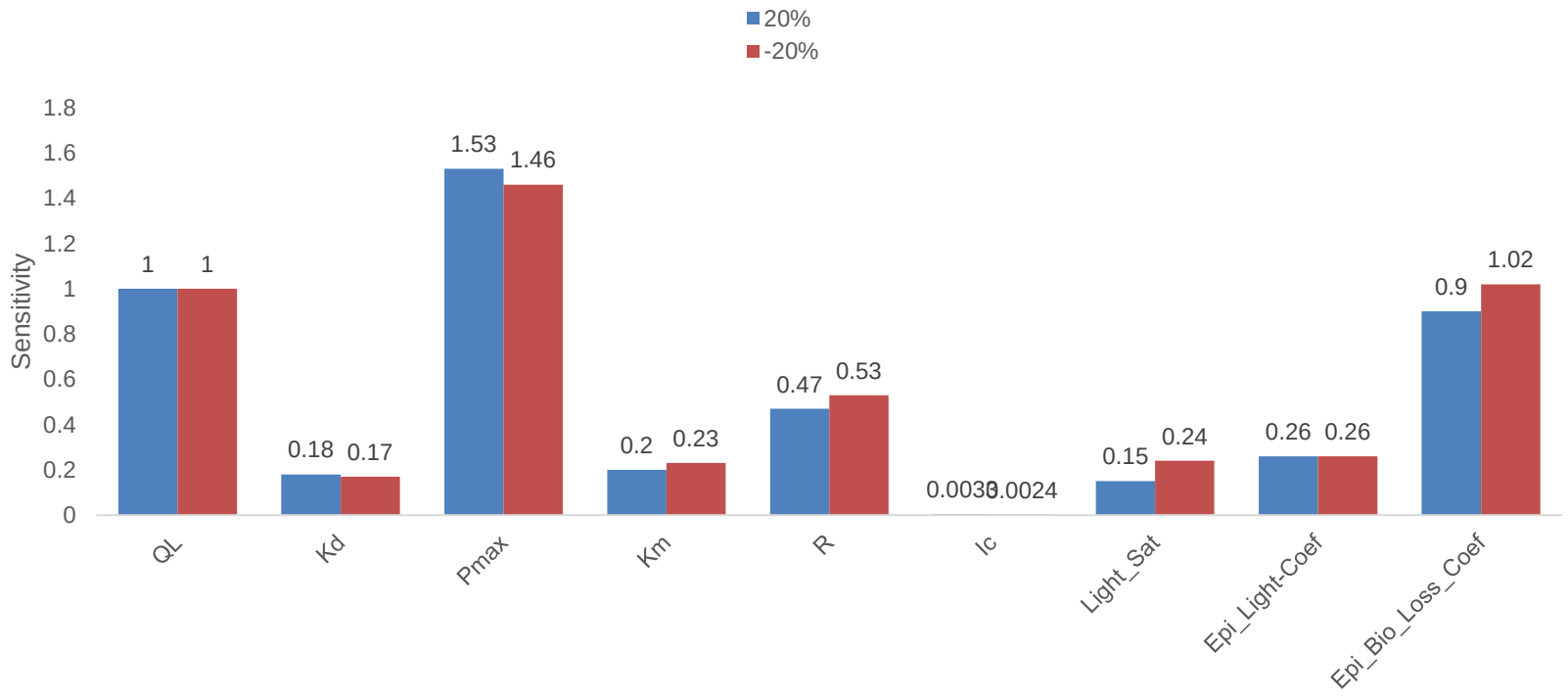

Figure 4-10. Results of sensitivity analyses for parameters.

CHAPTER 5
CONCLUSIONS

In Chapter 2, I showed that epiphytes on *V. americana* can attenuate a considerable portion of incident light. Direct measurements of light transmission through submersed epiphytes produced an empirical model that represents an important component of the numerical model developed in Chapter 4, and along with light requirements drawn from the literature, yielded a prediction regarding the threshold epiphytic load (4 to 5 mg DW cm^{-2} of leaf) that essentially stops growth of *V*. *americana* leaves.

In Chapter 3, the detrimental impacts of epiphytic loads on the growth of *V. americana* were quantified and evaluated in the field. This work confirmed the hypothesis from Chapter 2 regarding a threshold epiphytic load. This threshold represents a valuable indicator of the health of spring-fed aquatic ecosystems that complements traditional indicators based on water quality.

In Chapter 4, a simulation model was developed that relates available light to production of biomass for *V*. *americana* under different epiphytic loads. The model incorporated the statistical relationship from Chapter 2, the field data from Chapter 3, and relationships and parameters from the literature to predict growth of *V*. *americana* under different epiphytic loads. The model can guide water resource managers as they implement actions to protect macrophytes from epiphytic loads, restore healthy meadows of macrophytes, and manage Florida’s valuable, spring-fed systems.

APPENDIX A
CODE FOR CHAPTER 2

CurveExpert Code for Chapter 2:

```
 # this preamble is optional, but it makes things nicer.  Here, you can choose the
# name of your model, the equation (if applicable), and the latex form of the
equation
# (for nice rendering)
name         = ur"Forced_3_Parameter_Exponential_Decay"
nindvar      = 1
equation     = r"b+q0*exp(-x/a)"
latexequation = r"b+q0 \mathrm{exp}{\left(-x/a\right)}"
def evaluate(x,b,q0,a):
  xf = 0.0
  yf = 100.0
  b = yf - q0*exp(-xf/a)
  return b + q0 * exp(-x/a)
def initialize(x,y):
  """
  The initialize function is in charge of initializing the parameters, given the raw
data
  x and y (which are columns of data).  Obviously, any Python functions can be
used
  here.
  The return value from this function should be anything that can be translated
into
  a numpy array.  If you don't know what this means, don't worry; just follow the
  examples.
  """
  b = 20.55000000000000000E+00
  q0 = 100.000000000000000E+00
  a = 1.000000000000000E+00
  return (b,q0,a)
```

Code for Python Matplotlib Appendix:

```
import numpy as np
from scipy.optimize import curve_fit
import matplotlib
matplotlib.use('Agg')
import matplotlib.pyplot as plt
from functions import *
if __name__ == "__main__":
   #Total DW
   x = np.array([0.2182539683, 0.2678062678, 0.3336703741, 0.4011899703,
0.4126750184, 0.5556921564, 0.6975414523, 0.7233273056, 0.7333682556,
0.774025974, 0.7792860734, 0.8483516484, 0.9597818678, 1.073080481,
1.074923324, 1.185185185, 1.411042945, 1.631623213, 1.68281489, 1.731175229,
```

```
1.759543659, 1.884057971, 1.976047904, 1.983957219, 2.157407407, 2.911340206,
2.973262032, 2.980769231, 3.06763285, 3.127272727, 3.130374957, 3.255555556,
3.344068706, 3.484176279, 3.501922508, 3.628577868, 3.680555556, 3.75187294,
3.975225225, 4.018640351, 4.17989418, 4.233664559, 4.424390244, 4.529411765,
4.740740741, 5.025839793, 5.155502392, 5.171014493, 5.171945701, 5.313981616,
5.982142857, 6.203296703, 6.35625, 6.455026455, 7.804444444, 7.933333333,
8.354385965, 9.489230769, 11.33156966, 16.66147725])
        y = np.array([76.35382426, 77.32572675, 76.85355017, 87.14624233,
75.41629998, 70.25901862, 66.60361481, 54.86474553, 67.84346474, 60.24143158,
54.14845937, 57.35518262, 53.45346221, 62.05054586, 53.57278321, 60.33802166,
47.11178937, 59.50845763, 50.53201086, 44.62358724, 47.19197733, 38.73192891,
46.98181413, 45.01706591, 51.0922529, 27.42021176, 26.65652522, 40.1285566,
35.87361739, 25.40533619, 62.22260031, 24.42602135, 20.13887855, 37.23497851,
61.45734292, 13.625503, 26.91658861, 25.32638282, 14.14494296, 32.71531587,
19.02114614, 43.14799943, 13.01767064, 26.77101523, 14.56419496, 18.85469551,
24.98520182, 26.50361415, 11.45962702, 32.01269484, 13.54327294, 8.075660015,
9.344904253, 6.213800643, 8.68022516, 18.70946595, 4.484490645, 9.566883309,
12.3959923, 17.9341622])
        #=== Plot
        fig = plt.figure()
        ax = fig.add_subplot(111)
        xlabel = 'Epiphyte Biomass, mg DW $cm^{-2}$ of leaf'
        ax.set_xlabel(xlabel)
        ax.set_ylabel('Light Transmission (I/$I_0$) %')
        plt.scatter(x, y)
        xdata = np.linspace(0, 20, 1000)
        plt.xlim([0,20])
        plt.ylim([0,100])
        plt.grid()
        plt.savefig('scatter_DW.png')
        no_force_point(x, y, 'DW', xlabel)
        force_point(x,y,'DW', 0 , 100, xlabel)
    import numpy as np
    from scipy.optimize import curve_fit
    import matplotlib.pyplot as plt
    def no_force_point(x, y, file_name, xlabel, chla=None):
        if chla:
            x_max=50
        else:
            x_max=20
            for i in xrange(4):
            t = i+1
            print t
            popt, pcov = model_func_curve_fit(x, y, None, t, chla)
            residuals = y- model_func_one(x, popt[0], popt[1], popt[2])
            ss_res = np.sum(residuals**2)
```

```
        ss_tot = np.sum((y-np.mean(y))**2)
        r_squared = 1 - (ss_res / ss_tot)
        print "unconstraint model%s r_squared = %s"%(t, r_squared)
        #=== Plot
        fig = plt.figure()
        #fig.suptitle('Light Transmittion', fontsize=14, fontweight='bold')
        ax = fig.add_subplot(111)
        ax.set_xlabel(xlabel)
        ax.set_ylabel('Light Transmission %')
            plt.scatter(x, y)
        #plt.savefig('testplot.png')
                xdata = np.linspace(0, x_max, 1000)
            plt.plot(xdata, model_func(xdata, popt[0], popt[1], popt[2], t))
        text = model_text(popt, r_squared, t)
        plt.annotate(text, xy=(0.03, 0.95), xycoords='axes fraction', fontsize=12)
        plt.xlim([0,x_max])
        plt.ylim([0,100])
        plt.grid()
        plt.savefig('unconstraint_%s_model%s.png'%(file_name, t))
def force_point(x, y, file_name, force_x, force_y, xlabel, chla=None):
    x = np.insert(x, 0, force_x)
    y = np.insert(y, 0, force_y)
    if chla:
        x_max=50
    else:
        x_max=20
        for i in xrange(4):
        t = i+1
        sigma = np.ones(len(x))
        sigma[[0]] = 0.01
                popt, pcov = model_func_curve_fit(x, y, sigma, t, chla)
        residuals = y- model_func_one(x, popt[0], popt[1], popt[2])
        ss_res = np.sum(residuals**2)
        ss_tot = np.sum((y-np.mean(y))**2)
        r_squared = 1 - (ss_res / ss_tot)
        print "constraint model%s r_squared = %s"%(t, r_squared)
        #=== Plot
        fig = plt.figure()
        #fig.suptitle('Light Transmittion', fontsize=14, fontweight='bold')
        ax = fig.add_subplot(111)
        ax.set_xlabel(xlabel)
        ax.set_ylabel('Light Transmission %')
            plt.scatter(x, y)
        #plt.savefig('testplot.png')
                xdata = np.linspace(0, x_max, 1000)
            plt.plot(xdata, model_func(xdata, popt[0], popt[1], popt[2], t))
```

```
        text = model_text(popt, r_squared, t)
        plt.annotate(text, xy=(0.03, 0.95), xycoords='axes fraction', fontsize=12)
        plt.xlim([0,x_max])
        plt.ylim([0,100])
        plt.grid()
        plt.savefig('constraint_%s_model%s.png'%(file_name, t))
def model_func_curve_fit(x, y, sigma, t, chla=None):
    if t == 1 and sigma != None:
      return curve_fit(model_func_one, x, y, p0=(100 , 1, 1), sigma=sigma)
    elif t == 2 and sigma != None:
      return curve_fit(model_func_two, x, y, p0=(100 , 1, 1), sigma=sigma)
    elif t == 3 and sigma != None:
      return curve_fit(model_func_three, x, y, p0=(100 , 1, 1), sigma=sigma)
    elif t == 4 and sigma != None:
      return curve_fit(model_func_four, x, y, p0=(100 , 1, 1), sigma=sigma)
    elif t == 1 and sigma == None:
      return curve_fit(model_func_one, x, y, p0=(100 , 1, 1))
    elif t == 2 and sigma == None:
      return curve_fit(model_func_two, x, y, p0=(100 , 1, 1))
    elif t == 3 and sigma == None:
      return curve_fit(model_func_three, x, y, p0=(100 , 1, 1))
    elif t == 4 and sigma == None:
        if chla:
            return curve_fit(model_func_four, x, y, p0=(835, 0.001, 2.7))
        else:
            return curve_fit(model_func_four, x, y, p0=(100, 1, 1))
def model_func(x, a, b, c, t):
    if t == 1:
        return model_func_one(x, a, b, c)
    elif t == 2:
        return model_func_two(x, a, b, c)
    elif t == 3:
        return model_func_three(x, a, b, c)
    elif t == 4:
        return model_func_four(x, a, b, c)
def model_text(popt, r_squared, t):
    if t == 1:
        return model_text_one(popt, r_squared)
    elif t == 2:
        return model_text_two(popt, r_squared)
    elif t == 3:
        return model_text_three(popt, r_squared)
    elif t == 4:
        return model_text_four(popt, r_squared)
def model_text_one(popt, r_squared):
    return "$f(x)=ae^{-x/b}$ | a=%.3f, b=%.3f" % (popt[0],popt[1])
```

```
            #return "$f(x)=ae^{-x/b}$ | a=%.3f, b=%.3f, $R^{2}$=%.3f" % (popt[0],popt[1],
r_squared)
        def model_func_one(x, a, b, c):
            return a*(np.exp(-x/b))
        def model_text_two(popt, r_squared):
            return "$f(x)= c + ae^{-x/b}$ | a=%.3f, b=%.3f, c=%.3f" %
(popt[0],popt[1],popt[2])
            #return "$f(x)= c + ae^{-x/b}$ | a=%.3f, b=%.3f, c=%.3f, $R^{2}$=%.3f" %
(popt[0],popt[1],popt[2], r_squared)
        def model_func_two(x, a, b, c):
            return c + a*(np.exp(-x/b))
        def model_text_three(popt, r_squared):
            return "$f(x)= a/(1+x/b)$ | a=%.3f, b=%.3f" % (popt[0],popt[1])
            #return "$f(x)= a/(1+x/b)$ | a=%.3f, b=%.3f, $R^{2}$=%.3f" % (popt[0],popt[1],
r_squared)
        def model_func_three(x, a, b, c):
            return a/(1+x/b)
        def model_text_four(popt, r_squared):
            return "$f(x)= a*(1+c*x/b)^{-1/c}$ | a=%.3f, b=%.3f, c=%.3f" %
(popt[0],popt[1],popt[2])
            #return "$f(x)= a*(1+c*x/b)^{-1/c}$ | a=%.3f, b=%.3f, c=%.3f, $R^{2}$=%.3f" %
(popt[0],popt[1],popt[2], r_squared)
        def model_func_four(x, a, b, c):
              return a*(np.power((1+c*x/b), (-1/c)))
```

APPENDIX B
CODE FOR CHAPTER 4

Section:

```
# -*- coding: utf-8 -*-
from __future__ import unicode_literals

from math import exp, pow
from django.db import models
from django.utils import timezone

# Create your models here.
class Section(models.Model):
    leaf = models.ForeignKey('Leaf', on_delete=models.CASCADE)
    light = models.ManyToManyField('Light', null=True)
    section_rank = models.IntegerField()
    gross_photo = models.FloatField(null=True)
    respiration = models.FloatField(null=True)
    net_photo = models.FloatField(null=True)
    #loss_by_epi = models.FloatField(null=True)

def setCalNetPhoto(self):
        sum_gross_photo =0
        sum_respiration =0
        sum_net_photo = 0
        #sum_loss_by_epi = 0
        QL = self.leaf.plant.experiment.ql #1
        KD = self.leaf.plant.experiment.kd #1.56 #(1/m)
        PMAX = self.leaf.plant.experiment.pmax #0.077 mg CO2 m-2s-1
        IC = self.leaf.plant.experiment.ic #9.4 #(uE/s/m^2)
        LIGHT_SAT = self.leaf.plant.experiment.light_sat #846.15 #(uE/s/m^2)
        KM =self.leaf.plant.experiment.km #123.08 #(uE/s/m^2)
        EPI_LIGHT_COEF = self.leaf.plant.experiment.epi_light_coef #1
        EPI_BIO_LOSS_COEF = self.leaf.plant.experiment.epi_bio_loss_coef #1
        RESPIRATION = self.leaf.plant.experiment.respiration # 2.57mg
CO2/(m2*15min)
        ALGAE_BIOMASS = self.leaf.plant.experiment.algae_biomass

        for time in self.light.all().order_by('date_and_time'):
            time_depth = (time.water.depth - self.section_rank + 0.5)/100  #input
depth(cm), after/100, (m)
            if time_depth<0:
                time_depth=0
            water_attenuation_pct=exp(-1*KD*time_depth)


            if ALGAE_BIOMASS == None:
```

```
                    if self.section_rank>7:
                        algae_biomass= self.leaf.algae_biomass_ratio*(self.section_rank-
7)*(float(self.leaf.width))

                        algae_attenuation_pct = (EPI_LIGHT_COEF*0.8)*exp(-
1*algae_biomass/(EPI_LIGHT_COEF*3.63)) #0.8 #0.3*exp(-1*algae_biomass)
                    else:
                        algae_biomass=0
                        algae_attenuation_pct =1
                else:
                    #algae_biomass = ALGAE_BIOMASS
                    algae_biomass =
ALGAE_BIOMASS*(self.section_rank*float(self.leaf.width)*float(self.leaf.length))/(0.5*se
lf.leaf.section_num*(self.leaf.section_num+1))
                    algae_attenuation_pct = (EPI_LIGHT_COEF*0.8)*exp(-
1*algae_biomass/(EPI_LIGHT_COEF*3.63))

                if algae_biomass==0:
                    algae_attenuation_pct =1

                #print algae_biomass
                #print algae_attenuation_pct
                #print "#####"

                #print algae_attenuation_pct
                ######################################
                #print "%s * %s * %s"%(time.surface_light, water_attenuation_pct,
algae_attenuation_pct)
                #if time_available_light>846.15: P=Pmax=16.5*8.96*10^-4
                #else (if 140<available light<846.15) P=16.5*8.96*10^-4*availble
light/(123.08+availible light)
                #    else (if availible light=140) P=13.82*8.96*10^-4
                        #else (if 9.4 <availible light <140) P= 13.82*8.96*10^-4*avalible
light/(92.31+availble light)
                            #else P=0
        time_available_light=time.surface_light*water_attenuation_pct*algae_attenuation
_pct   #uE/m^2.s

                if time_available_light>=LIGHT_SAT:
                    gross_photo_rate=PMAX #mgCO2/(m^2*s)
                elif IC<time_available_light<LIGHT_SAT:

gross_photo_rate=PMAX*time_available_light/(KM+time_available_light)
#mgCO2/(m^2*s)
                else:
                    gross_photo_rate= 0
```

```
        gross_photo = gross_photo_rate*60*15*(1*self.leaf.width)/10000*0.68
#mgCO2/(15min)-->mgDW
                sum_gross_photo = sum_gross_photo + gross_photo

                if algae_biomass > 1:
                  if algae_biomass >= 4.5: # most epi
                    respiration = EPI_BIO_LOSS_COEF*0.15*5*gross_photo + 0.4*
gross_photo + RESPIRATION*(1*self.leaf.width)/10000*0.68
                    #respiration = 0.25*algae_biomass*gross_photo + 0.4* gross_photo +
RESPIRATION*(1*self.leaf.width)/10000*0.68
                  elif 2 < algae_biomass <= 4.5:
                    respiration = EPI_BIO_LOSS_COEF*0.2*algae_biomass*gross_photo
+ 0.4* gross_photo + RESPIRATION*(1*self.leaf.width)/10000*0.68
                  elif 1< algae_biomass <=2:
                    respiration = EPI_BIO_LOSS_COEF*0.4*algae_biomass*gross_photo
+ 0.4* gross_photo + RESPIRATION*(1*self.leaf.width)/10000*0.68
                else:   #less epi
                  respiration = EPI_BIO_LOSS_COEF*0.3*algae_biomass*gross_photo +
0.4* gross_photo + RESPIRATION*(1*self.leaf.width)/10000*0.68
                #if self.section_rank <= 45:
                  #if algae_biomass >= 0.2: # mg DW/cm^2
                      #respiration = (0.4* gross_photo + 4.15*0.2*gross_photo) +
RESPIRATION*(1*self.leaf.width)/10000*0.68
                  #elif 0.1<algae_biomass<0.2:
                      #respiration = (0.4* gross_photo + 2*algae_biomass*gross_photo) +
RESPIRATION*(1*self.leaf.width)/10000*0.68
                  #elif 1<algae_biomass<=0.1:
                      #respiration = (0.4* gross_photo + 12*algae_biomass*gross_photo)
+ RESPIRATION*(1*self.leaf.width)/10000*0.68
                  #else:
                      #respiration = (0.28* gross_photo) +
RESPIRATION*(1*self.leaf.width)/10000*0.68
                #else:
                    #respiration = (0.4* gross_photo + 1*gross_photo) +
RESPIRATION*(1*self.leaf.width)/10000*0.68
                #respiration = (0.4* gross_photo + 0.6*algae_biomass*gross_photo) +
RESPIRATION*(1*self.leaf.width)/10000*0.68
                sum_respiration = sum_respiration + respiration
                net_photo = QL*(gross_photo - respiration) #mgCO2/(m^2*s)-->mgDW
                sum_net_photo = sum_net_photo + net_photo
#1mgDW=1.467mgCO2~1.65mgCO2 #1mgC02=0.606~0.682mgDW
                #print "water_attenuation_pct %s"%water_attenuation_pct
                current_time = timezone.localtime(time.date_and_time).strftime("%Y-%m-
%d %H:%M")
```

```
                #print_out = "%s,%s,%s,%s,%s,%s,%s,%s,%s,%s,%s,%s"%(self,
current_time,time.surface_light,
                #                   time_depth, time.water.depth, water_attenuation_pct,
                #                   algae_biomass,algae_attenuation_pct,
                #                   time_available_light,
                #                   gross_photo_rate,net_photo,sum_net_photo)
                #with open("log/section.csv", "a") as myfile:
                #    myfile.write(print_out+'\n')
                #print print_out
                #print 'time: %s net_photo:%s time_availible_light: %s time_depth:
%s'%(time.date_and_time, net_photo, time_availible_light, time_depth)
            #print "sum_net_photo: %s"%sum_net_photo
            self.gross_photo = sum_gross_photo
            self.respiration = sum_respiration
            self.net_photo = sum_net_photo
            #exit()
            return self.net_photo
                #|7 days sum net photo-real data |^2=r2
                #outplot: x list all parameter and r^2
        sum-net-photo*growth rate=new growth #(CO2)
            (WHOLE LEAVE)
            '''
        def save(self, *args, **kwargs):
            if self.id != None:
                self.setCalNetPhoto()
            super(Section, self).save(*args, **kwargs)

            def __unicode__(self):
                return "Plant %s: Leaf: %s Section: %s" % (self.leaf.plant.id,
self.leaf.leaf_rank, self.section_rank)

            #./recreate.sh #(clean old data and input new data)
            #./createsuperuser.sh  #if I want to see database (website)
            #python manage.py cal_section  # calculate
            #python manage.py continue # continue
            #https://macrophyte-model-yangx.c9users.io/admin/macrophyte/light/ #website
            #https://macrophyte-model-yangx.c9users.io/admin/macrophyte/section/
            #sudo service postgresql start
            #sudo service redis-server start
            #https://bitbucket.org/y_xu/macrophyte_model

            #./start.sh
            #./recreate.sh
            #./celery_run.sh
            # http://24.91.12.125/admin/
            #bitbucket.org
```

```
            #./sql/section_sum.sh (ps:Calculate section net photo)
            #./sql/plant_epi.sh (ps:Calculate epi density-total blade)
            #  1.cd data -> 2.#./drop_create.sh  (remove old data)
              #3.#./rollback.sh (Run project see if it is right)
              #3.open a new terminal run#./sql/plant_epi.sh)
              #4. find result in file(sql/plant_epi.csv)

            #cd sql-> bash section_sum.sh
            #pg_dump macrophyte | gzip > macrophyte.gz ( download .gz)
```

Leaf:

```
        # -*- coding: utf-8 -*-
        from __future__ import unicode_literals

        from django.db import models
        from macrophyte.models import Section
        from django.db.models import F, FloatField, Sum

        # Create your models here.
        class Leaf(models.Model):
            plant = models.ForeignKey('Plant', on_delete=models.CASCADE)
            algae = models.OneToOneField('Algae', on_delete=models.CASCADE,
null=True)
            leaf_rank = models.IntegerField()
            age = models.IntegerField(null=True)
            length = models.FloatField(null=True)
            width = models.FloatField(null=True)
            section_num = models.IntegerField(null=True)
            algae_biomass_ratio = models.FloatField(null=True)
            #algae_density = models.FloatField(null=True)
            real_growth= models.FloatField(null=True)
            net_photo = models.FloatField(null=True)
            self_used_net_photo = models.FloatField(null=True)
            gross_photo_product = models.FloatField(null=True)
            respiration = models.FloatField(null=True)
            #r = models.FloatField(null=True)

            def setCalSectionNum(self):
                if int(float(self.length)) == float(self.length):
                    self.section_num = int(float(self.length))
                else:
                    self.section_num = int(float(self.length)) + 1
                return self.section_num
```

```
            #
self.algae_biomass_ration=float(self.algae.algae_biomass)/(float(self.width)*(section_nu
m-7)(section_num-7+1)/2)
            #(epi-DW mg)/(1*W)*(n*(n+1)/2)
            #def setCalAlgaeDensity(self):
            #    self.algae_density=
float(self.algae.algae_biomass)/(float(self.length)*float(self.width))    #(mg/cm^2)
            #    return self.algae_density

            def setCalAlgaeBiomassRatio(self):

                if int(self.section_num) > 7:
                    #self.algae_biomass_ratio
=(float(self.algae.algae_biomass)*float(self.width)*float(self.length))/(float(self.width)*(se
lf.section_num-7)*(self.section_num-7+1)/2)
                    self.algae_biomass_ratio
=float(self.algae.algae_biomass)/(float(self.width)*(self.section_num-
7)*(self.section_num-7+1)/2)
                    #print "%s = float(%s)/(float(%s)*(%s-7)*(%s-
7+1)/2)"%(self.algae_biomass_ratio, self.algae.algae_biomass, self.width,
self.section_num, self.section_num)
                else:
                    self.algae_biomass_ratio = 0
                return self.algae_biomass_ratio

            def setNetPhoto(self):
                result =
Section.objects.filter(leaf=self).aggregate(sum_net_photo=Sum(F('net_photo'),
output_field=FloatField()))
                self.net_photo = result['sum_net_photo']
                if self.net_photo == None:
                    self.net_photo = 0
                #self.r = result['sum_net_photo']-self.real_growth

                #print "R^2 for leaf %s is %s"%(self.leaf_rank, r)

                return self.net_photo
                # def R=abs(sum net photo-nb_dw) return R
                #   each leaf has one R^2=R*R
                #   I want to know the sum of all leaves R^2 and return the value

            def setGrossPhotoProduct(self):
                result =
Section.objects.filter(leaf=self).aggregate(sum_gross_photo_product=Sum(F('gross_ph
oto'), output_field=FloatField()))
                self.gross_photo_product = result['sum_gross_photo_product']
```

```
            if self.gross_photo_product == None:
                self.gross_photo_product = 0
            return self.gross_photo_product

        def setRespiration(self):
            result =
Section.objects.filter(leaf=self).aggregate(sum_respiration=Sum(F('respiration'),
output_field=FloatField()))
            self.respiration = result['sum_respiration']
            if self.respiration == None:
                self.respiration = 0
            return self.respiration

        def setSelfUsedNetPhoto(self):
            if self.net_photo < 0:
                self.self_used_net_photo = 0
                return self.self_used_net_photo

            if self.age <= 3:
                self.self_used_net_photo = self.net_photo
            elif 3 < self.age <= 9:
                if self.net_photo > 52.3:
                    self.self_used_net_photo = 52.3
                else:
                    self.self_used_net_photo = self.net_photo

            elif 9 < self.age <= 15:
                if self.net_photo > 56.16:
                    self.self_used_net_photo = 56.16
                else:
                    self.self_used_net_photo = self.net_photo

            elif 15 < self.age <= 21:
                if self.net_photo > 40.56:
                    self.self_used_net_photo = 40.56
                else:
                    self.self_used_net_photo = self.net_photo

            elif 21 < self.age <= 27:
                if self.net_photo > 16.55:
                    self.self_used_net_photo = 16.55
                else:
                    self.self_used_net_photo = self.net_photo

            elif 27 < self.age <= 33:
                if self.net_photo > 11.70:
```

```
                self.self_used_net_photo = 11.70
            else:
                self.self_used_net_photo = self.net_photo

        elif self.age > 33:
            self.self_used_net_photo = 0
        return self.self_used_net_photo

        #return self.LeaveIncreasePerShoot
    #@property
    #def setTide(self):
    #    return 1


    def save(self, *args, **kwargs):
        if self.algae != None:
            self.setCalSectionNum()
            self.setCalAlgaeBiomassRatio()
            #self.setCalAlgaeDensity()

        super(Leaf, self).save(*args, **kwargs)

    def __unicode__(self):
        return "Plant %s Leaf %s" % (self.plant.id, self.leaf_rank)

#https://macrophyte-model-yangx.c9users.io/admin
Plant:
# -*- coding: utf-8 -*-
from __future__ import unicode_literals

from django.db import models
from macrophyte.models import Leaf
from django.db.models import F, FloatField, Sum

# Create your models here.
class Plant(models.Model):
    experiment = models.ForeignKey('Experiment', on_delete=models.CASCADE)
    predicted_growth = models.FloatField(null=True)
    gross_photo_product = models.FloatField(null=True)
    respiration = models.FloatField(null=True)
    real_growth = models.FloatField(null=True, default=0)
    net_photo = models.FloatField(null=True)
    new_leaf = models.FloatField(null=True)

    # # predicted growth = growth rate* plant net photo
    #predicted growth vs. real growth (real photo product)
```

```
            #@property
            #def setTide(self):
            #    return 1
            def setNewLeaf(self):
                self.new_leaf = 0
                for leaf in Leaf.objects.filter(plant=self):
                    if leaf.self_used_net_photo == 0:
                        pass
                    elif leaf.age <= 3:
                        self.new_leaf = self.new_leaf + leaf.net_photo
                    else:
                        self.new_leaf = self.new_leaf + (leaf.net_photo -
leaf.self_used_net_photo)
                return self.new_leaf

            def setNetPhoto(self):
                result = Leaf.objects.filter(plant=self,
net_photo__gte=0).aggregate(sum_net_photo=Sum(F('net_photo'),
output_field=FloatField()))
                self.net_photo = result['sum_net_photo']
                if self.net_photo == None:
                  self.net_photo = 0
                return self.net_photo

            def setGrossPhotoProduct(self):
                result =
Leaf.objects.filter(plant=self).aggregate(sum_gross_photo_product=Sum(F('gross_phot
o_product'), output_field=FloatField()))
                self.gross_photo_product = result['sum_gross_photo_product']
                return self.gross_photo_product

            def setRespiration(self):
                result =
Leaf.objects.filter(plant=self).aggregate(sum_respiration=Sum(F('respiration'),
output_field=FloatField()))
                self.respiration = result['sum_respiration']
                return self.respiration

            def setPredictedGrowth(self): #predicted_Growth
                #L_FRACTION = self.experiment.l_fraction

                self.predicted_growth = self.net_photo #* L_FRACTION # Ftaction of net
photo allocated to leaves
                return self.predicted_growth

            def save(self, *args, **kwargs):
```

```
    super(Plant, self).save(*args, **kwargs)

class Meta:
    ordering = ['-experiment','id']

def __unicode__(self):
    return "Experiment: %s Plant: %s" % (self.experiment.id, self.id)
```

LIST OF REFERENCES

Agustí, S., S. Enríquez, H. Frost-Christensen, K. Sand-Jensen, and C.M. Duarte. 1994. Light harvesting among photosynthetic organisms. *Functional Ecology* 8: 273-279.

Akaike, H. 1973. Information theory as an extension of the maximum likelihood principle. In *Second International Symposium on Information Theory*, ed. B. Petrov, and F. Csáki. Akadémiai Kiadó.

Asaeda, T., M. Sultana, J. Manatunge, and T. Fujino. 2004. The effect of epiphytic algae on the growth and production of *Potamogeton perfoliatus* L. in two light conditions. *Environmental and Experimental Botany* 52(3): 225-238.

Askenasy, E. 1880. *Über eine neue Methode, um die Vertheilung der Wachsthumsintensität in wachsenden Theilen zu bestimmen.* Varl Winter's Universitätsbuchhandlung in Heidelberg.

Batiuk, R.A., R.J. Orth, K.A. Moore, W.C. Dennison, and J.C. Stevenson. 1992. *Chesapeake Bay submerged aquatic vegetation habitat requirements and restoration targets: A technical synthesis. Report number PB-93-196665/XAB.* Gloucester Point: Virginia Institute of Marine Science.

Best, E.P., and W.A. Boyd. 1999. *A simulation model for growth of the submersed aquatic macrophyte Eurasian watermilfoil (Myriophyllum spicatum L.). No. WES-TR-A-99-3.* Vicksburg: Army Engineer Waterways Experiment Station.

Best, E.P., and W.A. Boyd. 2001. *A simulation model for growth of the submersed aquatic macrophytes American wildcelery (Vallisneria americana Michx.).* US Army Crops of Engineers. Engineer Research and Development Center.

Blanch, S.J., G.G. Gant, and K.F. Walker. 1998. Growth and recruitment in *Vallisneria americana* as related to average irradiance in the water column*. Aquatic Botany* 61: 181–205.

Blanco, F.F., and M.V. Folegatti. 2005. Estimation of leaf area for greenhouse cucumber by linear measurements under salinity and grafting. *Science of Agriculture* 62(4): 305-309.

Bocci, M., G. Coffaro, and G. Bendoricchio. 1997. Modelling biomass and nutrient dynamics in eelgrass (*Zostera marina* L.): application to the lagoon of Venice (Italy) and Oresund (Denmark). *Ecological Modeling* 102: 67-80.

Bonn, M.A. 2004. *Visitor profiles, economic impacts and recreational aesthetic values associated with eight priority Florida springs located in the St. Johns River Water Management District. Special Publication SJ2004-SP35.* Palatka: St. Johns River Water Management District.

Borowitzka, M.A., P.S. Lavery, and M. van Keulen. 2006. Epiphytes of seagrasses. In *Seagrasses: Biology, Ecology and Conservation,* ed. A. Larkum, R.J. Orth, and C. Duarte. Springer Netherlands 441-461 pp.

Borowitzka, M.A., R.C. Lethbridge, and L. Charlton. 1990. Species richness, spatial distribution and colonisation pattern of algal and invertebrate epiphytes on the seagrass *Amphibolis griffithii*. *Marine Ecology Progress Series* 64: 281-291.

Borum, J. 1987. Dynamics of epiphyton on eelgrass (*Zostera marina* L.) leaves: relative roles of algal growth, herbivory, and substratum turnover. *Limnology and Oceanography* 32(4): 986-992.

Borum J., and S. Wium-Andersen. 1980. Biomass and production of epiphytes on eelgrass (*Zostera marina* L.) in the Øresund, Denmark. *Ophelia* 1: 57-64.

Brook, H.K. 1981. *Guide to the physiographic divisions of Florida.* Gainesville: Florida Cooperative Extension Service, Institute of Food and Agricultural Sciences, University of Florida.

Brush, M.J., and S.W. Nixon. 2002. Direct measurements of light attenuation by epiphytes on eelgrass *Zostera marina*. *Marine Ecology Progress Series* 238: 73-79.

Buia, M.C., and L. Mazzella. 1991. Reproductive strategies of the Mediterranean seagrasses, *Posidonia oceanica* (L.) Delile, *Cymodocea nodosa* (Ucria) Aschers., and *Zostera noltti* Hornem. *Aquatic Botany* 40: 343-362.

Bulthuis, D.A., and W.J. Woelkerling. 1983. Biomass accumulation and shading effects of epiphytes on leaves of the seagrass, *Heterozostera tasmanica*, in Victoria, Australia. *Aquatic Botany* 16: 137-148.

Burnell, O.W., B.D. Russell, A.D. Irving, and S.D. Connell. 2014. Seagrass response to CO_2 contingent on epiphytic algae: indirect effects can overwhelm direct effects. *Oecologia* 176(3): 871-882.

Burnham, K.P., and D.R. Anderson. 2001. Kullback-Leibler information as a basis for strong inference in ecological studies. *Wildlife Research* 28: 111-119.

Burnham, K.P., and D.R. Anderson. 2002. *Model selection and multimodel inference: A practical information-Theoretic Approach.* Springer-Verlag.

Burt, J.S., G.A. Kendrick, R.J. Masini, and C.J. Simpson. 1995. *Light and Posidonia sinuosa seagrass meadows in the temperate coastal waters of Western Australia. II. Effect of epiphyte species assemblages and biomass on attenuating light to the leaf surface. Technical Series 61.* Perth: Department of Environmental Protection.

Cambridge, M.L., A.W. Chiffings, C. Brittan, L. Moore, and A.J. McComb. 1986. The loss of seagrass in cockburn sound, Western Australia. II. Possible causes of seagrass decline. *Aquatic Botany* 24: 269-285.

Canfield, D.E., and M.V. Hoyer. 1988. Influence of nutrient enrichment and light availability on the abundance of aquatic macrophytes in Florida streams. *Canadian Journal of Fisheries and Aquatic Sciences* 45: 1467-1472.

Capone, D.G., P.A. Penhale, R.S. Oremland, and B.F. Taylor. 1979. Relationship between productivity and N_2 (C_2H_2) fixation in a *Thalassia testudinum* community. *Limnology and Oceanography* 24(1): 117-125.

Carter, V., N.B. Rybicki, J.M. Landwehr, and M. Naylor. 2000. *Light requirements for SAV survival and growth. Chesapeake Bay submerged aquatic vegetation water quality and habitat based requirements and restoration targets: a second technical synthesis. Chesapeake Bay Program 4-15.* USEPA.

Cattaneo, A., G. Galanti, and S. Gentinetta. 1998. Epiphytic algae and macroinvertebrates on submerged and floating leaved macrophytes in an Italian lake. *Freshwater Biology* 39(4): 725-740.

Cebrián, J., and C.M. Duarte. 1994. The dependence of herbivory on growth rate in natural plant communities. *Functional Ecology* 518-525.

Cebrián J., S. Enríquez, M. Fortes, N. Agawin, J.E. Vermaat, and C.M. Duarte. 1999. Epiphyte accrual on *Posidonia oceanica* (L.) Delile leaves: implications for light absorption. *Botanica Marina* 42: 123-128.

Chambers, P.A., and J. Kalff. 1985. Depth distribution of biomass of submerged aquatic macrophyte communities in relation to Secchi depth. *Canadian Journal of Fisheries and Aquatic Sciences* 42: 701-709.

Chambers, P.A., and J. Kalff. 1987. Light and nutrient in the control of aquatic plant community structure: I. *In situ* experiments. *Journal of Ecology* 75: 611-619.

Chapelle, A., A. Ménesguen, J.M. Deslous-Paoli, P. Souchu, N. Mazouni, A. Vaquer, and B. Millet. 2000. Modelling nitrogen, primary production and oxygen in a Mediterranean lagoon. Impact of oysters farming and inputs from the watershed. *Ecological Modeling* 127: 161-181.

Choice, Z.D., T.K. Frazer, and C.A. Jacoby. 2014. Light requirements of seagrasses determined from historical records of light attenuation along the Gulf coast of Peninsular Florida. *Marine Pollution Bulletin* 81(1): 94-102.

Coffaro, G., and A. Sfriso. 1997. Simulation model of *Ulva rigida* growth in shallow water of the Lagoon of Venice. *Ecological Modeling* 102: 55-66.

Cohen, M.J. 2007. *Sources, transport and transformations of Nitrate-N in the Florida environment. Final Report SJ2007-SP10.* St. Johns River Water Management District.

Czerny, A.B., and K.H. Dunton. 1995. The effects of *in situ* light reduction on the growth of two subtropical seagrasses, *Thalassia testudinum* and *Halodule wrightii*. *Estuaries and Coasts* 18(2): 418-427.

Demarty, M., and Y.T. Prairies. 2009. In sity dissolved organic carbon (DOC) release by submerged macrophytes-epiphyte communities in southern Quebec lakes. *Canadian Journal of Fisheries and Aquatic Sciences* 66: 1522-1531.

Dennison, W.C., R.J. Orth, K.A. Moore, J.C. Stevenson, V. Carter, S. Kollar, P.W. Bergstrom, and R.A. Batiuk. 1993. Assessing water quality with submersed aquatic vegetation. *BioScience* 43(2): 86-94.

Dixon, L.K. 2000. Establishing light requirements for the seagrass *Thalassia testudinum*: an example from Tampa Bay, Florida. *CRC Press, LLC*.

Doust, J.L., and G. LaPorte. 1991. Population sex ratios, population mixtures and fecundity in a clonal dioecious macrophyte, *Vallisneria americana*. *The Journal of Ecology* 79: 477-489.

Doyle, R.D. 2001. Effects of waves on the early growth of *Vallisneria americana*. *Freshwater Biology* 46: 289-397.

Drake, L.A., F.C. Dobbs, and R.C. Zimmerman. 2003. Effects of epiphyte load on optical properties and photosynthetic potential of the seagrasses *Thalassia testudinum* banks ex Konig and *Zostera marina* L. *Limnology and Oceanography* 48: 456-463.

Duarte, C.M. 1991. Seagrass depth limits. *Aquatic Botany* 40: 337-363.

Duarte, C.M. 1992. Nutrient concentration of aquatic plants: patterns across species. *Limnology and Oceanography* 37: 882-889.

Duarte, C.M., N. Marba, N. Agawin, J. Cebrian, S. Ennquez, M.D. Fortes, M.E. Gallegos, M. Merino, B. Olesen, K. Sand-Jensen, J. Uri, and J.E. Vermaat. 1994. Reconstruction of seagrass dynamics: age determinations and associated tools for the seagrass ecologist. *Marine Ecology Progress Series* 107: 195-209.

Duarte, C.M., Y.T. Prairie, T.K. Frazer, M.V. Hoyer, S.K. Notestein, R. Martinez, A. Dorsett, and D.E. Canfield. 2010. Rapid accretion of dissolved organic carbon in the springs of Florida: the most organic-poor natural waters. *Biogeosciences* 7: 4051-4057.

Dunn, A.E., D.R. Dobberfuhl, and D.A. Casamatta. 2008. A survey of algal epiphytes from *Vallisneria americana* michx. (Hydrocharitaceae) in the Lower St. Johns River, Florida. *Southeastern Naturalist* 7(2): 229–244

Elkalay, K., C. Frangoulis, N. Skliris, A. Goffart, S. Gobert, G., Lepoint, and J. Hecq. 2003. A model of the seasonal dynamics of biomass and production of the seagrass *Posidonia oceanica* in the Bay of Calvi (Northwestern Miditerranean). *Ecological Modeling* 167: 1-18.

Environmental Growth Chambers. Accessed at: http://www.egc.com/useful_info_lighting.php.

Erickson, R.O., and F.J. Michelini. 1957. The plastochron index. *American Journal of Botany* 44: 297-305.

FAWN, Florida Automated Weather Network. 2015. Institute of Food and Agricultural Sciences, University of Florida, Gainesville, Florida. Accessed at: http://fawn.ifas.ufl.edu/data/reports/

Fitzpatrick, J.R., and H. Kirkman. 1995. Effects of prolonged shading stress on growth and survival of the seagrass *Posidonia australis* in Jervis Bay, New South Wales, Australia. *Marine Ecology Progress Series* 127: 279-289.

Fong, C.W., S.Y. Lee, and R.S. Wu. 2000. The effects of epiphytic algae and their grazers on the intertidal seagrass *Zostera japonica*. *Aquatic Botany* 67(4): 251-261.

Frankovich, T.A., and J.C. Zieman. 1994. Total epiphyte and epiphytic carbonate production on *Thalassia testudinum* across Florida Bay*. Bulletin of Marine Science* 54: 679-695.

Frankovich, T.A., and J.C. Zieman. 2005. Periphyton light transmission relationships in Florida Bay and the Florida Keys, USA. *Aquatic Botany* 83: 14-30.

Frazer, T.K. 2000. *Coastal nitrate assessment: Nutrient assimilation capacity of five gulf coast rivers. Second annual project summary.* Tampa: Southwest Florida Water Management District, Surface Water Improvement and Management Program.

Frazer, T.K., M.V. Hoyer, S.K. Notestein, J.A. Hale, and D.E. Canfield. 2001. *Physical, chemical and vegetative characteristics of five gulf coast rivers.* Gainesville: University of Florida.

Frazer, K.T., S.K. Notestein, and W.E. Pine, Jr. 2006. *Changes in the physical, chemical and vegetative characteristics of the Homosassa, Chassahowitzka and Weeki Wachee Rivers.* Submitted to Southwest Florida Water Management District Surface Water Improvement and Management Program.

Glazer, B.T. 1999. *Analysis of physical, chemical, and biological factors inhibiting growth and restoration of submerged vascular plants in Delaware's Indian River and Rehoboth Bays.* Lewes: University of Delaware.

Gosselain, V., C. Hudon, A. Cattaneo, P. Gagnon, P. Planas, and D. Rochefort. 2005. Physical variables driving epiphytic algal biomass in a dense macrophyte bed of the St. Lawrence River (Quebec, Canada). *Hydrobiologia* 534: 11-22.

Gregg, W.W., and F.L. Rose. 1985. Influences of aquatic macrophytes on invertebrate community structure, guild structure, and microdistribution in streams. *Hydrobiologia* 128: 45-56.

Hauxwell, J.A., C.W. Osenberg, and T.K. Frazer. 2004. Conflicting management goals: manatees and invasive competitors inhibit restoration of a native macrophhyte. *Ecological Applications* 14: 57-586.

Hauxwell, J.A., T.K. Frazer, and C.W. Osenberg. 2007. An annual cycle of biomass and productivity of *Vallisneria americana* in a subtropical spring-fed estuary. *Aquatic Botany* 87: 61-68.

Heffernan, J.B., D.M. Liebowitz, T.K. Frazer, J.M. Evans, and M.J. Cohen. 2010. Algal blooms and the nitrogen-enrichment hypothesis in Florida springs: evidence, alternatives, and adaptive management. *Ecological Applications* 20: 816-829.

Hootsmans, M.J.M., and J.E. Vermaat. 1991. Macrophytes, a key to understanding changes caused by eutrophication in shallow freshwater ecosystems. IHE, Delft, The Netherlands, IHE Report Series.

Howard-Williams, C., B.R. Davies, and R.H.M. Cross. 1978. The influence of periphyton on the surface structure of a *Potamogeton pectinatus* L. leaf. *Aquatic Bot*any 5: 87-91.

Hoyer, M.V., T.K. Frazer, S.K. Notestein, and D.E. Canfield. 2004. Vegetative characteristics of three low-lying Florida coastal rivers in relation to flow, light, salinity and nutrients. *Hydrobiologia* 528: 31-43.

Iizumi, H., and A. Hattori. 1982. Growth and organic production of eelgrass (*Zostera marina* L.) in temperature waters of the Pacific Coast of Japan. III. The kinetics of nitrogen uptake. *Aquatic Bot*any 12: 245-256.

Jones, G.W., S.B. Upchurch, K.M. Champion, and D.J. Dewitt. 1997. *Water quality and hydrology of the Homosassa, Chassahowitzka, Weeki Wachee, and Aripeka spring complexes, Citrus and Hernando Counties, Florida - Origin of increasing nitrate concentrations. Southwest Florida Water Management Program*. Ambient Ground-Water Quality Monitoring Program.

Kelly, M.G., B. Moeslund, and N. Thyssen. 1981. Productivity measurement and the storage of oxygen in the aerenchyma of aquatic macrophytes. *Archiv für Hydrobiologie* 92: 1-10.

Kemp, W.M., R. Bartleson, L. Murray. 2000. *Epiphyte contributions to light attenuation at the leaf surface. In: Chesapeake Bay submerged aquatic vegetation water quality and habitat-based requirements and restoration targets: a second technical synthesis.* United States Environmental Protection Agency 55-69.

Kemp, W.M., R. Batiuk, R. Bartleson, P. Bergstrom, V. Carter, C.L. Gallegos, W. Hunley, L. Karrh, E.W. Koch, J.M. Landwehr, K.A. Moore, L. Murray, M. Naylor, N.B. Rybicki, J.C. Stevenson, and D.J. Wilcox. 2004. Habitat requirements for submerged aquatic vegetation in Chesapeake Bay: water quality, light regime, and physical-chemical factors. *Estuaries* 27: 363-377.

Kimber, A., C.E. Korschgen, and A.G. Van Der Valk. 1995. The distribution of *Vallisneria americana* seeds and seedling light requirements in the Upper Mississippi River. *Canadian Journal of Botany* 73: 1966-1973.

Kirk, J.T.O. 1994. Light and photosynthesis in aquatic ecosystems. Cambridge University Press.

Kiørbe, T. 1980. Production of *Ruppia cirrhosa* (Petagna) Grande in mixed beds in Ring Kobing Fjord (Denmark). *Aquatic Botany* 9:135-143.

Knight, R.L., and S.K. Notestein. 2008. Springs as Ecosystems. In: Brown, M.T., K.C. Reiss, M.J. Cohen, J.M. Evans, K.R. Reddy, P.W. Inglett, K.S. Inglett, T.K. Frazer, C.A. Jacoby, E.J. Phlips, R.L. Knight, S.K. Notestein, and K.A. McKee. 2008. *Summary and synthesis of the available literature on the Effects of nutrients on spring organisms and systems.* Report to the Florida Department of Environmental Protection, Tallahassee, Florida.

Korschgen, C.E., and W.L. Green. 1988. *American wild celery (Vallisneria americana): ecological considerations for restoration. U.S. Fish and Wildlife Service. Fish and Wildlife Technical Report 19-24.*

Kremer, B.P. 1981. Metabolic implications of non-photosynthetic carbon fixation in brown macroalgae. *Phycologia* 20(3): 242-250.

Kurtz, J.C., D.F. Yates, J.M. Macauley, R.L. Quarles, F.J. Genthner, C.A. Chancy, and R. Devereux. 2003. Effects of light reduction on growth of the submerged macrophyte *Vallisneria americana* and the community of root-associated heterotrophic bacteria. *Journal of Experimental Marine Biology and Ecology* 291(2): 199-218.

Lamoreaux, R.J., W.R. Chaney, and K.M. Brown. 1978. The plastochron index: a review after two decades of use*. American Journal of Botany* 65: 586-593.

Lauridsen, T.L., E. Jeppesen, and M. Søndergaard. 1994. Colonization and succession of submerged macrophytes in shallow Lake Vaeng during the first five years following fish manipulation. *Hydrobiologia* 275(1): 233-242.

Lin H.J. 1995. Responses of epiphytes on eelgrass (*Zostera marina* L.) to nutrient enrichment. PhD thesis, University of Rhode Island, Kingston, RI.

Lindeboom, H.J., and B.H.H. DeBree. 1982. Daily production and consumption in an eelgrass (*Zostera marina*) community in saline Lake Grevelingen: discrepancies between the O_2 and ^{14}C method. *Netherlands Journal of Sea Research* 16: 362-379.

Lorenti, M., L. Mazzella, and M.C. Buia. 1995. Light limitation of *Posidonia oceanica* (L.) Delile leaves and epiphytes at different depths. *Rapports de la Commision Internationale de la Mer Méditerranée* 34.

Losee R.F., and R.G. Wetzel. 1983. Selective light attenuation by the periphyton complex. In *Periphyton of freshwater ecosystems*. Wetzel, R.G. (ed). Springer.

Ludwig, J.A., and D.J. Tongway. 1995. Spatial organization of landscapes and its function in Semi-Arid Woodlands, Australia. *Landscape Ecology* 10: 51-63.

Madden, C.J., and W.M. Kemp. 1996. Ecosystem model of an estuarine submersed plant community, calibration an simulation of eutrophication responses. *Estuaries* 19: 457-474.

Mattson, R.A., J.H. Epler, and M.K. Hein. 1995. Description of benthic communities in karst, spring-fed streams of north central Florida. *Journal of the Kansas Entomological Society* 68: 18-41.

Mazzella, L., and J. Ott. 1984. Seasonal changes in some features of *Posidonia oceanica* (L.) Dellile leaves and epiphytes at different depths. In *Proceedings of the International workshop on Posidonia oceanica beds*, ed. C.F. Boudouresque, A.J. de Grissac, J. Olivier, and G.I.S. Posidonie. G.I.S. Posidonie.

Mazzella, L., and R.S. Alberte. 1986. Light adaptation and the role of autotrophic epiphytes in primary production of the temperate seagrass, *Zostera marina* L. *Journal of Experimental Marine Biology and Ecology* 100(1-3): 165-180.

McFarland, D.G. 2006. *Reproductive ecology of Vallisneria americana Michaux*. *SAV-06-4*. Vicksburg: Engineer research and development center.

Montana Department of Environmental Quality. 2011. Sample collection and laboratory analysis of Chlorophyll-a standard operation procedure. Accessed at: http://deq.mt.gov/Portals/112/Water/WQPB/QAProgram/Documents/PDF/SOPs/WQPBWQM-011v6_FNL.pdf

Muenscher, W.C. 1936. The germination of seeds of *Potamogeton*. *Annals of Botany* 50(200): 805-821.

Munch, D.A., D.J. Toth, C. Huang, J.B. Davis, C.M. Fortich, W.L. Osburn, E.J. Phlips, E.L. Quinlan, M.S. Allen, M.J. Woods, P. Cooney, R.L. Knight, R.A. Clarke, and S.L. Knight. 2006. *Fifty-year retrospective study of the ecology of Silver Springs, Florida. Publication Number: SJ2007-SP4.* Palatka: St. Johns River Water Management District.

Neckles, H.A., R.L. Wetzel, and R.J. Orth. 1993. Relative effects of nutrient enrichment and grazing on epiphyte macrophyte (*Zostera marina L*) dynamics. *Oecologia* 93: 285-295.

Nelson, T.A., and J.R. Waaland. 1997. Seasonality of eelgrass, epiphyte, and grazer biomass and productivity in subtidal eelgrass meadows subjected to moderate tidal amplitude. *Aquatic Bot*any 56: 51-74.

Notestein S.K. 2001. *Physical, chemical, and vegetative characteristics of the Chassahowitzka river.* Gainesville: University of Florida.

Odum, H.T. 1957. Trophic structure and productivity of Silver Springs, Florida. *Ecological Monographs* 27(1): 55-112.

Orth, R.J., and J. van-Montfrans. 1984. Epiphytes seagrass relationships with an emphasis on the role of micrograzing: a review. *Aquatic Botany* 18: 43-69.

Orth, R.J., and K.A. Moore. 1983. Chesapeake Bay: an unprecedented decline in submerged aquatic vegetation. *Science* 222: 51-53.

Oshima, Y., M.J. Kishi, and T. Sugimoto. 1999. Evaluation of the nutrient budget in a seagrass bed. *Ecological Modeling* 115: 19-33.

Ott, J.A. 1979. Persistence of a seasonal growth rhythm in *Posidonia oceanica* (L.) Delile under constant conditions of temperature and illumination. *Marine Biology Letters* 1: 99-104.

Ott, J.A. 1980. Growth and production in *Posidonia oceanica* (L.) Delile. *Marine Ecology* 1(1): 47-64.

Patriquin, D. 1973. Estimation of growth rate, production and age of the marine angiosperm *Thalassia testudinum* Konig. *Caribbean Journal of Science* 13: 111-123.

Penhale, P.A., and W.O. Smith. 1977. Excretion of dissolved organic carbon by eelgrass (*Zostera marina*) and its epiphytes. *Limnology and Oceanography* 22(3): 400-407.

Penning de Vries, F.W.T., and H.H. VanLaar. 1982. Simulation of growth processes and the model BACROS. Simulation of plant growth and crop production, Pudoc, Wageningen 114-131.

Phillips, G., D. Eminson, and B. Moss. 1978. A mechanism to account for macrophyte decline in progressively eutrophicated freshwaters. *Aquatic Botany* 4: 103-126.

Pinckney, J., H. Paerl, P. Tester, and T. Richardson. 2001. The role of nutrient loading and eutrophication in estuarine ecology. *Environmental Health Perspectives* 109: 699-706.

Pirc, H. 1985. Growth dynamics in *Posidonia oceanica* (L.) Delile. *Marine Ecology* 6(2): 141-165.

Plus, M., A. Chapelle, A. Ménesguenb, J.M. Deslous-Paolic, and I. Auby. 2003. Modelling seasonal dynamics of biomasses and nitrogen contents in a seagrass meadow (*Zostera noltii* Hornem.): application to the Thau lagoon (French Mediterranean coast). *Ecological Modeling* 161(3): 211-236.

Ramus, J. 1981. The capture and transduction of light energy. In *The biology of seaweeds*, ed. C.S. Lobban, and M.J. Wynne. Botanical Monographs, Blackwell Scientific Publications.

Rogers, J.W., D.G. McFarland, and J.W. Barko. 1995. Evaluation of the growth of *Vallisneria americana* Michx. in relation to sediment nutrient availability. *Lake and Reservoir Management* 11: 57-66.

Rogers, K.H., and C.M. Breen. 1981. Effects of epiphyton on *Potamogeton crispus* L. leaves. *Microbial Ecology* 7(4): 351-363.

Rosenau, J.C., G.L. Faulkner, C.W. Hendry Jr., and R.W. Hull. 1977. Springs of Florida. Florida Department of Natural Rescources. Bureau of Geology Bulletin No.32: 461.

Sand-Jensen, K. 1977. Effect of epiphytes on eelgrass photosynthesis. *Aquatic Botany* 3: 55-63.

Sand-Jensen, K. 1990. Epiphyte shading its role in resulting depth distribution of submerged aquatic macrophytes. *Folia geobotanica and phytotaxonomica* 25: 315-320.

Sand-Jensen, K., C. Prahl, and H. Stokholm. 1982. Oxygen release from roots of submerged aquatic macrophytes. *Oikos* 38: 349-354.

Sand-Jensen, K., and J. Borum. 1984. Epiphyte shading and its effect on photosynthesis and diel metabolism of *Lobelia dortmanna* L. during the spring bloom in a Danish lake. *Aquatic Botany* 20: 109-119.

Sand-Jensen, K., N.P. Revsbech, and B.B. Jorgensen. 1985. Microprofiles of oxygen in epiphyte communities on submerged macrophytes. *Marine Biology* 89: 55-62.

Sand-Jensen, K., and M. Søndergaard. 1981. Phytoplankton and epiphyte development and their shading effect on submerged macrophytes in lakes of different nutrient status. *International Review of Hydrobiology* 66(4): 529-552.

Scott, T.M., G.H. Means, R.C. Means, and R.P. Meegan. 2002. *First magnitude springs of Florida: Florida Geological Survey Open File Report 85.*

Scott, T.M., G.H. Means, R.P. Meegan, R.C. Means, S.B. Upchurch, R.E. Copeland, J. Jones, T. Roberts, and A. Willet. 2004. *Springs of Florida. Florida Geological Survey Bulletin No. 66.*

Sculthorpe, C.D. 1985. The biology of aquatic vascular plants. Koeltz Scientific Books. Konigstein, Germany.

Seddon, S., R.S. Connolly, and K.S. Edyvane. 2000. Large-scale seagrass die back in northern Spencer Gulf, South Australia*. Aquatic Botany* 66: 297-310.

Short, F.T. 1980. A simulation model of seagrass production system. In: Handbook of seagrass biology: an ecosystem perspective. Phillips, R.C., and C.P. McRoy (eds). Garland STPM Press.

Short, F.T., and C.M. Duarte. 2001. Methods for the measurement of seagrass growth and production. In *Global seagrass research methods*, ed. F.T. Short, and R.G. Coles. Amsterdam: Elsevier Science.

Silberstein, K., A. Chiffings, and A. McComb. 1986. The loss of seagrass in Cockburn Sound, Western Australia. III. The effect of epiphytes on productivity of *Posidonia australis* Hook. F. *Aquatic Botany* 24: 355-371.

Smart, R.M., J.W. Barko, and D.G. McFarland. 1994. *Competition between Hydrilla verticillata and Vallisneria americana under different environmental conditions. Technical report NO. WES/TR/EL-A-94-1.* Vicksburg: Army engineer waterways experiment station.

Spence, D.H.N. 1976. Light and plant response in freshwater. In *Light as an ecological factor*, ed. R. Bainbridge, G.C. Evans, and O. Rackham. Blackwell Science Publications.

Springs Management Plan. 2016. Southwest Florida water Management District. Accessed at: http://www.swfwmd.state.fl.us/publications/files/Springs_Management_Plan.pdf.

Stankelis, R.M., M.D. Naylor, and W.R. Boynton. 2003 Submerged aquatic vegetation in the mesohaline region of the Patuxent estuary: Past, present, and future status. *Estuaries* 26: 186-195.

Stankelis R.M., W.R. Boynton, and J.M. Frank. 1999. Submerged aquatic vegetation (SAV) habitat evaluation. Chapter 1. In *Ecosystems processes component level interpretive report No 16*. Solomons: Chesapeake Biological Laboratory, University of Maryland System.

Stevenson, R.J., A. Pinowska, A. Albertin, and J.O. Sickman. 2007. *Ecological condition of algae and nutrients in Florida springs: The Synthesis Report.* Tallahassee: Prepared for the Florida Department of Environmental Protection.

Sytsma, M.D., and L.W.J. Anderson. 1993. Transpiration by an emergent macrophyte:source of water and implications for nutrient supply. *Hydrobiologia* 271: 97-108.

Thayer, G.W., W.J. Kenworthy, and M.S. Fonseca. 1984. *Ecology of eelgrass meadows of the Atlantic coast: a community profile (No. FWS/OBS-84/02).* National Marine Fisheries Service, Beaufort, NC (USA). Beaufort Lab., Virginia Univ., Charlottesville (USA). Department of Environmental Sciences.

Titus, J., and M.A. Adams. 1979. Coexistence and the comparative light relations of the submersed macrophytes *Myriophyllym spicatum* L. and *Vallisneria americana* Michx. *Oecologia* 40: 273-286.

Titus, J., R.A. Goldstein, M.S. Adams, J.B. Mankin, R.V. O'Neill, P.R. Weiler, H.H. Shugart, and R.S. Booth. 1975. A production model for *Myriophyllum spicatum* L. *Ecology* 56: 1129-1138.

Twilley, R., W. Kemp, K. Staver, J. Stevenson, and W. Boynton. 1985. Nutrient enrichment of estuarine submersed vascular plant communities. I. Algal growth and effects on production of plants and associated communities. *Marine Ecology Progress Series* 23: 179-191.

United States Fish and Wildlife Service. 1988. *Crystal River National Wildlife Refuge annual narrative report. Chassahowitzka National Wildlife Refuge.* Homosassa, Florida.

van-Dijk, G.M. 1993. Dynamics and attenuation characteristics of periphyton upon artificial substratum under various light conditions and some additional observations on periphyton upon *Potamogeton pectinatus* L. *Hydrobiologia* 252: 143-161.

van-Donk, E., and W.J. van de Bund. 2002. Impact of submerged macrophytes including charophytes on phyto-and zooplankton communities: allelopathy versus other mechanisms*. Aquatic Botany* 72(3): 261-274.

Vásquez-Elizondo, R.M., and S. Enríquez. 2017. Light absorption in coralline algae (Rhodophyta): a morphological and functional approach to understanding species distribution in a coral reef lagoon. *Frontiers in Marine Science* 4: 297.

Vermaat, J.E., J.A.J. Beijer, R. Gijlstra, M.J.M. Hootsmans, C.J.M. Philippart, N.W. van den Brink, and W. van Vierssen. 1993. Leaf dynamics and standing stocks of intertidal *Zostera noltii* Hornem. and *Cymodocea nodosa* (Ucria) Ascherson on the Banc d'Arguin (Mauritania). *Hydrobiologia* 258: 59-72.

Vermaat, J.E., and M.J.M. Hootsmans. 1994. Periphyton dynamics in a temperature-light gradient. Lake Veluwe, a macrophyte-dominated system under Eutrophication Stress, Springer Netherlands.

Waycott, M., C.M. Duarte, T.J. Carruthers, R.J. Orth, W.C. Dennison, S. Olyarnik, A. Calladine, J.W. Fourqurean, K.L. Heck, A.R. Hughes, and G.A. Kendrick. 2009. Accelerating loss of seagrasses across the globe threatens coastal ecosystems. *Proceedings of the National Academy of Sciences* 106(30): 12377-12381.

Westlake, D.F. 1978. Rapid exchange of oxygen between plant and water. *Proceedings International Association of Theoretical and Applied Limnology*. Verhandlungen des Internationalen Verein Limnologie 20: 2363–2367

Wetland Solutions, Inc. 2010. *An ecosystem-level study of Florida's springs. FWC Project Agreement No.08010*.

Wigand, C., J. Wehr, K. Limburg, B. Gorham, S. Longergan, and S. Findlay. 2000. Effect of *Vallisneria americana* (L.) on community structure and ecosystem function in lake mesocosms. *Hydrobiologia* 418: 137-146.

Yobbi, D.K. 1992. *Effects of tidal stage and ground-water levels on the discharge and water quality of springs in costal Citrus and Hernando Counties. United States Geological Survey. WRI 92-4069.*

Yobbi, D.K., and L.A. Knockenmus. 1989. *Salinity and flow relations and effects of reduced flow in Chassahowitzka River and Hommossassa River estuaries, Southwest Florida.* U.S. Geological Survey. Water Resources Investigations Report 88-4044.

Zieman, J.C., 1968. *A study of the growth and decomposition of the seagrass: Thalassia testudinam.* Miami: University of Miami.

Zieman, J.C., and R.G. Wetzel. 1980. Productivity in seagrasses: methods and rates. In *Handbook of seagrass biology: an ecosystem perspective*, ed. R.C. Phillips, and C.P. McRoy. Garland STPM Press.

Zieman, J.C., S.A. Macko, and A.L. Mills. 1984. Role of seagrasses and mangroves in estuarine food webs: temporal and spatial changes in stable isotope composition and Amino acid content during decomposition. *Bulletin of Marine Science* 35(3): 380-392.

Zimmerman, R.C., A. Cabello-Pasini, and R.S. Alberte. 1994. Modelling daily production of aquatic macrophytes from irradiance measurements: a comparative analysis. *Marine Ecology Progress Series* 114: 185-196.

Zupo, V., M.C. Buia, and L. Mazzella. 1997. A production model for *Posidonia oceanica* based on temperature. *Estuarine Coastal Shelf Sciences* 44: 483-492.

BIOGRAPHICAL SKETCH

Jing Guan was born in Qingdao, China, a beautiful coastal city. Camping, hiking, and swimming instilled in her a fundamental interest and enchantment with the natural world. Her interests in natural science took hold, and since secondary school, she has indulged in all kinds of scientific experiments. As part of the generation born in the 1980s in China, she witnessed overpopulation, deterioration of water resources and exhaustion of fishery resources. Her enthusiasm for natural sciences and a desire to make a difference motivated her to pursue an associate's degree focused on Fisheries Sciences and Aquaculture. Undergraduate studies and an internship at a fisheries research institution deepened her understanding of Environmental Science and brought her into a new realm, aquatic science. Subsequently, she went to the University of Florida to study water treatment, management of water quality and hydro-ecological restoration. She obtained her M.S from the Department of Soil and Water Sciences. While in Florida, she was particularly drawn toward the unique spring systems and felt heartbroken when she saw the anthropogenic impacts they endure. Her strong interest in Florida's spring systems led her to conduct research that integrates epiphytic algae, macrophytes, and spring-fed systems. Jing plans to continue working on applied aquatic science around the world.